FAKULTÄT
FÜR !NFORMATIK
Faculty of Informatics

Real-time Ray Tracing on the GPU

Ray Tracing using CUDA and kD-Trees

DIPLOMARBEIT

zur Erlangung des akademischen Grades

Diplom-Ingenieur

im Rahmen des Studiums

Visual Computing

eingereicht von

Günther Voglsam
Matrikelnummer 9955844

an der
Fakultät für Informatik der Technischen Universität Wien

Betreuung: Associate Prof. Dipl.-Ing. Dipl.-Ing. Dr.techn. Michael Wimmer
Mitwirkung: Dipl.-Ing. Dr. Robert F. Tobler

Wien, 29.04.2013

(Unterschrift Günther Voglsam) (Unterschrift Betreuung)

FAKULTÄT
FÜR !NFORMATIK
Faculty of Informatics

Real-time Ray Tracing on the GPU

Ray Tracing using CUDA and kD-Trees

MASTER'S THESIS

submitted in partial fulfillment of the requirements for the degree of

Diplom-Ingenieur

in

Visual Computing

by

Günther Voglsam
Registration Number 9955844

to the Faculty of Informatics
at the Vienna University of Technology

Advisor: Associate Prof. Dipl.-Ing. Dipl.-Ing. Dr.techn. Michael Wimmer
Assistance: Dipl.-Ing. Dr. Robert F. Tobler

Vienna, 29.04.2013 (Signature of Author) (Signature of Advisor)

Erklärung zur Verfassung der Arbeit

Günther Voglsam
Hubertusstrasse 7, 4470 Enns

Hiermit erkläre ich, dass ich diese Arbeit selbständig verfasst habe, dass ich die verwendeten Quellen und Hilfsmittel vollständig angegeben habe und dass ich die Stellen der Arbeit - einschließlich Tabellen, Karten und Abbildungen -, die anderen Werken oder dem Internet im Wortlaut oder dem Sinn nach entnommen sind, auf jeden Fall unter Angabe der Quelle als Entlehnung kenntlich gemacht habe.

(Ort, Datum)	(Unterschrift Günther Voglsam)

Acknowledgements

I want to thank Michael Wimmer at the *Institute of Computergraphics and Algorithms* for his support for the thesis, as well as the members of the *VRVis Forschungs-GmbH* for making this thesis happen in such a pleasant environment. At the VRVis I want to say special thanks to Robert F. Tobler, Michael Schwärzler and Christian Luksch for all their support and the numerous discussions we had.

I also want to thank the *Faculty of Computer Science* at the *Vienna University of Technology* for the financial support to acquire the needed hardware to make this thesis happen.

Finally I'd like to thank my colleagues from the *Computer Graphics Club* for all the interesting discussions and their friendship.

Abstract

In computer graphics, ray tracing is a well-known image generation algorithm which exists since the late 1970s. Ray tracing is typically known as an offline algorithm, which means that the image generation process takes several seconds to minutes or even hours or days.

In this thesis I present a ray tracer which runs in real-time. Real-time in terms of computer graphics means that 60 or more images per second (*frames per second*, FPS) are created. To achieve such frame rates, the ray tracer runs completely on the graphics card (GPU). This is possible by making use of Nvidia's *CUDA*-API. With CUDA, it is possible to program the processor of a graphics card similar to a processor of a CPU. This way, the computational power of a graphics card can be fully utilized. A crucial part of any ray tracer is the acceleration data structure (ADS) used. The ADS is needed to efficiently search in geometric space. In this thesis, two variants of so called *kD-Trees* have been implemented. A kD-Tree is a binary tree, which divides at each node a given geometric space into two halves using an axis aligned splitting plane.

Furthermore, a CUDA library for the rendering engine *Aardvark*, which is the in-house rendering engine at the VRVis Research Center, was developed to access CUDA functionality from within Aardvark in an easy and convenient way.

The ray tracer is part of a current software project called "HILITE" at the VRVis Research Center.

Kurzfassung

Die Strahlen-Verfolgung („Ray-Tracing“) ist ein Verfahren zur Berechnung von Bildern, dass seit den späten 1970er-Jahren bekannt ist. Dieses Verfahren ist typischerweise ein so genannter „off-line“ Algorithmus, was bedeutet, dass die Berechnung für ein Bild zwischen mehreren Sekunden oder Minuten bis hin zu mehreren Stunden oder gar Tagen benötigen kann.

Im Zuge dieser Diplomarbeit wurde ein Programm zur Strahlen-Verfolgung („*Raytracer*“) entwickelt, der die Erzeugung von Bildern in Echtzeit ermöglicht. „Echtzeit“ im Sinne der Computer-Graphik bedeutet dabei, 60 oder mehr Bilder pro Sekunde berechnen und anzeigen zu können. Um solch hohe Bilderzeugungsraten erreichen zu können, wird der Raytracer komplett auf der Graphikkarte (GPU) ausgeführt. Ermöglicht wird dies durch verwenden der Technologie *CUDA*. CUDA wurde vom Graphikkarten-Hersteller Nvidia entwickelt und erlaubt es, den Prozessor einer Graphikkarte in ähnlicher Art und Weise zu programmieren wie den einer CPU. Damit ist es möglich, die volle Rechenleistung einer Graphikkarte auszunutzen. Ein wichtiger Teil eines Raytracers sind dessen Beschleunigungsdatenstrukturen. Diese werden verwendet, um das Aufsuchen von Objekten im geometrischen Raum zu beschleunigen. In dieser Diplomarbeit wurden so genannte kD-Bäume in zwei unterschiedlichen Varianten implementiert. Ein kD-Baum ist ein binärer Baum, bei dem jeder Knoten einen gegebenen geometrischen Raum durch achsparallele Ebenen in zwei Unterräume teilt.

Zusätzlich wurde für die Programmierung des Raytracers eine CUDA Bibliothek für „Aardvark“ entwickelt. Aardvark ist die hauseigene Rendering-Engine des VRVis Forschungs-GmbH. Die Bibliothek erlaubt es, CUDA-Funktionalität innerhalb von Aardvark ohne großen Initialaufwand verwenden zu können.

Der Raytracer ist Teil eines größeren Software-Projekts namens „HILITE“, welches am VRVis umgesetzt wird.

For my grandfather

Albert Weichhart

1919 - 2012

Contents

CHAPTER 1

Introduction

1.1 About Ray Tracing

Ray tracing is one of the classic rendering algorithms. It arose already in the late 1970s. Ray tracing simulates the transport of light in a scene by shooting rays of light from the eye-point into the scene. Those rays are then intersected with the scene objects. If a ray hits a surface which is reflective like a mirror, the ray bounces off the surface and the path of the ray is further traced. Moreover, if a ray hits an object made of a transparent material, the ray gets refracted and is traced through this transparent object. However, when the ray hits an object with diffuse material or no object at all, the tracing of the ray stops. Figure 1.2 shows the basic ray-tracing scheme and Figure 1.1 shows a typical example of a ray-traced image. The strength of ray tracing is that it can generate images with correct reflection and correct refraction, as well as correct hard shadows, with relatively low programming effort in contrast to rasterization (see below). The basic ray-tracing algorithm is described in detail in Section 2.3 and throughout the thesis, various properties are discussed with particular attention paid to real-time ray tracing.

Figure 1.1: Example ray tracing image. [Tra06]

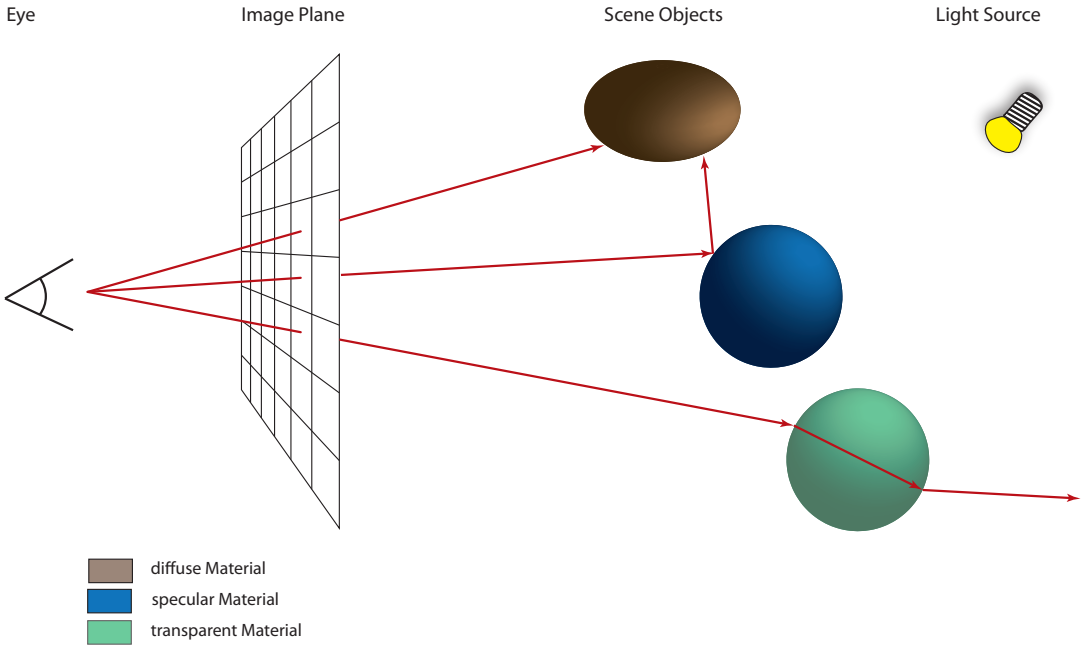

Figure 1.2: Ray-tracing scheme. Light rays are traced from the eye-point into the scene through each pixel. The rays are intersected with the objects in the scene and if the object's material is either reflecting or transparent, one or more follow-up rays are traced.

As opposed to ray tracing, *rasterization* has been the dominant rendering algorithm for several decades. In order to generate an image using rasterization, the whole scene geometry is projected onto the image plane. For each pixel, it is determined which polygon covers the space of the pixel. To ensure that polygons farther away do not overwrite pixels of polygons nearer to the image plane, a depth buffer is maintained. The depth buffer stores for each pixel the distance of the polygon currently drawn at this pixel. Using a depth test, the polygons which are farther away than the one at the corresponding location in the depth buffer are discarded, and therefore only the polygons nearest to the image plane are drawn.

Graphics cards are highly optimized for rendering using rasterization. However, dealing with rasterization becomes tricky when images with a realistic look are desired. Therefore, several extension algorithms have been invented to render effects like shadows, reflection, refraction, depth-of-field and others. These algorithms are usually either hard to implement, computationally expensive or do not meet the desired image quality because of algorithmic simplifications. Many of those effects like correct reflection and refraction as well as hard shadows, however, come naturally with the ray-tracing algorithm, and other effects can be implemented into a ray tracer without much effort.

1.2 Programmable Graphics Hardware and Ray Tracing

Looking at the evolution of graphics cards during the last decade, they became more and more flexible and programmable. Instead of using only a hard-wired pipeline for rendering images, the so-called *fixed function pipeline*, nowadays this pipeline can be programmed at several stages. This flexibility eventually led to the point where graphics cards were fully programmable. Five years ago, the graphics cards vendor Nvidia supplied an API called *CUDA* for accessing their fully programmable hardware to make use of the computational power of these graphics cards for other purposes than rendering using rasterization.

The original purpose of graphics cards was calculating a color for each pixel on the screen. This can be done in a parallel manner, and, due to this fact, graphics cards are highly parallel processors. Also, ray tracing can be calculated in parallel by many independent threads or processors. Hence, calculating ray-traced images on those fully programmable graphics cards instead on CPUs became an interesting topic. However, the hardware architecture of graphics cards was not perfectly suited for ray tracing, mainly because random memory accesses were comparably slow in graphics memory as opposed to CPU-RAM. Latest graphics cards generations try to remedy this drawback by implementing faster memory access and a cache hierarchy [Coo10].

Depending on the complexity of the scene, a ray-traced image can take from a few seconds or minutes, up to several hours or even more to render. In computer graphics, the term "*real-time*" usually refers to a frequency of 60 or more images per second, each of which has to be generated by the application. The frequency at which the images can be generated is called the *frame rate*. It is often expressed in *frames per second* (FPS). Even on a modern high-end computer, it is very hard to achieve such high frame rates using the CPU to ray trace an image. But when exploiting the computational power of modern, massively parallel GPUs, these frame rates can become possible. However, this still depends highly on the complexity of the scene and the

concrete implementation, as well as on the used acceleration structures and other optimizations (see Chapter 3.1), but real-time ray tracing is possible nowadays.

1.3 Aim of the Thesis

This thesis is part of the HILITE project [Gmb] at the VRVis Forschungs-GmbH. The aim of this project is to give a highly realistic, interactively modifiable preview of the illumination of architectural scenes. The main lighting computations are done using advanced rasterization techniques like GPU-based light simulation using lightmaps, together with a photon simulation done on the CPU. Since reflections are view-dependent and the application is interactive, correct reflections cannot be precalculated when moving through the scene. Several attempts have been made to render correct reflections on curved surfaces with rasterization [EMD+05] [EMDT06] [RH06]. All these methods, however, are either not accurate enough, can not handle concave geometry or can not handle 2^{nd}-order reflections. Therefore, a real-time ray tracer was needed. The idea was to integrate the ray tracer into the rasterization-based algorithms to form a hybrid rendering system. Attempts for hybrid rendering systems as a combination of rasterization and ray tracing have been done already by Beister et al. [MB05] and Cabeleira [Cab10]. Both utilized the rasterization algorithm on the GPU to generate an image and enhanced it with a ray tracer running on the CPU, which is in both cases only capable of creating first-hit reflections and refractions.

The goal of this thesis was to realize a ray tracer on the GPU which is capable of running at interactive to real-time frame rates. The implementation of the *whole* ray tracer on the GPU led to several challenging tasks. The first one is that the GPU can run many (up to thousands) of threads in parallel, which made new designs of the implemented algorithms necessary. Furthermore, recursion was not or not sufficiently supported at the time of implementing the ray tracer. This required iterative solutions. Finally, the development tools for GPU programming are not that advanced yet as they are for the CPU. Hence, the lack of debugging possibilities made it hard to debug a bigger program running entirely on the GPU. Solutions for that are presented in Section 6.6.

As a prerequisite to implementing a GPU ray tracer, a library for accessing the GPU computing capabilities from within the VRVis-internal rendering engine Aardvark was needed. The goal was further to provide easy, high-level access to CUDA through this library. Based on this CUDA library, a CUDA ray tracer has been developed. It was designed in such a way that it can be used from within any Aardvark application. Furthermore, since the ray tracer should be able to integrate into the main program of the HILITE project, the HILITE-Viewer, an interface and data conversion should be provided by the ray tracer, which proved to be a demanding task. The CUDA library will be described in detail in Chapter 5 and the CUDA ray tracer in Chapter 6.

1.4 Contributions

This thesis has two contributions of a more practical nature and three contributions which can be called scientific. They will be summarized in this section.

1.4.1 CUDA Library

The first contribution is a CUDA library developed for the VRVis-internal rendering engine Aardvark. Aardvark is used as a base framework for many scientific projects. The CUDA library now makes it possible to utilize the power of GPU computing for various projects. One of those projects is the CUDA ray tracer, which was also developed for this thesis (see next contribution).

The CUDA library provides access to CUDA-functionality on a high level of abstraction from within Aardvark, which is written in C#. The library is explained in detail in Chapter 5. The most important features of the library are:

- Management of CUDA-Context, -Device, -Modules and -Functions: By using the library, CUDA contexts can be created easily as well as modules and functions can be loaded in a convenient way.
- Memory manager: The CUDA resources are managed with a memory manager, which automatically cleans up unused resources on the GPU.
- Data types: Ready-to-use data types for arrays and struct-like data are provided. Those data types can be worked with as with normal C#-data types and are automatically made available for inside a CUDA kernel. Page-locked arrays are supported too.
- Simple kernel launch: The launch of a CUDA kernel can be done almost as simple as calling any C#-function.
- Graphics resource sharing: DirectX graphics resources, like textures and buffers, can be shared with CUDA. Functionality for sharing of OpenGL resources can be added with very little effort as well.
- Full support for CUDA-Streams, CUDA-Events and -Timers, and so on. Almost every feature of the CUDA API 3.x is available via the CUDA library.

1.4.2 CUDA Ray tracer

The second contribution is the CUDA ray tracer itself. It is called *CURA* and utilizes the CUDA library. CURA will be described in detail in Chapter 6. Some of the features are:

- A ray tracer which runs completely on the GPU, so the CPU is free for other tasks.
- Real-time to interactive frame rates, depending on the scene complexity.
- The ray tracer uses kD-Trees in two variants:
  - *Object-kD-Tree*: One kD-Tree per scene object.
  - *Über-kD-Tree*: One kD-Tree for the whole scene. The leaves of this tree are the Object-kD-Trees.

  Both are described in Sections 6.4 and 7.3.

- The main purpose of the ray tracer is to render static scenes, however, scene updates and hence animations are supported as well.

- The used graphics resources are shared between CUDA and Direct X for efficient rendering.

- Fully configurable at runtime.

- Since the implemented ray tracer can be used by any Aardvark application, CURA serves as an example on how to use the CUDA ray tracer inside Aardvark projects.

- Last but not least, the ray tracer has already been built into the HILITE-Viewer by another student concurrently to writing this thesis.

1.4.3 Über-kD-Tree

One of our contributions is a new data structure which we call the *Über-kD-Tree*. It is a kD-Tree with kD-Trees in its leaves. The leaf kD-Trees are kd-Trees per geometrical object and we call them *Object-kD-Tree*. The main reason why we developed this data structure is that in the final application, the HILITE-Viewer, objects need to be added and deleted interactively at runtime. To spare costly rebuilds of data structures in case of an addition or deletion of an object, just the usually small Über-kD-Tree needs to be rebuilt, which can be done quite fast.

The Über-kD-Tree is described in Section 4.5, details on the implementation are given in Section 6.4 and results using this data structure are presented in Section 7.3.

1.4.4 A new debugging Method

Debugging kD-Trees is hard, and it is even harder when they are implemented on the GPU, for several reasons. First, on the GPU a kD-Tree or any other data structure is "flattened" to an array and uses indices as pointers between the nodes. This makes traversing the data structure harder because indices, which also encode leaves, have to be processed. Second, recursive function calls are nowadays supported on GPUs, but slow. Hence, iterative methods have to be used which leads in turn to several special cases which occur only seldom.

Since GPU debugging capabilities are still limited, the only way to debug such code is to rewrite the GPU code for the CPU and debug it there. However, an image to be rendered consists of a few-thousand to a few-million pixels and only some of them exhibit erroneous results. For this reason it is not possible nor necessary to debug the complete rendering of the whole image.

As a solution to this, I introduced the so-called "debug pixel". It is one pixel fixed on the screen for which debugging can be triggered on the CPU. When moving around with the camera in the scene, one can point the debug pixel to a pixel which shows a wrong result and trigger debugging for this pixel only. This way, special cases can be debugged well.

The debug method is further described in Section 6.6.

1.4.5 Presentation of Algorithms for the GPU

There are several papers released which deal with real-time ray tracing on the GPU. However, it is hard to find information on complete algorithms for GPUs, especially iterative and parallel versions of the ray tracing algorithm for CUDA, as well as several techniques for the traversal of kD-Trees. For this reason, Chapter 4 describes and summarizes the complete algorithms for iterative and parallel ray tracing for GPUs and several traversal methods for GPUs for kD-Trees.

CHAPTER 2

Theory

In this chapter, the theoretical foundations for generating an image from virtual scenes are explained. First, the rendering equation is introduced. Ray tracing provides a partial solution to the rendering equation. Later on, an overview is given on how to model properties of materials before presenting methods of practical solutions of the rendering equation. For the classification of rendering algorithms, the light transport notation is presented. Finally, the basic ray-tracing algorithm is explained in detail in the last section of this chapter.

2.1 The Rendering Equation

In order to generate realistic-looking images, the propagation of light in a scene has to be calculated. The rendering equation is a mathematical formulation of how light disperses in a scene and can be used to classify diverse rendering algorithms, depending on which parts of the rendering equation the algorithms can solve, approximate or which parts are omitted. The rendering equation was published simultaneously by Kajiya [Kaj86] and Immel et al. [ICG86] in 1986. Equation 2.1 shows the original Kajiya version.

$$I(x, x') = g(x, x') \left[\epsilon(x, x') + \int_S \rho(x, x', x'') I(x', x'') \, \mathrm{d}x''\right]. \tag{2.1}$$

where

$I(x, x')$ is the intensity of light passed from point x' to point x,

$g(x, x')$ is a geometry term which encodes the occlusion between the two points,

$\epsilon(x, x')$ is the emitted light from point x' to x,

S is the union of all surfaces in the scene and

$\rho(x, x', x'')$ is the intensity of the light scattered from x'' to x via x'. ρ is the BRDF.

The alternative and nowadays more common form of the rendering equation from Immel et al. [ICG86] is as follows:

$$L_o(p, \omega_o) = L_e(p, \omega_o) + L_s(p, \omega_o). \tag{2.2}$$

where

$L_o(p, \omega_o)$ is the outgoing radiance from point p in the direction of ω_o,

$L_e(p, \omega_o)$ is the emitted radiance from point p in the direction of ω_o and

$L_s(p, \omega_o)$ is the scattered radiance from p in the direction of ω_o.

L_s itself can be expanded to

$$L_s(p, \omega_o) = \int_{\Omega} \rho(p, \omega_i, \omega_o)\, L_i(p, \omega_i)\, cos\theta \, \mathrm{d}\omega_i. \tag{2.3}$$

where

Ω is the hemisphere of the incoming radiance,

$\rho(p, \omega_i, \omega_o)$ is the amount of the reflected radiance at point p for incoming radiance with angle ω_i and outgoing radiance with angle ω_o. This is the BRDF.

$L_i(p, \omega_i)$ is the incoming radiance at point p from direction ω_i. It can also be seen as the outgoing radiance from a point p' with angle $-\omega_i$, thus $L_i(p, \omega_i) = L_o(p', -\omega_i)$. This is in turn the same as the first hit of a ray from the point p in the direction ω_i. It is usually expressed by the *visibility function* h with $p' = h(p, -\omega_i)$, which then gives $L_o(p', -\omega_i) = L_o(h(p, -\omega_i), \omega_i)$ (see Figure 2.1, left) [Lás99].

$cos\,\theta$ corresponds to the geometric term from Kajiya's rendering equation. θ is the angle of incident, which is the angle between the surface normal at point p and the incoming radiance. Thus, if the angle increases, the available energy is distributed over a greater area, decreasing the amount of energy per unit area (see Figure 2.1, right).

It is hard to solve the rendering equation analytically. One problem is the recursion. Every incoming radiance L_i at point p is the L_o of another point p', which in term has other incoming L_i's of other points p'', and so on. Because of the law of conservation of energy, no additional energy can be produced or emitted at a recursion level, but energy can be absorbed by the material. This means that the deeper the level of recursion, the lower the available energy, and thus the contribution to the final image is also comparatively small. Some rendering algorithms therefore stop the recursion either at a fixed maximum level, or if the energy of a recursion level is below a certain threshold.

Another problem is that the integral over the hemisphere Ω has infinitely many incoming directions. This is the reason why the hemisphere can only be approximated by sampling.

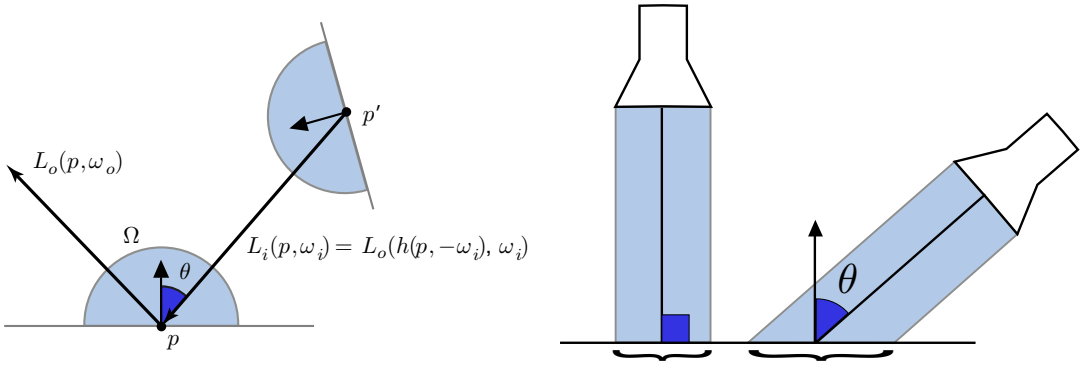

Figure 2.1: Left: Incoming and outgoing radiance at point p from point p'. Right: $Cos\,\theta$-Term. If the incident angle θ increases, the amount of energy per unit area decreases. (Figures adapted from [Gue08].)

2.1.1 BRDF, BTDF, BSDF

BRDF is the abbreviation for *bidirectional reflectance distribution function*. It is used to describe the reflection characteristics of a surface, i.e., it describes how incident light is scattered and reflected. Since light can only be reflected into the upper hemisphere, the BRDF is defined only for this region. Formally, the BRDF is a function which takes four parameters, the incoming and outgoing directions in spherical coordinates (Equation 2.4). If the two-dimensional position on a surface is included, the BRDF has six parameters, as in the rendering equation (Equation 2.1).

$$\rho(\omega_i, \omega_o) = \frac{L_o(\omega_o)}{L_i(\omega_i)\, cos\theta_i\, \mathrm{d}\omega_i}. \tag{2.4}$$

BRDFs must fulfill several properties to be called *physically plausible* [Lás99]. First, a BRDF must satisfy the *Helmholtz reciprocity*, which means that the BRDF is symmetric with regard to the incoming and outgoing directions:

$$\rho(\omega_i, \omega_o) = \rho(\omega_o, \omega_i). \tag{2.5}$$

This property is important, because this allows ray tracing to be performed in the opposite (backward) direction. Furthermore, a BRDF must satisfy the law of *energy conservation*. This means that the reflected amount of light is less or equal to the incoming light:

$$\int_\Omega \rho(\omega_i, \omega_o) \leq 1. \tag{2.6}$$

A BRDF for a material with perfect specular reflection reflects the light in one direction only. If a material exhibits perfect diffuse reflection, light is scattered equally in all directions into the upper hemisphere. Real-world materials, however, consist of a combination of diffuse and specular reflection properties, like rough specular or directional diffuse materials (see Figure 2.2). To model realistic-looking surfaces, models can be created by measuring the behavior

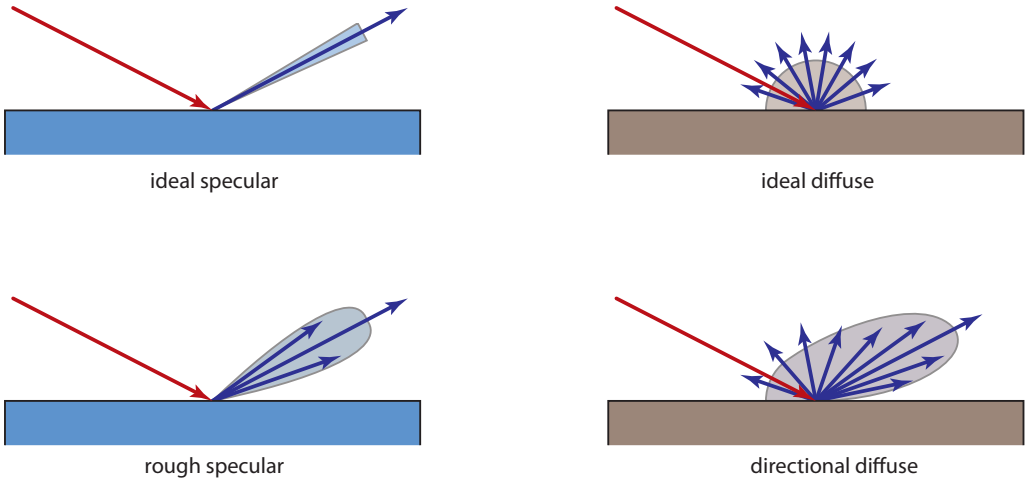

Figure 2.2: Reflection and scattering. Ideal specular reflection reflects light only in one direction, whereas an ideal diffuse surface scatters the incoming light equally in all directions. Real-world materials, however, are a combination of both, like a rough specular or directional diffuse material.

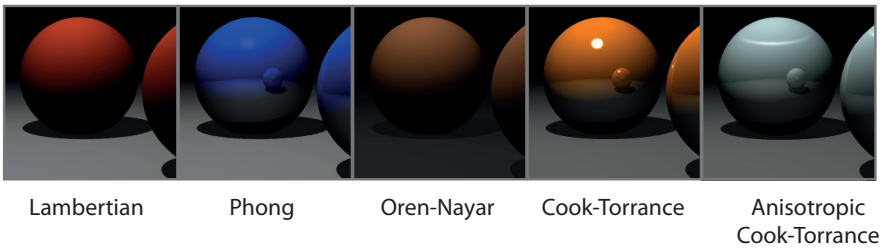

Figure 2.3: BRDF examples. Different analytical BRDF-models are shown. [Gue08]

of real materials under defined illumination. The results are then either stored in a table, or an analytical model is created or fitted to the measured data. Some examples of analytical models can be seen in Figure 2.3.

As stated above, BRDFs only describe the reflection into the upper hemisphere. Hence, for transparent materials, the BTDF, the *bidirectional transmittance distribution function*, is defined for the lower hemisphere (the backside, or interior) in a similar way. BRDF and BTDF form finally together the BSDF, the *bidirectional scattering distribution function*.

2.1.2 Solution Attempts of the Rendering Equation

Since the rendering equation is hard to solve, several algorithms have been developed which simplify the rendering problem and give only an approximate solution. They can be divided into

the following three groups [Lás99]:

- **Local Illumination methods**

  The simplest way to solve the rendering equation is by only considering light coming directly from a light source and omitting the light reflected, refracted and scattered between surfaces. Because only local properties of the material of the surface and the given light source(s) are considered, this type of light is called *direct light* [Hec90]. Local illumination methods are usually simple and fast to calculate, however, due to simplifications of the rendering equation, sacrificing realism of the resulting image.

- **Recursive Ray tracing**

  Recursive ray tracing, also called *visibility ray tracing*, enhances the local illumination model by allowing recursion of the rendering equation for perfectly reflective and refractive materials. To prevent infinite recursion, usually a maximum recursion depth is defined. For recursive ray tracing, the rendering equation can be written as follows [Lás99]:

$$\begin{aligned} L_o(p,\omega_o) = L_e(p,\omega_o) + \int_\Omega \rho(p,\omega_i,\omega_o)\, L_{LS}(h(p,-\omega_i),\omega_i)\, cos\theta \,\mathrm{d}\omega_i + \\ \rho_r(p,\omega_r,\omega_o)\, L_o(h(p,-\omega_r),\omega_r) + \rho_t(p,\omega_t,\omega_o)\, L_o(h(p,-\omega_t),\omega_t). \end{aligned} \tag{2.7}$$

  where

  L_{LS} is the incoming radiance from a light source,

  ω_r and ω_t are the ideal directions for reflection and transparency, respectively, and

  ρ_r and ρ_t are the BRDFs for reflection and transparency.

  Hence, recursive ray tracing can handle materials with perfect reflection and refraction. However, diffuse surfaces can still only handle direct light. To be able to also solve the diffuse inter-reflection of surfaces, global illumination solutions are needed. Many of those solutions use ray tracing as a basis for the algorithms. The ray tracing algorithm will be described in detail in the following sections. In this thesis, we will describe the implementation of a recursive ray tracer. However, it should be possible to use this ray tracer also in global illumination solutions.

- **Global Illumination solutions**

  In the real world, light bounces off from surfaces and reflects and refracts not only for perfectly specular or transparent materials, but scatters in various directions, according to the type of material. This further means that the illumination of a surface depends also on the light bounced off from all other surfaces, the so called *indirect light*. Hence, for properly solving the rendering equation, this scattering has to be considered as well.

Symbols		Regular Expressions	
L	Light Emission	*	0-n
D	Diffuse reflection or refraction	+	1-n
S	Specular reflection or refraction	[]	0-1
E	Eye interaction	|	**or**
		()	Precedence

Classification of some rendering algorithms	
LDE	Ray Casting
LD*E	Radiosity
L[D]S*E	Ray Tracing
L(D|S)*E	Path Tracing; all possible light paths

Table 2.1: Light Transport Notation

Algorithms which are able to calculate indirect lighting are called global illumination algorithms. Well known examples are radiosity, path tracing and photon tracing. Figure 2.4 shows a comparison of the different solution attempts of the rendering equation. It can be seen that the more physically correct a rendering solution is, the more time it takes to compute the image.

2.2 Light Transport Notation

A convenient way to describe the capabilities of different rendering algorithms is to use the *light transport notation* [Hec90]. With a small string, all possible paths of a ray or photon traversing the scene can be described (see Table 2.1). Letters describe the type of interaction. They can be combined with symbols to form regular expressions. The capabilities of some well-known rendering algorithms are also given in Table 2.1.

A path LD*E means that an algorithm is able to handle several bounces of rays or photons between diffuse surfaces, like the classical radiosity algorithm does. All possible paths would be described as L(D|S)*E, which means that there can be arbitrarily many diffuse or specular bounces. Classic ray tracing can handle paths of the form L[D]S*E, which means that when traced from the eye, there can be many (or none) specular reflections or refractions, but a maximum of only one diffuse bounce. Examples of possible paths are shown in Figure 2.5.

2.3 The Ray Tracing Algorithm

2.3.1 Overview

Ray tracing is a rendering algorithm which simulates the propagation of light in a scene. Ray tracing can handle correct reflection and refraction as well as pixel-accurate hard shadows. By implementing even more effects, like depth-of-field, motion blur and the like, ray tracing can generate realistic-looking images for many types of scenes.

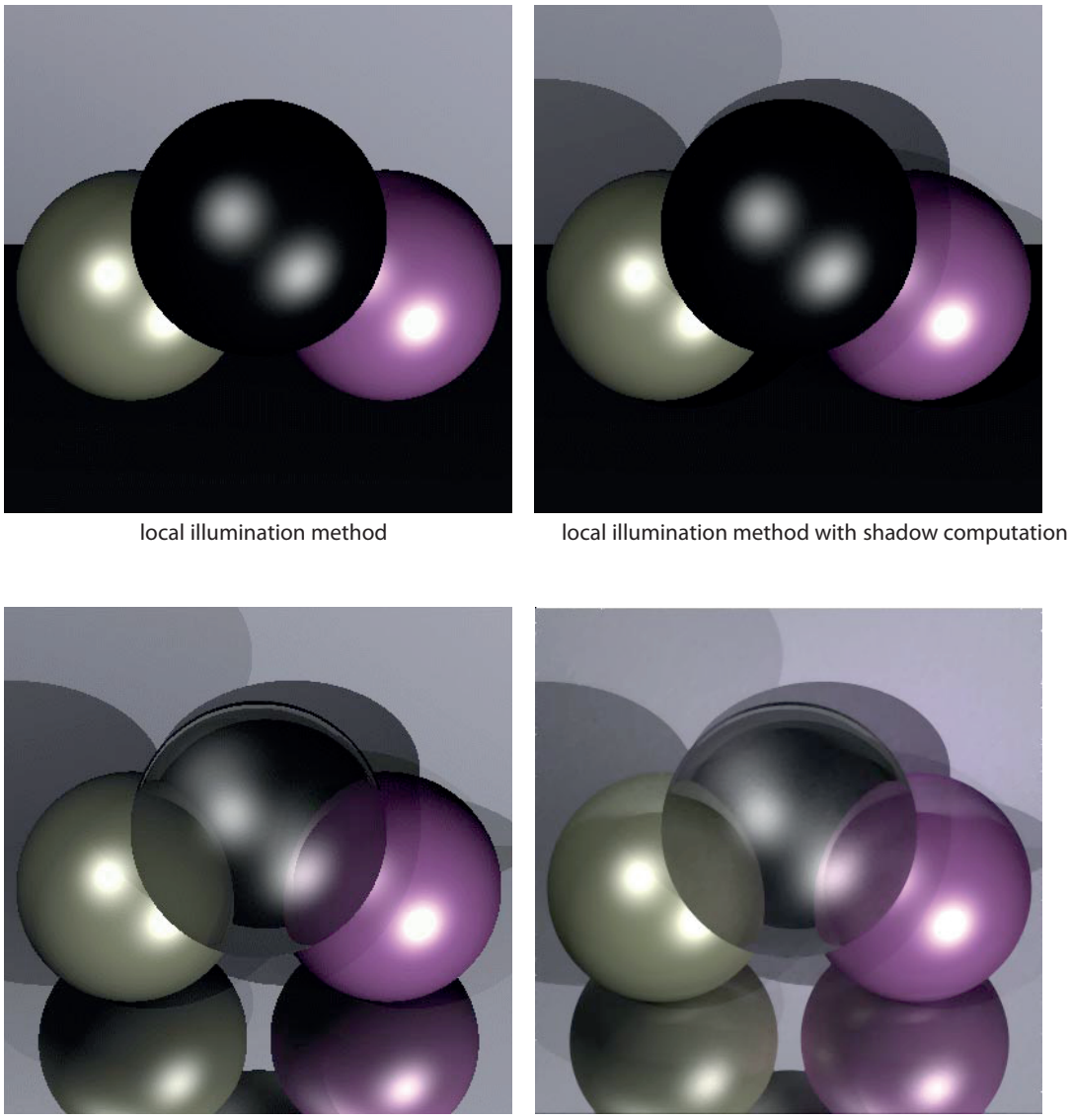

Figure 2.4: Comparison of different rendering solutions. The local illumination took 90 seconds to render (95 seconds with shadows), the ray tracing image was computed in 135 seconds and the global illumination solution took 9 hours for generating the image. [Lás99]

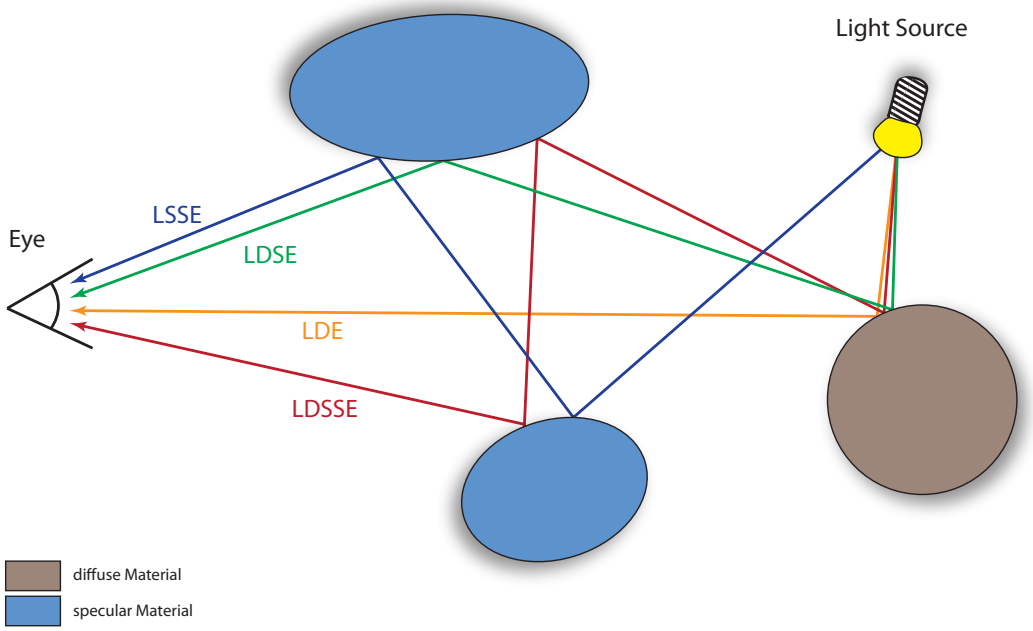

Figure 2.5: Light Transport Notation showing some possible light paths.

In light transport notation, ray tracing can handle paths of the form L[D]S*E. This means when shooting a ray from the eye, the algorithm can simulate paths of light with multiple (or no) ideal specular reflections until it hits a diffuse surface.

Originally, the light rays have been shot into the scene from the light source. The paths of the rays through the scene have been followed until the eye was hit. However, only a few of those rays hit the eye and so this approach was wasteful. Therefore, the direction of the rays has been reversed and nowadays the rays are shot from the eye into the scene.

The basic version of the modern ray-tracing algorithm was published in 1979 by Turner Whitted [Whi80] and is hence often called *Whitted style ray tracing*. In the following, the basic ray-tracing algorithm as well as some extensions will be explained.

2.3.2 Basic Ray Tracing Algorithm

The basic Whitted ray-tracing algorithm is given in Algorithm 1. It starts with creating an *eye ray* or *primary ray* for each pixel. The pixels lie in the image plane and therefore the origins of all primary rays lie on this image plane. The exact position of the origins correspond to the location of the pixels in world space. The direction of the primary rays point from the eye position towards the pixel in the image plane (see Figure 2.6).

Then the tracing of the primary ray starts. The ray is intersected with the objects in the scene and the nearest intersection, if any, is selected. The intersection of the rays with the objects in the scene is the most time-consuming part of the ray tracing algorithm. In the original publication,

it consumed 95% of the total run time. Strategy on how to reduce unneccessary intersection operations is therefore crucial for reasonable rendering performance for ray tracing. The chapter on acceleration data structures (Chapter 3.1) gives details about various strategies on how to reduce those intersection tests.

If no hitpoint is found, the background color is returned and the calculations for this pixel are finished. If a hit is recorded, *shadow tests* for all light sources are performed. For this, for each light source a *shadow ray* is created. The origin of the shadow ray is the hitpoint of the nearest intersection and the ray's direction points towards a light source. If there is at least one object between the hitpoint and light source, the hitpoint is in shadow with respect to this light source. Thus, the hitpoint is not shaded with the given light source. When testing the shadow ray for an intersection, the test can be terminated as soon as any intersection is found, which is faster than looking for the closest intersection. The shadow test is done for all light sources in the scene. If, however, the hitpoint is visible from a given light source, the hitpoint is shaded with local shading techniques like Lambert or Phong shading.

The next step is to cast *reflected rays*, if the material at the hitpoint is specularly reflecting. The origin of the reflected ray is the hitpoint. In ray tracing, all specularly reflecting materials are ideal. This means that the outgoing direction of the reflection ray encloses the same angle with the normal of the surface at the hitpoint as the incoming ray (see Figure 2.7, left). Now the tracing recursively starts again with the reflected ray as the ray to be processed. When the tracing of this ray, and all rays possibly following due to other reflections or refractions, are calculated, the tracing stops. There are two common ways to end the recursion of tracing rays. One is to define a maximum recursion level and to stop the recursion when the maximum level is reached. A maximum level of 2 usually gives already good results. The other way to end the recursion would be a more physically-based one. As mentioned in Section 2.1, the radiance gets lower with each bounce. Therefore, one can set a minimum threshold for the contribution and stop the recursion if this threshold is reached.

For transparent materials, *refraction rays* are traced in a similar way as the reflection rays. The main difference is that the direction for the refraction rays depends on the material properties, more precisely on the index-of-refraction of the material a ray enters and of the material the ray is leaving (see Figure 2.7, right).

After all reflection and refraction rays are traced, the final color for this pixel has been calculated. What remains is to write the color into the output buffer. When a color for all pixels is calculated, the algorithm has finished and the image can be displayed.

Ray Tree

When a ray hits a transparent object, this ray creates a reflection and a refraction ray. Hence, at every intersection point, a maximum of two follow-up rays can be created. This can be represented by a binary tree called a *ray tree* (see Figure 2.8). The root is the primary ray, and if this ray hits an object which has a reflecting surface, a reflection ray is created. If the surface is also transparent, a refraction ray is created as well. In the ray tree, the left child is the reflection ray and the right child the refraction ray [Suf07]. By looking at the ray tree it can be seen that with the support for reflection and transparency, a single primary ray can create a deep tree of

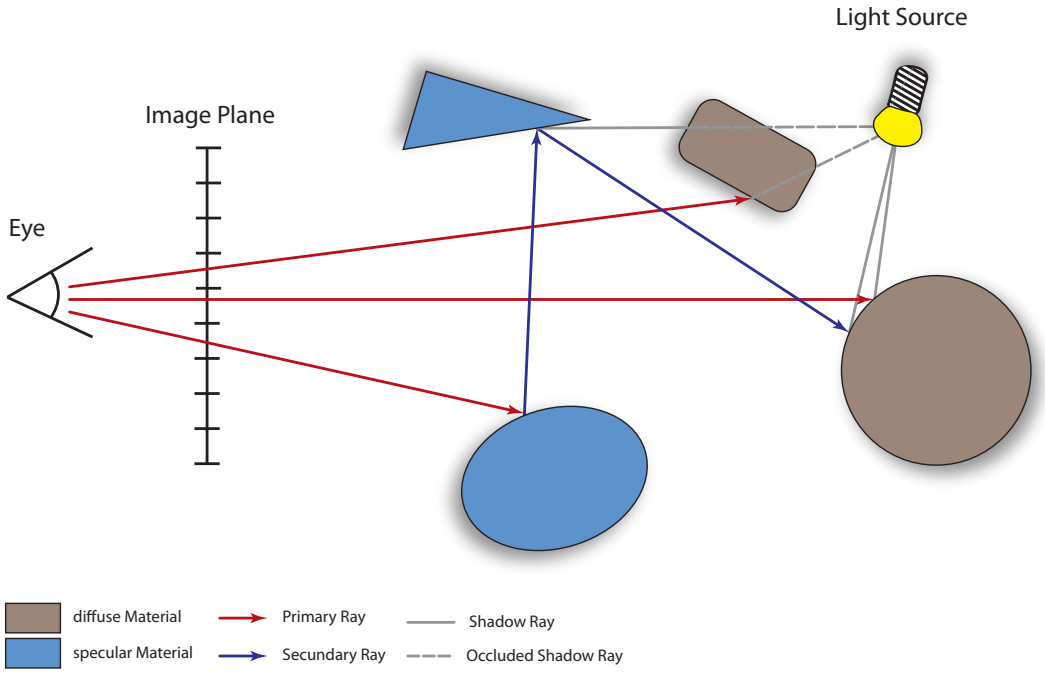

Figure 2.6: Basic ray tracing algorithm. Primary rays are sent from the eye through a pixel and intersect the objects in the scene. If a specular material is hit, a reflected ray is created. Finally, when a diffuse material is hit, the shadow rays are cast to test if the given hitpoint is in shadow.

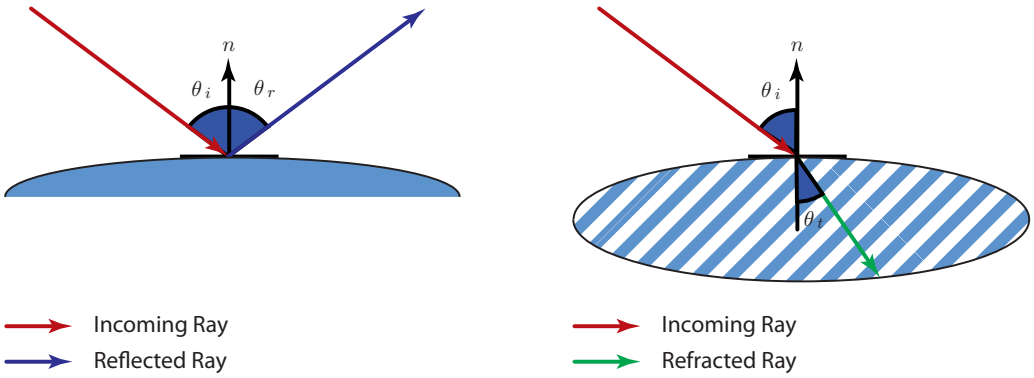

Figure 2.7: Left: Reflection. The outgoing angle is equal to the incident angle for perfectly specular materials. Right: Refraction. The angle of the refracted ray depends on the material properties of the inner and outer materials.

Algorithm 1 Basic Ray Tracing Algorithm (continued on next page)

```
1:  procedure DoRayTracing()
2:      for each pixel (x, y)
3:          primaryRay ← CreatePrimRay(x, y)
4:          outputColor ← Trace(primaryRay)
5:          WriteOutput(x, y, outputColor)
6:      end for each
7:  end procedure
8:
9:  function CreatePrimRay(x, y)
10:     origin ← point on image plane at pixel (x, y)
11:     direction ← (pixel location in the world) - (eye-point position)
12:     return Ray(origin, direction)
13: end function
14:
15: function Trace(ray)
16:     color ← black
17:     hit ← Intersect(ray, scene)
18:
19:     if hit then
20:         color += Shade(ray, hitPoint)
21:         if Material is reflective then
22:             reflectionRay ← Ray(hitPoint, reflected(ray.direction))
23:             color += Trace(reflectionRay)
24:         end if
25:         if Material is transparent then
26:             refractionRay ← Ray(hitPoint, refracted(ray.direction))
27:             color += Trace(refractionRay)
28:         end if
29:     else
30:         color ← BackgroundColor
31:     end if
32:
33:     return color
34: end function
```

rays. Usually a maximum tree level is defined to stop the fan out of the tree and hence omit further tracing.

Packet Traversal

The simplest way to trace rays is to trace one by one. However, nearby rays are likely to hit similar objects. Hence, it would be beneficial to trace those rays together to utilize cached

Algorithm 1 Basic Ray Tracing Algorithm (continued from previous page)

```
35: function SHADE(ray, hitPoint)
36:     color ← black
37:
38:     for each light source
39:         shadowRay ← Ray(hitPoint, (light source position − hitPoint))
40:         inShadow ← CASTSHADOWRAY(shadowRay)
41:         if inShadow then          → hitpoint is in shadow with respect to this light
                                        source ⇒ do not shade hitPoint with this light
42:             continue
43:         else
44:             color += CALCULATELOCALSHADING()
45:         end if
46:     end for each
47:
48:     return color
49: end function
```

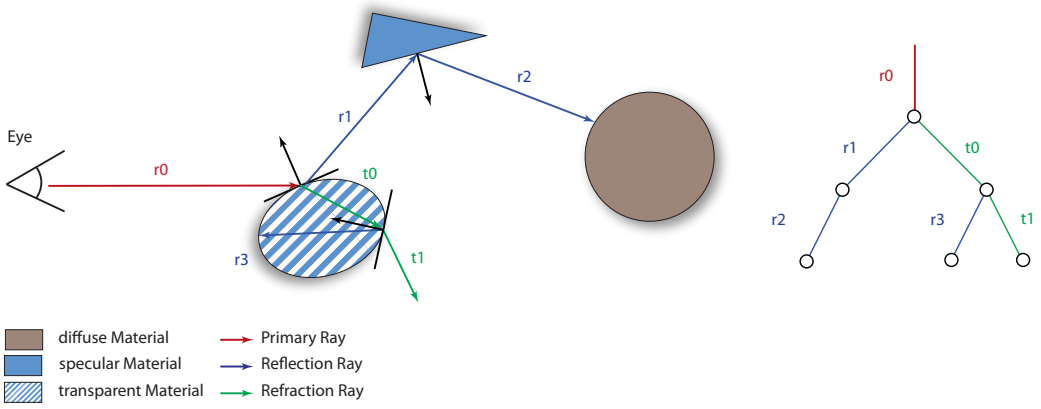

Figure 2.8: In the left image, a ray is traversed through the scene. The corresponding ray-tree is shown on the right side. The tree is made up of the rays, starting by the primary ray. Each intersection in the scene corresponds to an inner node of the tree.

memory access. This can be done using *packet traversal*. The main idea behind packet traversal is to create a frustum of rays and trace them together. The frustum can be created by four boundary rays which form a pyramid-styled frustum. These four rays, or all rays in this frustum if there are other rays in it, can then be traced with SIMD (*Single Instruction Multiple Data*) on CPUs. If one of the rays has already finished by having found the nearest intersection, this ray has to be marked as inactive while the remaining rays of the frustum continue the traversal.

Packet traversal can gain considerable speedup for coherent rays. Primary rays are inherently

coherent and packet traversal pays off most for them. Secondary rays, like shadow, reflection and refraction rays, are much less coherent and hence gain far less speedup.

CHAPTER 3

Background and Related Work

The first part of this chapter describes the most common acceleration data structures for ray tracing. Since kD-Trees have been implemented in this thesis (see Section 6.4), they are discussed thoroughly. Because splitting strategies are important for the construction and the resulting quality of acceleration data structures, they are described as well. The second part of this chapter presents Nvidia's CUDA API in detail, paying attention to the software as well as the hardware side of CUDA. After that, in the last part of this chapter, adaptations of the basic ray-tracing algorithm, presented in Section 2.3, for parallel and GPU rendering are examined.

3.1 Acceleration Data Structures for Ray Tracing

3.1.1 Motivation

Ray tracing as it is known today was first published by Turner Whitted in 1979 [Whi80]. At that time it was far from a real-time technology. The creation of images took minutes to several hours, depending on the scene complexity and the screen size (Figure 3.1). Whitted observed that his ray-tracing application spent about 95% of the rendering time with intersection tests. Accordingly, strategies for reducing and eliminating unnecessary intersection tests have been developed. Those led to the invention of special data structures, called *acceleration data structures* (ADS). They aim for efficiently culling those parts of the scene a given ray does not intersect. By culling those parts, the computationally expensive ray-primitive intersection calculations can be reduced and hence rendering time can be saved. The most important ADS will be discussed in the following.

3.1.2 Brute Force

The simplest form of having an acceleration data structure is the absence of it. Hence, when rendering an image, every ray has to be intersected with every primitive in the scene. However,

Figure 3.1: Image from the original Whitted paper [Whi80]. Rendering time was 74 minutes at a resolution of 640x480 pixels. No acceleration data structures have been used back then.

this is only feasible for scenes with only a few primitives. For performance comparison, this "type" of acceleration data structure was also implemented in this thesis' ray tracer.

3.1.3 KD-Trees

In 1985, Kaplan [M.R85] introduced kD-Trees in the computer graphics domain. They had been developed by Bentley in 1975 [Ben75] for general purpose associative searching in k-dimensional data.

KD-Trees are a special form of *binary space partitioning*-trees (BSP-Trees). BSP-trees are binary trees and every node of the tree splits the 3D space into two disjoint regions by a plane dividing the space. The root node spawns a box over the whole scene and every tree level recursively divides the space by a splitting plane. Planes for BSP-trees can be oriented in an arbitrary way. Since this makes inside-outside (or left-right) tests more expensive to calculate, those planes are often restricted to be axis aligned. Using axis-aligned planes is a common way to divide space, this type of acceleration data structure has its own name, called a *kD-Tree*.

To make the cutting of space more efficient, it is often the case that for every other level in the tree hierarchy, the axis to which the splitting plane is aligned to is switched in a round-robin manner: x-axis first, y-axis next, then the z-axis, again the x-axis and so on.

The primitives of the scene are stored in the leaves of the tree. All inner nodes only store the axis of subdivision, being either the x-, y- or z-axis, and the position of the splitting plane on this axis.

Further, algorithmic extensions exist such that large chunks of empty space can be cut off efficiently, as well as breaking the round-robin manner to divide along the axis promising the most effective split.

Since planes divide the scene, it can happen that a plane cuts through a primitive. There are several ways to handle such a situation. One way is to split the primitive into two halves and sort the split parts into the corresponding child nodes. Another strategy would be to include the unsplit primitives into both children. This is faster to construct than the previous approach, however, due to the duplication of the primitives, this leads to higher memory consumption.

The kD-Trees are known to be the best acceleration data structures in terms of rendering performance [Hav00], since they clip away parts of the scene very efficiently. Therefore, kD-Trees are the acceleration data structures which were chosen to be implemented in two different types for this thesis (see Chapter 6).

Classic Construction Algorithm

KD-Trees are constructed in a top-down manner (see Figure 3.2). First, the bounding box including all the primitives of the whole scene is created. Then the splitting position is chosen. The position depends on the used splitting strategy, some of which are described in Section 3.1.7. When the position for the split is found, the splitting plane divides the primitives into two sets. For the left and the right side of the plane, a node is created in the tree hierarchy and the corresponding primitives are sorted into their nodes.

Some of the primitives may be intersected by the splitting plane, and they need special treatment. One solution is to include the intersected primitives in both sets, the left and the right one. This can be done easily and quickly, however, this leads to duplication of the primitives, which in turn leads to higher overall memory consumption.

The other possibility is to split the primitives along the plane. There are two major ways to do so. The first, and computationally more expensive one, is to split the primitives itself accurately with the plane. The other one would be to create an axis aligned bounding box (AABB) for the primitive to be split, and split only the AABB with the plane. Since with kD-Trees the planes are always axis aligned too, the split can be performed very efficiently. This is sometimes referred to as the *boxed kD-Tree builder*.

The search for the position of the new splitting planes is then done recursively for the former left and right child nodes. This recursion lasts until a leaf node has to be created. There are several different criteria for creating a leaf node. An often used criterion is to define a fixed number of primitives, under which a node is not to be split anymore. Another, more seldom used criterion, is that a fixed tree height is defined. When using the Surface Area Heuristic (see Section 3.1.7), a leaf node can be created when the cost of splitting a node is higher than not to split it.

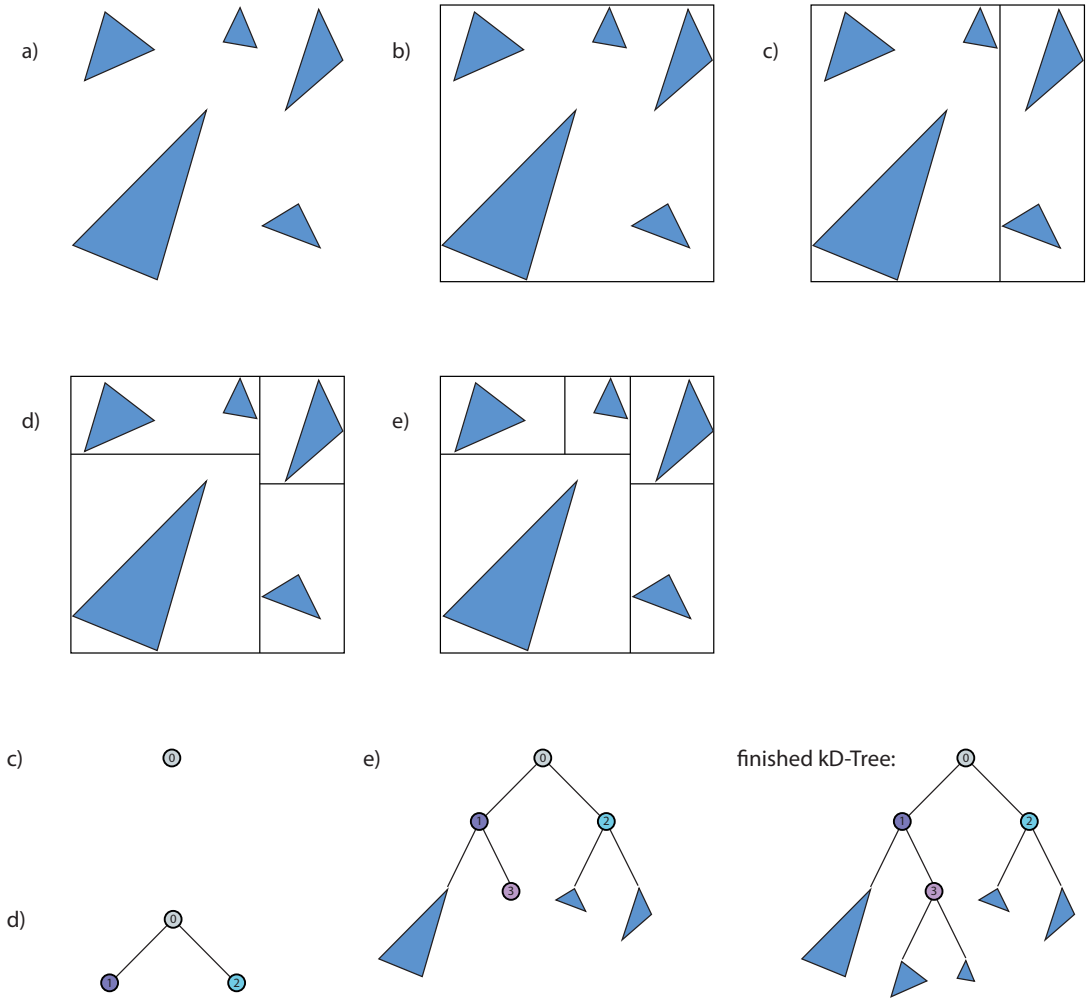

Figure 3.2: Classic kD-Tree construction algorithm: a) A soup of primitives (here: triangles) for which the kD-Tree has to be created. b) Around the primitives, a tight bounding box is constructed. c) The first splitting plane is inserted. In the corresponding kD-Tree, this plane serves as the root of the tree. d) Next, the two cells created by the previous splitting plane are again divided by inserting splitting planes. The new splitting planes again create nodes for the kD-Tree. e) One more splitting plane is inserted in the upper left cell, such that in each cell (in this example) only one primitive is left. For all cells which are not further subdivided, the corresponding primitives are inserted into the tree as leafs, and the kD-Tree construction is finished.

Approaches for Parallel Construction

The classic construction algorithm for kD-Trees is not well suited for massively parallel machines like GPUs. The power of GPUs can only be utilized when all threads are busy all the time. The classic algorithm, however, only allows to start a few new threads with every level. Therefore, other ways to build the hierarchy have to be found.

One way for parallelization is to start a thread for each primitive and let each thread test its primitive against a splitting candidate. Another way is, if there are enough nodes, to parallelize over the nodes of a tree level and let each thread calculate the split for its node. Zhou et al. [ZHWG08] use a combination of both. They choose their parallelization scheme depending on the currently processed tree level and hence on the amount of primitives per node and on the number of nodes per tree level.

Another common scheme is to set a fixed number of splitting locations and evaluate those in parallel. Danilewsky [DPS10] has implemented a fast kD-Tree builder by using this binned splitting planes. In order to use the full potential of the GPU, five different stages (i.e., kernels) for different sized nodes were implemented.

All of the parallel algorithms have in common that they try to fully utilize the GPU all the time. Therefore, the parallelization scheme may be switched during the processing of the algorithm.

Recursive Traversal

When the intersection of a ray with the scene is performed, the data structure has to be traversed. The standard way for traversing a kD-Tree is to recursively traverse the nodes of the tree. A pseudo code of this traversal is shown in Algorithm 2.

First, in order to intersect the ray with the scene, the ray is intersected with the bounding box of the scene. If the ray hits the bounding box, the values for t_{min} and t_{max} of the ray are set and the traversal of the data structure begins.

Then the root node is tested if the ray intersects the part left or right of the splitting plane, or both. In case of the ray intersecting only the left or the right part, the traversal continues with the corresponding left or right child-node and the t-values of the ray are adapted, depending on which side of the plane the ray is. If both are intersected, the node which is closer to the ray origin is traversed first and the other node is traversed if the other traversal path does not return an intersection.

The traversal continues recursively until a leaf node is reached. Then, all primitives in the leaf node are tested for an intersection with the ray. If there are one or more intersections found, the closest one is returned. The traversal for this ray is then finished. Otherwise, if no intersection in the leaf node is found, the recursive call returns without intersection. In case any of the traversed node's splitting planes has been crossed, the other tree path now is traversed. This is done until either an intersection is found, or no more recursive calls are left.

Rope Trees

KD-Trees with ropes, or *rope trees*, are special types of kD-Trees. When a leaf, i.e. its respective primitives, is intersected with a ray and no intersection has been found, the traversal through the

Algorithm 2 Recursive kD-Tree Traversal (continued on next page)

```
1:  function IntersectScene(ray)
2:      if ray does not hit Scene.BoundingBox then
3:          return no hit
4:      end if
5:
6:      foundHit ← IntersectNode(root, ray)
7:
8:      if foundHit then
9:          return primitive which was hit
10:     else
11:         return no hit
12:     end if
13: end function
14:
15: function IntersectLeaf(node, ray)
16:     nearestIntersection ← no intersection
17:
18:     for each primitive in leaf
19:         hit ← intersect primitive with ray
20:         if hit and hit is nearer then nearestIntersection then
21:             nearestIntersection ← hit
22:         end if
23:     end for each
24:
25:     return nearestIntersection
26: end function
```

tree, looking for ray-primitive intersections, continues. This is normally done by continuing the tree traversal at the last node where the ray intersected both children and the traversal descended into the nearer child. Now, the child which is further away has to be traversed. In a recursive implementation of the tree traversal, the continuation of the traversal comes naturally with the recursion. If the traversal was implemented in an iterative manner (see Section 4.4.1), the traversal continues with the last node on the stack. However, both variants need to further traverse parts of the tree, which consumes time.

To remedy this, Havran et al. [HBZ98] introduced rope trees. With rope trees, every leaf has a link, a *rope*, to its neighboring leaves on each of its sides. When in 3D, a leaf cell hence has six sides and one rope for each side. This way, when a ray does not intersect any of the primitives in a leaf, the traversal can quickly continue by following the rope to the neighboring leaf which is pierced by the ray. The ray-primitive intersection tests can now be executed immediately for this leaf without the need to further traverse the tree.

In the general case, a leaf has more than one neighboring leaf cell on a side (see Figure 3.3).

Algorithm 2 Recursive kD-Tree Traversal (continued from previous page)

```
27: function IntersectNode(node, ray)
28:     foundHit ← no hit
29:     if node is leaf then
30:         foundHit ← IntersectLeaf(node, ray)
31:         return foundHit
32:     end if
33:
34:     if ray is entirely on left of node's splitting plane then
35:         foundHit ← IntersectNode(node.ChildLeft, ray)
36:         return foundHit
37:     end if
38:     if ray is entirely on right of node's splitting plane then
39:         foundHit ← IntersectNode(node.ChildRight, ray)
40:         return foundHit
41:     end if
42:
43:     if ray crosses node's splitting plane then
44:         if node.ChildLeft is nearer than node.ChildRight then
45:             foundHit ← IntersectNode(node.ChildLeft, ray)
46:             if foundHit then
47:                 return foundHit
48:             end if
49:
50:             foundHit ← IntersectNode(node.ChildRight, ray)
51:             if foundHit then
52:                 return foundHit
53:             end if
54:         else
55:             foundHit ← IntersectNode(node.ChildRight, ray)
56:             if foundHit then
57:                 return foundHit
58:             end if
59:
60:             foundHit ← IntersectNode(node.ChildLeft, ray)
61:             if foundHit then return foundHit
62:             end if
63:         end if
64:     end if
65: end function
```

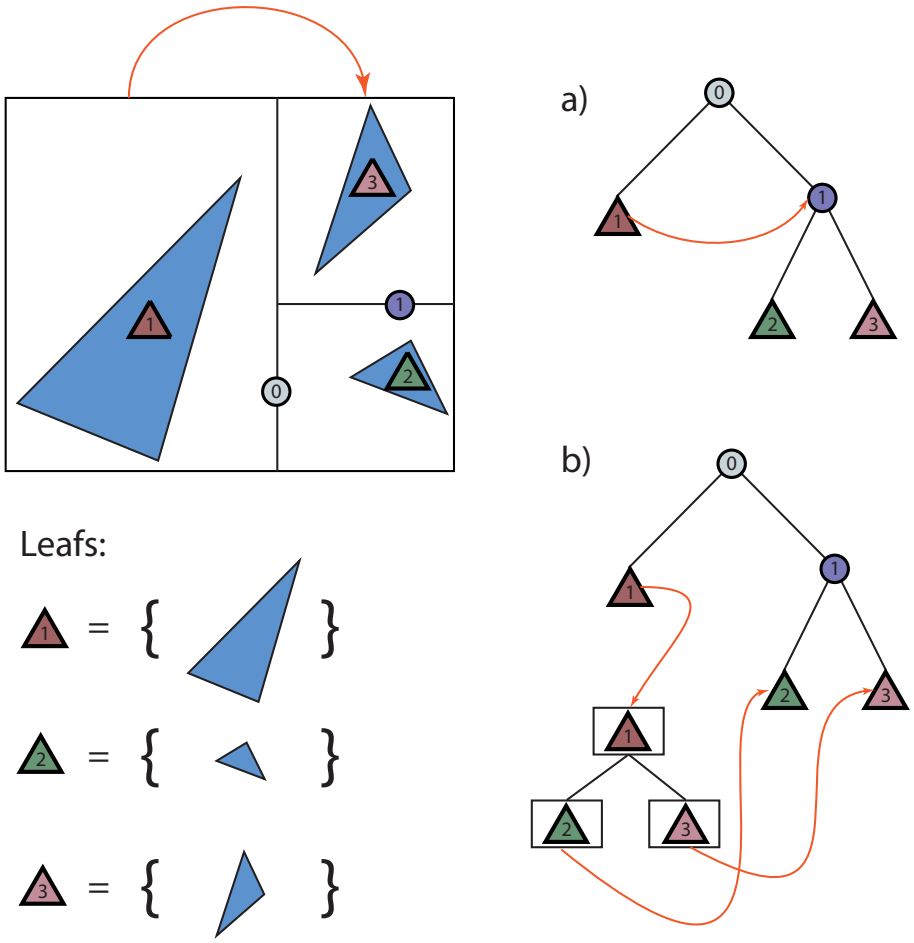

Figure 3.3: Rope tree example. A small example showing one single rope from leaf 1 to its neighboring leafs 2 and 3. In Figure a), the rope points to the lowest node in the kD-Tree which holds all adjacent leafs to leaf 1. In Figure b), the rope points to a treelet. The treelet is a small kD-Tree which the ray needs to traverse in order to decide with which adjacent leaf it should continue the traversal.

Since it would be inefficient to store a list of ropes for each of the six sides, there are two common strategies to handle such a situation. The first one is that the rope points to the lowest kD-Tree node that holds all the neighboring leaf nodes (Figure 3.3a). The second method is that the rope points to an external *treelet*, which is a small external kD-Tree (Figure 3.3b). This treelet is than traversed by the ray to find the actual neighbor leaf.

With rope trees, kD-Tree traversal can be significantly accelerated. However, the downside of rope trees is that due to storing additional ropes and bounding boxes for each leaf, the memory consumption for rope trees is considerably higher as for normal kD-Trees.

3.1.4 Bounding Volume Hierarchies

Another highly efficient acceleration data structure are *bounding volume hierarchies* (BVH). They have been introduced by Kay and Kajia [KK86] in 1986. A bounding volume is a preferably convex and geometrically simple geometric object, like a sphere or a box, tightly enclosing a usually complex object in the scene. This way it can quickly be tested if a ray intersects or misses the original object at all. If a ray does not hit the bounding volume of an object, it can't hit the original object. Only if the ray hits the bounding volume, the ray may also hit the original object in the scene, and the usually much more expensive intersection test with the object of the scene has to be executed.

BVHs are hierarchies built by using such bounding volumes. Most BVHs nowadays use axis aligned bounding boxes (AABB) as bounding volumes, because they are relatively inexpensive to test against, usually fit an arbitrary object tight enough and can easily be combined to hierarchies. However, spheres or oriented bounding boxes (arbitrary cuboids) are also used [HQL$^+$10], albeit far less often, even if they may fit the enclosed objects tighter.

As with kD-Trees, BVHs form a tree, but in this case a tree of bounding volumes. Usually the arity of the nodes is two, which means that every node can have two bounding volumes as children. Both children are fully enclosed by the parent node. An arity greater than two is possible, but hardly used in praxis.

BVHs can be constructed top-down or bottom-up. For the bottom-up way, first, some primitives are grouped together into a bounding volume. Then, nearby bounding volumes are combined to a new bounding volume. This is repeated until the whole scene is encapsulated in the hierarchy. For the top-down approach, first a bounding volume for all primitives in the scene is built. Then, the primitives contained in the scene are divided into usually two children, each of them again having its own bounding box. This is recursively repeated until the bounding volumes contain only a given number of primitives. The decision where to split the bounding volumes can be done in several ways, see Section 3.1.7.

It is important to note that the bounding volumes are not necessarily disjoint regions (see Figure 3.4). Consider for example two nearby triangles. If they are near enough, their bounding boxes can overlap. It is an important property of BVHs that the bounding volumes may overlap. Thus, if a node has two overlapping child nodes and a ray intersects both bounding volumes of those child nodes, both of those nodes have to be tested against intersection and hence have to be further traversed down the tree. This is the main reason why BVHs are not as efficient as kD-Trees are. The big advantage, on the other hand, is that BVHs consume far less memory than kD-Trees. The maximum memory needed for a BVH is known in advance, since every primitive in the hierarchy is included exactly only once. Note that kD-Trees can have more references to primitives in case of "cut" primitives (primitives split by a splitting plane).

Algorithmic extensions for BVHs exist to prohibit the overlapping of the nodes' bounding volumes by introducing spatial splits like SBVH [SFD09] or FBVH [GPP$^+$10]. Both aim at minimizing redundant intersections tests, which results in faster traversals. The SBVH and FBVH can be considered as hybrids between BVHs and kD-Trees.

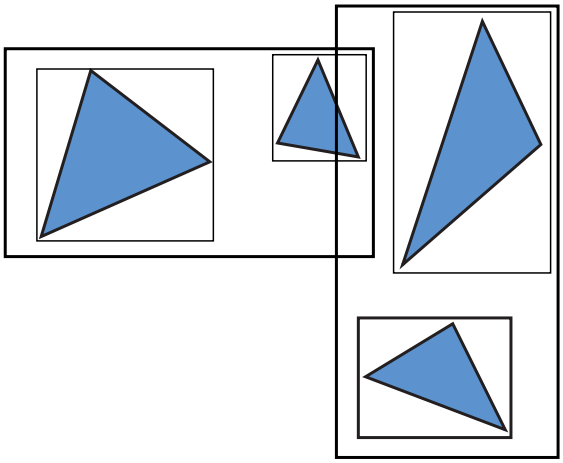

Figure 3.4: Overlapping BVH cells. Since BVH cells no not have to be disjoint regions, they can overlap if the bounding box of a primitive penetrates the bounding box of another cell. If a ray intersects both cells, the ray intersects the overlapping region and the primitives of both cells have to be tested for intersection with the ray.

3.1.5 Other Common Acceleration Data Structures

Another ADS is the *uniform grid*. Uniform grids have the advantage of being simple and can be constructed very fast. However, they are not optimal for non-balanced scenes. This means, if the primitives are not evenly distributed in the scene, which is hardly the case in a general scene, the rendering performance of grids can be relatively slow. This is because in some cells of the grid there are lots of primitives to test against, whereas in other areas there are hardly any primitives in a cell. A typical example is the "teapot in a stadium". In this case it is hard to choose the optimal resolution of the grid. Kalojanov et al. [KBS11a] for example have investigated the use of two-level nested grids of different solutions to remedy this.

The last presented ADS is the *Octree*. An Octree is basically an AABB divided into eight equally sized AABBs, which are then again recursively divided, and so on. Octrees are also fast to construct, however, the tree of arity eight is very wide. For ray tracing, however, deeper hierarchies usually perform better because they more efficiently cut off regions of the scenes which are not relevant for a given ray.

A comparison of the mentioned ADS is given in Figure 3.5.

3.1.6 Divide-and-Conquer Schemes

Recently a new and quite promising approach has emerged. This approach does not need the explicit construction of any acceleration data structure. Usually, all the acceleration structures mentioned before have to be explicitly constructed *before* any ray can traverse it. If the scene geometry changes, due to animations or the like, with a few exceptions, the whole data structure has to be rebuilt first before starting ray traversal to render an image. One exception would be

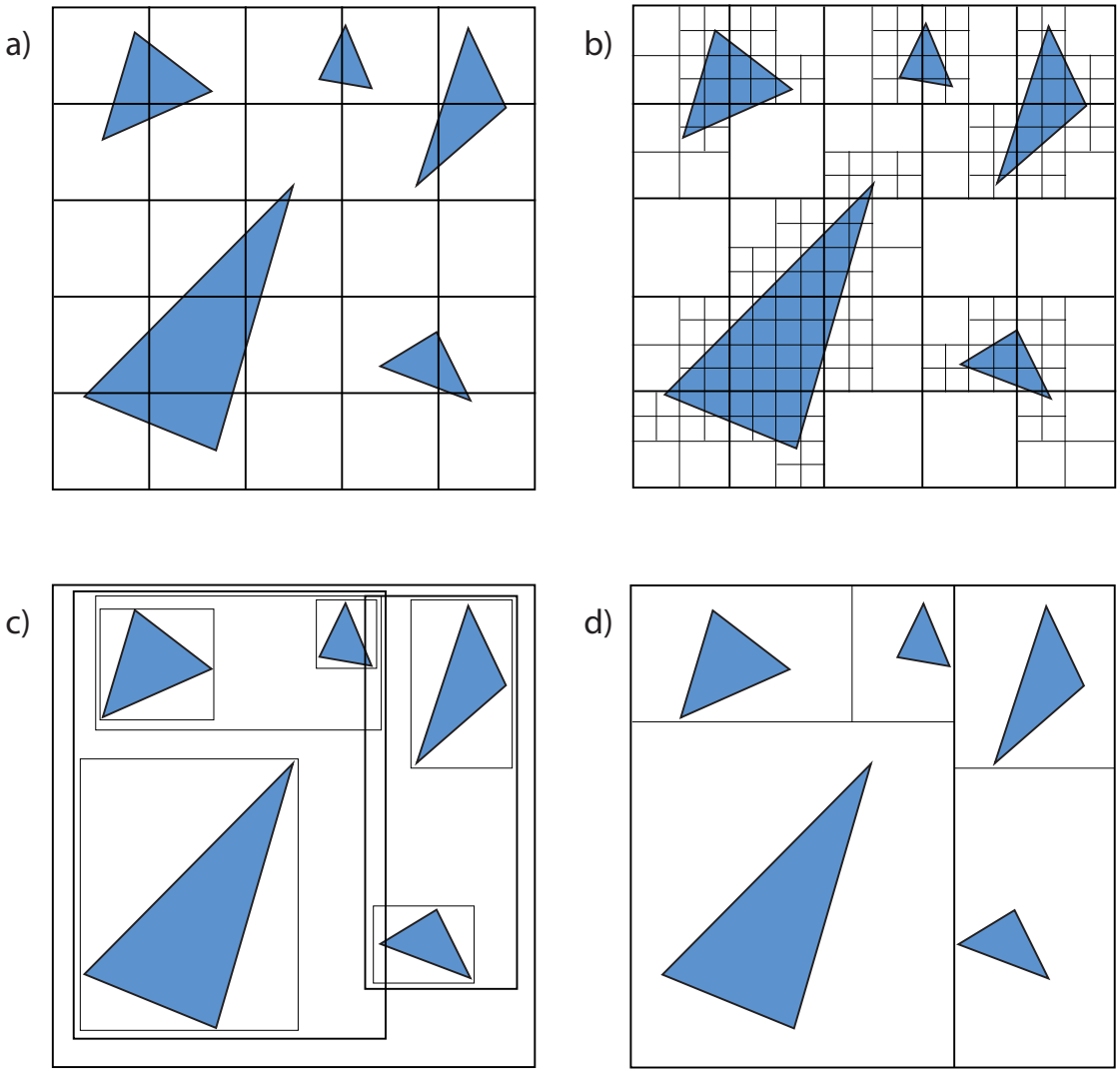

Figure 3.5: Different acceleration data structures: a) Regular grid, b) Octree, c) Bounding Volume Hierarchies and d) kD-Tree.

BVH-refitting, which however usually degrades tree quality over time and hence occasionally needs a complete rebuild.

To remedy rebuilding an ADS, they can be built *on-the-fly*. This differs from the rebuild in the way that the ray traversal can start immediately, and the ADS is constructed while the ray traverses the scene. This way, fully dynamic scenes can be ray traced efficiently. Furthermore, this approach usually takes up far less memory then all other approaches. The on-the-fly constructed ADS can basically be of any type.

The lazy construction of ADS has been already proposed in 1987 by Arvo and Kirk [AK87]. Recently, Mora [Mor11b] investigated divide-and-conquer strategies for kD-Trees and Keller

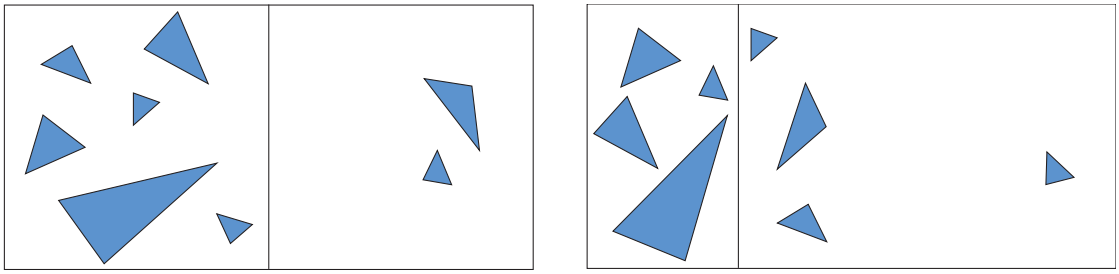

Figure 3.6: Left: Spatial median bad case. The resulting tree hierarchy for the left cell will be much deeper than for the one on the right side. Right: Object median bad case. The cell on the right encapsulates a big area of empty space. This space will be divided further and further, leading to unnecessary traversal steps.

and Wächter [AK11] as well as Áfra [Áfr12] for BVHs. Efficient algorithms and implementations are subject of current and future research.

3.1.7 Splitting Strategies

The quality of some of the ADS, like kD-Trees and BVHs, strongly depends on where the splitting planes have been placed. Several strategies for choosing the splitting positions exist. The most common ones are described below.

Spatial Median

The simplest form, and hence quite often used, is to position the split plane in the geometric middle of the longest axis. However, when the primitives are not evenly distributed in the scene, and in the majority of scenes this will be the case, this does not provide a very good choice for the split, since one subtree of the node will become much deeper than the other one (see Figure 3.6, left).

Object Median

Another easy possibility is to split at the object median. Such a split will result in half of the objects lying on the one and the other half at the other side of the splitting plane. This can however lead to some geometrically unnecessarily big nodes. Consider an object consisting of many primitives in the middle of the scene, and an object with only a few primitives at the very end of the scene. With an object median split, a node would span over primitives of the small object and a few primitives of the complex object, encapsulating the whole empty space in between, which would in turn lead to unnecessary traversal steps (see Figure 3.6, right).

Surface Area Heuristic

Several other strategies for positioning the splitting planes than the ones mentioned above exist. Some of them work with heuristics. One of them has proven to be particularly useful and is used

frequently.

To find good positions for splitting a node is crucial for an ADS to be of good quality. Good quality for an ADS means that its traversal and intersection with a given ray is as efficient as possible in such a way that the parts of the scene which are not pierced by the ray are culled as soon as possible.

The *Surface Area Heuristic* (SAH), introduced by Goldsmith in 1987 [GS87], is a heuristic commonly used to estimate the cost of intersecting an arbitrary ray with an ADS. When constructing an ADS, the resulting hierarchy is considered to be optimal when the cost of the SAH is minimized and hence traversing the structure with a ray is relatively fast. The SAH presumes that the rays are uniformly distributed in the scene, that they do not stop at any primitive and that the ray hits the scene's bounding box at all.

Exact SAH

Assume that a ray hits a node in any ADS and the node can be represented by any bounding box or volume. Given that a ray hits this parent node N_p, the conditional probability P of a ray hitting one of its child-nodes N_c is related to the ratio of their surface areas SA [PGSS06]:

$$P(N_c|N_p) = \frac{SA(N_c)}{SA(N_p)} \tag{3.1}$$

The SAH is then defined as the expected cost of traversing the parent node itself and the cost of intersecting the left and the right child node as shown in Equation 3.2:

$$C = C_t + C_L\, P(N_p|N_l) + C_R\, P(N_p|N_r), \tag{3.2}$$

where C is the cost for a random ray intersecting a node, C_t is the cost for traversing the node itself, C_L and C_R are the costs of traversing the left and right subtrees respectively and N_l and N_r the left and the right nodes.

The cost for the subtrees C_L and C_R can only be calculated when this subtrees are built. For this reason, a *greedy local approximation* is used to evaluate the SAH [ZHWG08]. For this it is assumed that the children are leaf nodes and the cost of intersecting them is replaced by the cost of intersecting a primitive multiplied by the number of primitives in each of them (Equation 3.3).

$$C = C_t + C_i\, n_l\, P(N_p|N_l) + C_i\, n_r\, P(N_p|N_r), \tag{3.3}$$

where C_i is the cost for intersecting a primitive and n_l and n_r are the number of primitives in the left and right child nodes respectively.

When the conditional probabilities in the above equation are expanded, the formula for the *exact SAH* is obtained as given in Equation 3.4.

$$C = C_t + C_i\, \frac{n_l\, SA(N_l) + n_r\, SA(N_r)}{SA(N_p)}. \tag{3.4}$$

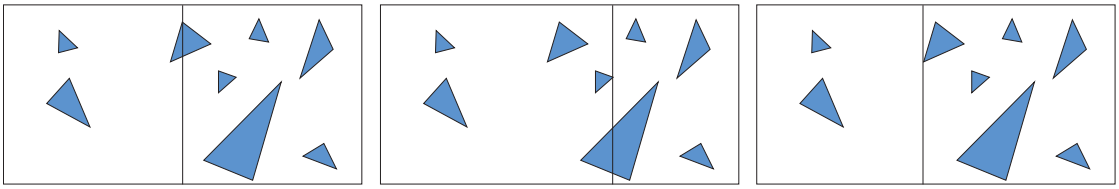

Figure 3.7: Comparison of the splitting strategies (from left to right): Spatial median, object median and split using the SAH.

At some point in the hierarchy construction, the cost for splitting a node will be higher than the cost of adding a leaf node. The cost for creating a leaf node is the cost of intersecting all primitives in it, as shown in Equation 3.5.

$$C_{Leaf} = C_i \, n_p, \tag{3.5}$$

where C_{Leaf} is the cost for making this node a leaf node and n_p is the number of primitives in the node.

To create a hierarchy using SAH, the SAH must be computed for every splitting candidate. For example for kD-Trees, for every possible splitting plane the SAH cost has to be calculated. A common way to calculate the SAH is to use a *sweep builder*. Again, for kD-Trees, the interesting splitting positions are the borders of bounding boxes of the primitives. The sweep builder "sweeps" through all those candidates and calculates a value for each. The one with the minimal cost is considered the optimal splitting plane and the split is performed with it.

A comparison of the resulting splits is shown in Figure 3.7.

Binned SAH

Using a sweep builder can be expensive because usually there are many splitting candidates. Another approach is to use only a fixed number of splitting candidates which are placed on predefined positions, so called *bins*. The SAH is calculated for each of the bins and the one with the minimal cost is selected. The quality of hierarchies created using a binned SAH algorithm is only slightly lower compared to an exact SAH [DPS10].

Binned SAH construction is used frequently for constructing ADS on the GPU, especially for kD-Trees and BVHs. This is because the cost at the bins can be calculated in parallel efficiently. A popular method for calculating the number of primitives left and right of each splitting candidate is *min-max binning* [DPS10, SSK07, PGSS06] (see Figure 3.8). Two arrays L and H are created, both having the length of the number of bins. Each array entry corresponds to a bin and is used as a counter. The entry at position i stores the events occurring between the $(i-1)$-th and the i-th event. In the array L, for every lower bound of a primitive, the counter at the corresponding position is increased. Likewise, in the array H, all the higher bounds are counted. To get the number of primitives left and right to a splitting candidate as well as the ones intersected by the splitting candidate, a suffix sum on L and a prefix sum on H are calculated. Having done that, each entry $(i+1)$ in array L holds the number of primitives right and in array H, entry i holds the number of primitives left of a given splitting candidate. The number of intersected

primitives can be calculated by subtracting the number of primitives left and right from the total number of primitives. With this information, SAH values for each splitting candidate can be calculated.

The resolution of the bins can either be fixed or adaptively chosen for each node, depending on the number of primitives. Furthermore, resampling of a bin can be done. Likewise, the SAH function could also be evaluated first only at each n-th event and then at a finer resolution. Min-max binning can be done efficiently in parallel by using parallel primitives operations like *scan* and *reduction*. A comparison between using a sweep builder and binned SAH and their splitting candidates is given in Figure 3.9.

Empty Space Cutoff

Finally, for large regions of empty space, an empty space cutoff is possible. Usually a threshold for the ratio of empty space to an axis is set. If the ratio for the empty space and the given axis is above the threshold, the split will be placed such that the empty space is encapsulated in a single node.

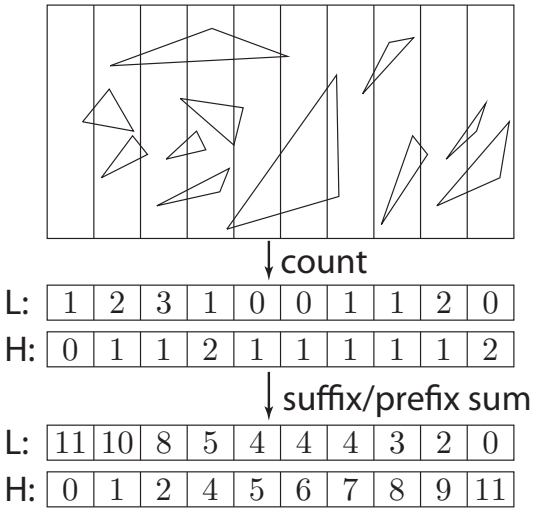

Figure 3.8: Min-max binning example using 10 bins. An array entry at position i stores the events occurring between the $(i-1)$-th and the i-th event. First, the array L counts for each entry the lower bounds of the primitives and the array H all the higher bounds. Then, a suffix sum over L and a prefix sum over H is computed. After that, in L each array entry $(i+1)$ holds the number of primitives completely to the right and in H entry i holds the number of primitives completely to the left. The number of primitives which lie partially on both sides can be computed by subtracting the number of primitives to the left and right from the total number of primitives. (Figure adapted from [DPS10].)

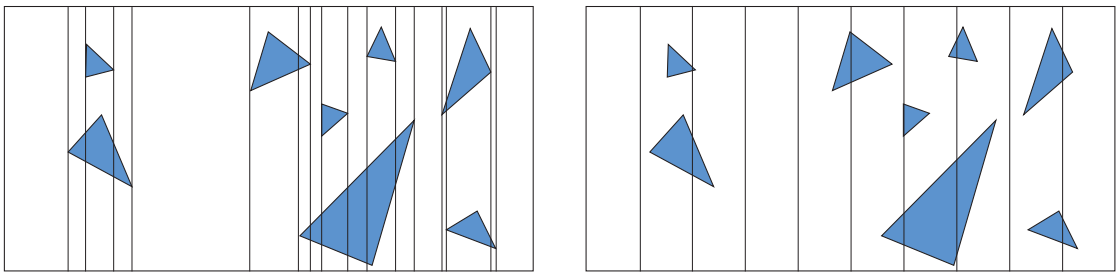

Figure 3.9: Left: SAH splitting candidates using a sweep builder. At each border of a primitive, a splitting candidate is created. Right: SAH splitting candidates using binning with 10 bins. The splitting candidates are created at fixed locations only.

3.2 CUDA

3.2.1 Motivation for General Purpose Programming on Graphics Hardware

Modern graphics cards are fully programmable, highly parallel, massively multithreaded many-core processors with tremendous computational power (Figure 3.10). Many-core processors calculate ("render") the graphics output pixel by pixel in many threads per processor.

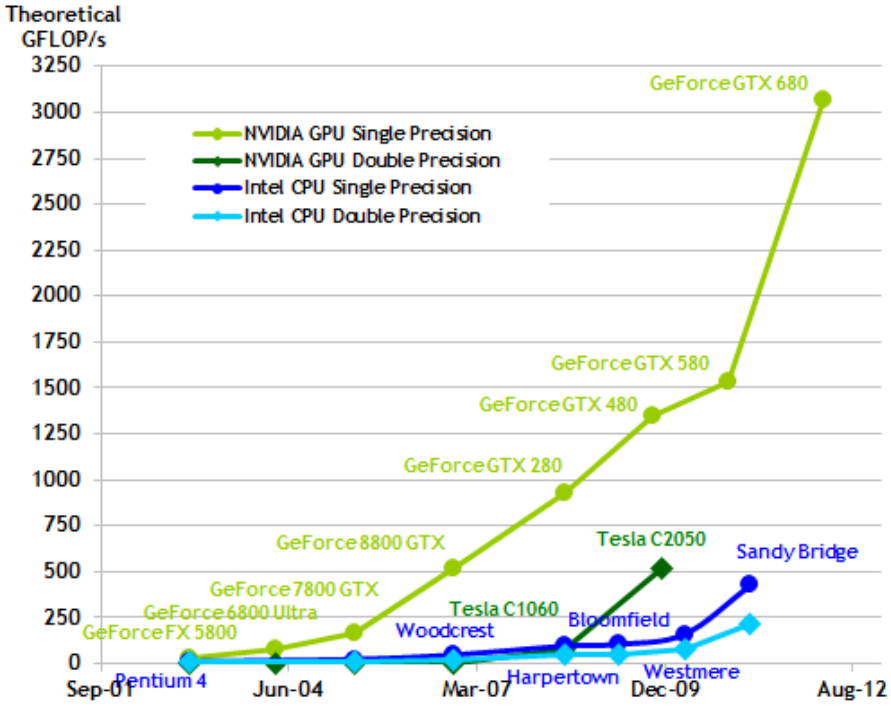

Figure 3.10: Evolution of computational power of GPU and CPU [Cooc].

Early graphics cards implemented the so called *fixed-function pipeline* in hardware. Only specific parameters could be set via a Graphics-API like OpenGL or Microsoft's DirectX. As graphics hardware evolved, parts of this fixed-function pipeline were made programmable through so-called *shaders*. Eventually, the graphics cards consisted of many processors, each of which could work independently. Since graphics cards, or *graphics processing units* (GPUs), have tremendous computational power, Nvidia introduced an API and programming model called *CUDA* (see next Section) to use this computational power not only for graphics, but also for other calculations.

3.2.2 CUDA

CUDA [Cooa] stands for *Compute Unified Device Architecture* and was introduced in 2007 by graphics card vendor Nvidia. CUDA is a general-purpose parallel programming model for graphics cards. CUDA was originally only supported on Nvidia GPUs. However, Nvidia re-

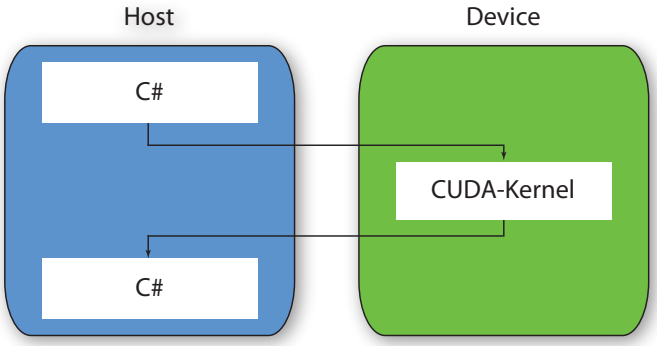

Figure 3.11: The host program first allocates memory on the CUDA device and copies data to the GPU. Then, it starts the CUDA kernel on the device. After the kernel has finished its calculations, the host typically copies back the results from the device to the host.

leased their LLVM-code and now CUDA can be programmed from any language that LLVM supports [Coob]. With CUDA, it is possible to not only render traditional graphics using rasterization with APIs like OpenGL or Microsoft's DirectX, but also to execute basically any other general purpose code on graphics cards.

Programming Model

A CUDA program consists of two different parts. One running on the *host*, which is usually a CPU. The other one is executed on the *device*, typically a CUDA-capable GPU (Figure 3.11). If a graphics card contains two GPUs ("dual GPU cards"), they also contain two CUDA devices. The host program starts the device program, called a *kernel*. The host program also typically allocates memory on the device, copies data to the device, copies back results from the device to the host and frees memory on the device. CUDA host programs are usually written in C or C++, but third party bindings for C#, Fortran or other languages exist as well.

The CUDA programming model for the host consists of two different APIs, the *CUDA C/C++* API, or *runtime* API, and the CUDA *Driver* API. Both APIs can be used to manage the device, the (parallel) execution, the memory management, sharing of resources used by graphics APIs like OpenGL or DirectX, and so on. The CUDA C/C++ API is a higher-level API than the Driver API and allows for more convenient programming, while on the other hand sacrificing flexibility. A program using this API further needs a runtime DLL when executed. The C-styled Driver API, on the contrary, reveals the programmer full access to all features with the price of higher complexity. However, a program written for the Driver API accesses the Nvidia graphics driver's API directly, hence no further DLLs are needed.

The CUDA device programs are the kernels executed on the CUDA device. They are implemented in CUDA device code, which is very similar to traditional C++. As of version 4.x of the CUDA toolchain, programming constructs like class inheritance, namespaces, templates and others are supported.

Compute Capability

The *CUDA Compute Capability* defines the hardware capabilities of a CUDA device. Nvidia introduced CUDA in 2007 with the release of the G80 chip, which was used in the Geforce 8 series of graphics cards. The generation of those cards featured the CUDA compute capability in its first version 1.0. With every revision or release of a new graphics chip, the CUDA compute capabilities were enhanced. Devices of CUDA compute capability equal or greater than 2.0 are able to handle recursive functions. The current generation of graphics cards is the 600 series (Kepler), exposing Compute Capability 3.2.

Execution Model

A CUDA *kernel* (a CUDA device program) is started by the host. To use the full power of the GPU, kernels are executed in parallel, one thread for one instance of a kernel. The CUDA programming model has a three-level hierarchy for arranging the parallel threads (see Figure 3.12). Threads are grouped into *blocks*. All blocks form the *grid*. The layout of the grid, i.e. how the threads are arranged into blocks, is defined by the host program. For easier addressing with two- or three-dimensional problems, blocks and grids can be defined using two (blocks also in three) dimensions.

It is common that each thread accesses a portion of a global chunk of memory and works on that data. For a thread to be able to access its data in the memory chunk, CUDA provides built-in variables for thread-index and block-index as well as thread-dimensions and block-dimensions. Using them, the global *thread-ID* can be calculated. With the thread-ID, for example an offset can be retrieved to access the correct data in memory.

When a kernel is started, the grid is launched. One instance of a CUDA kernel is calculated by one single thread, which itself is part of a thread-block. If viewed from the hardware side, a CUDA device consists of several *streaming multiprocessors* (SM). Each of them can execute several blocks, but each block is executed only on a single SM.

When a grid is launched, every available SM executes a block (see Figure 3.13). Each started thread is executed in parallel. However, the hardware executes threads in bundles called *warps* (see Figure 3.14). A warp consists of 32 threads. Those 32 threads run together in lockstep, which means that every one of those 32 threads has to execute the same hardware instruction. Nvidia calls this *SIMT*, which stands for *Single Instruction, Multiple Threads* (similar to the common term *SIMD*, which stands for *Single Instruction Multiple Data*). The lockstep further implies that if one of the threads of a warp branches, all other threads have to follow that code path even if they would not need to. To efficiently implement programs in CUDA, this issue has to be addressed by designing appropriate parallel algorithms.

Memory Hierarchy

The CUDA architecture consists of multiple memory spaces (Figures 3.15 and 3.16). The biggest memory space is called the *global memory*. It can be accessed by all threads, and each thread can read and write to it. To prevent threads from writing to the same location simultaneously, atomic operations exist. However, access to the global memory is relatively slow.

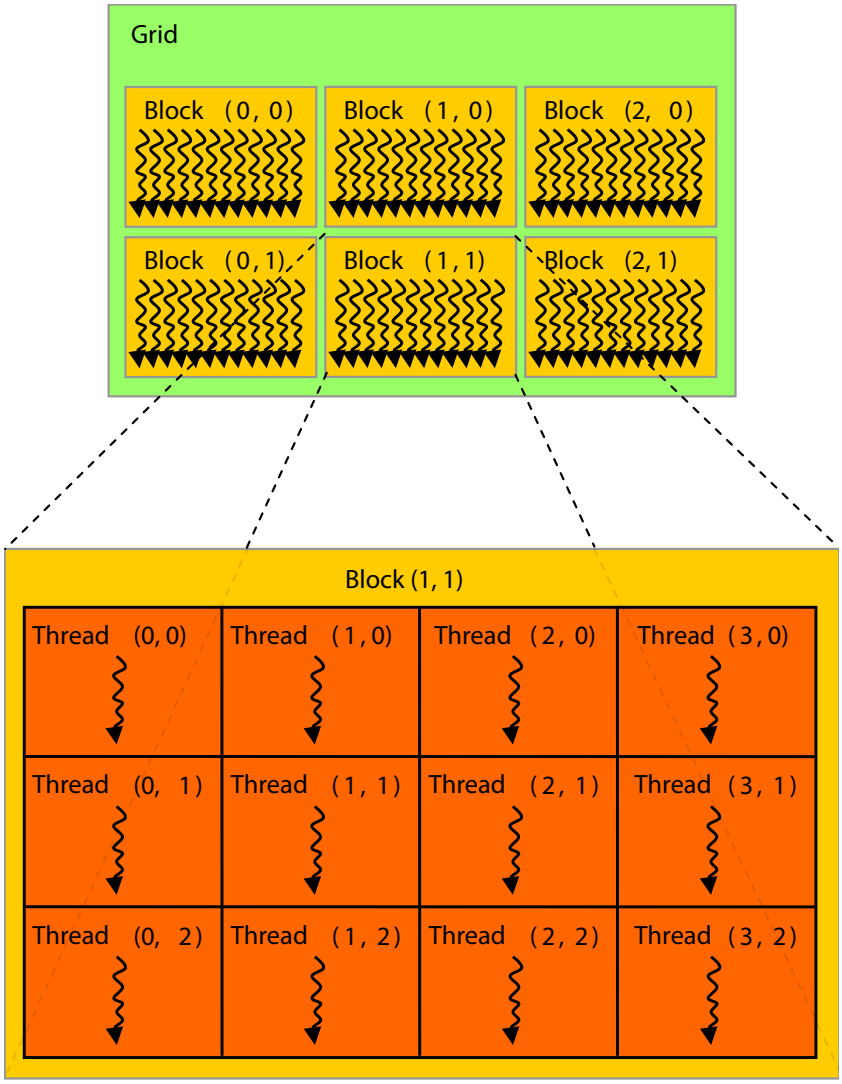

Figure 3.12: CUDA execution model. Parallel threads are grouped into blocks, blocks form the grid. (Figure adapted from [Cooc])

Therefore, access patterns such that data can be efficiently cached should be used. There is also a memory space called *constant memory*, which is "read only" for a thread, but it can be read from faster. However, the constant memory is quite small.

Another memory space is the *local memory*. It is local per thread, and can be read by and written to only by its thread. However, this memory is not located on the chip of the SM, but in the VRAM of the graphics card, where also the global and constant memory reside. Thus, the local memory is usually not significantly faster than the global memory.

In contrast, the *shared memory* is a memory space per block and resides on the chip of the SM. Consequently, the shared memory is very fast to access. Each thread of the same

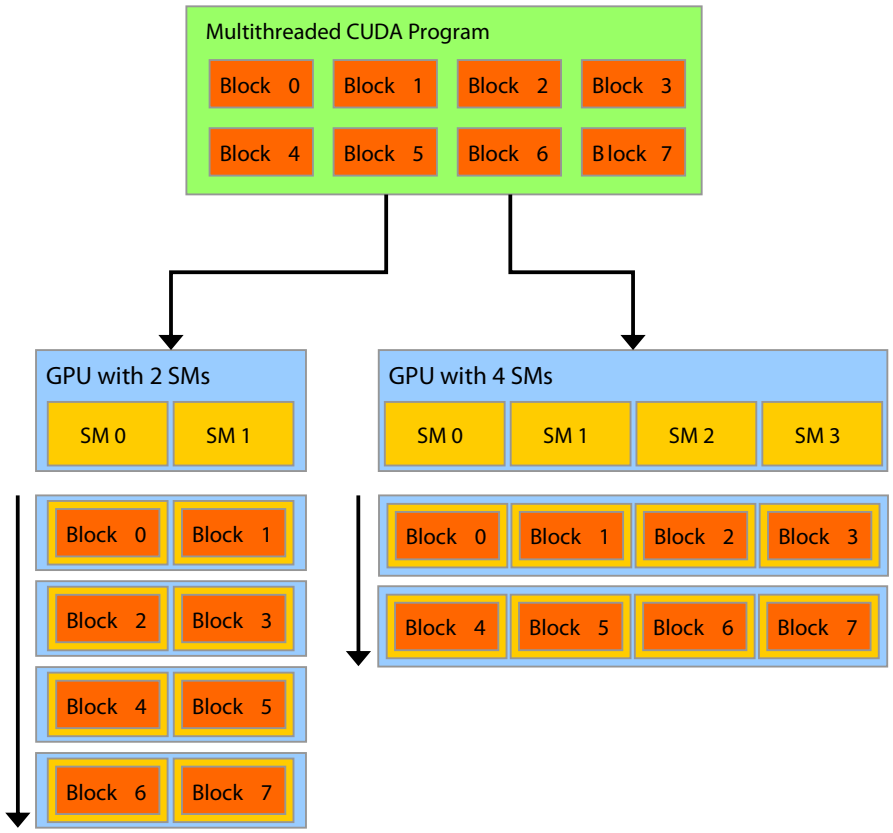

Figure 3.13: CUDA Scalability. A multithreaded CUDA kernel consists of several blocks. A block is executed on a streaming multiprocessor (SM). The GPU starts as many blocks in parallel as SMs are available. (Figure adapted from [Cooc])

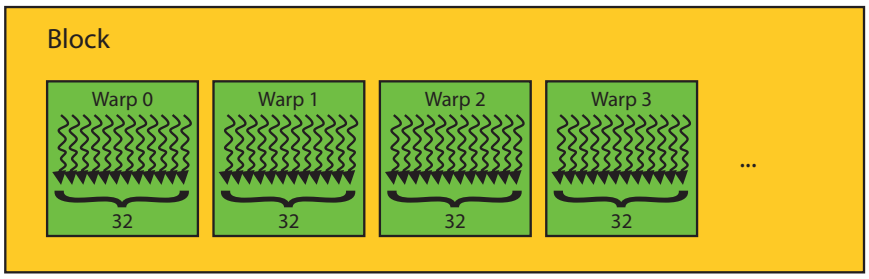

Figure 3.14: CUDA Warps. The GPU executes threads in bundles of 32 threads. Those bundles are called *warps*. Each thread of a warp executes the same instruction. This means, if one of the threads branches, all other threads in this warp need to follow this branch too.

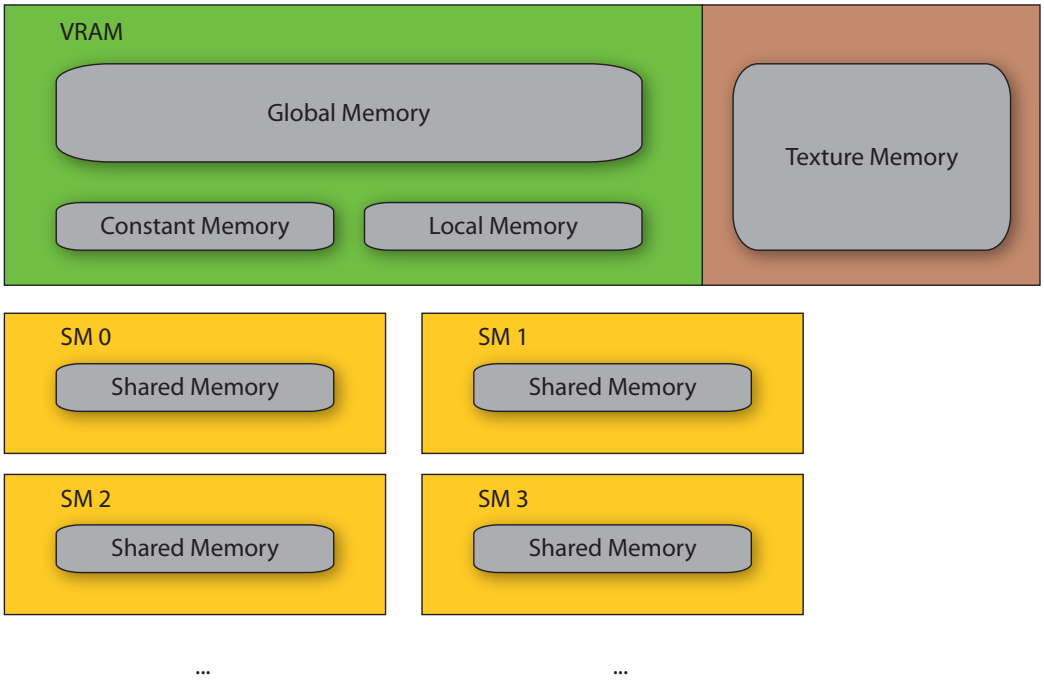

Figure 3.15: CUDA memory hierarchy. The GPU consists of several memory areas. The VRAM holds the global, constant and local memory as well as the texture memory, which has special addressing modes. Each streaming multiprocessor (SM) has an on chip shared memory.

block shares the same memory (hence the name). A thread should use its own portion of the memory. To access a thread's data, an offset needs to be calculated using the built-in thread-index variables. Shared memory is limited to 64KB on current hardware.

A memory space stemming from the graphics processing aspect of graphics cards is the *texture memory*. The texture memory was initially used in computer graphics to store and access diverse image data. It was, however, soon used as a buffer for arbitrary data. Since a pixel in the image data often needed to be sampled or interpolated with nearby pixels, the texture memory has different access patterns and is more suited for random memory access. Data residing in the texture memory can be accessed in constant time, whereas for the other memory areas the access time depends on alignment of the memory access pattern and therefore on the cache efficiency.

When designing an algorithm for CUDA, it is therefore beneficial to consider the diverse memory spaces.

Graphics Resources Sharing

When programming computer graphics applications, data like vertex positions, textures and such, have to be managed. Usually, graphics APIs like OpenGL or DirectX are used. The mentioned *graphics resources* are passed to that API such that the graphics card can use those

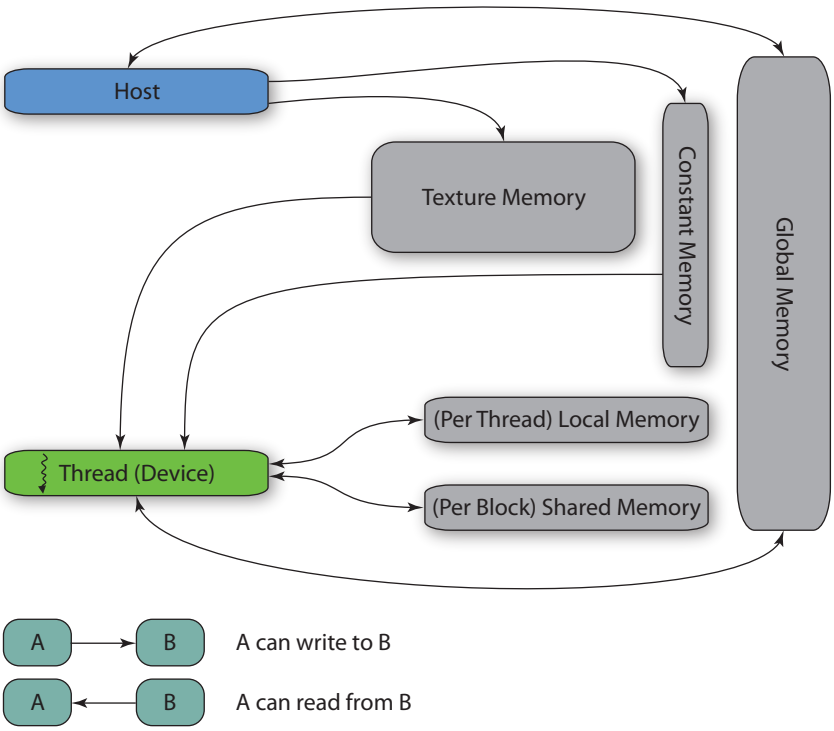

Figure 3.16: Memory access. The host and the threads from the device can read and write from and to different memory locations. The only memory where both can read from and write to is the global memory. Hence, data exchange is usually handled via this memory.

resources to render images. These resources then reside in the memory of the graphics card. When using CUDA in a graphics application, it is often the case that the CUDA kernels need to access the graphics data, e.g. to modify vertex positions for animations. It would be inefficient to copy the data of the graphics resources into CUDA buffers, modify them, and copy the data back to the graphics resources. Therefore, the CUDA API provides possibilities to share the graphics resources of OpenGL or DirectX, read and write to them directly without having to copy the data back and forth. In terms of a CUDA ray tracer this is important, since the CUDA ray tracing kernel can directly write into the frame buffer of the graphics API, which is then directly displayed by the application using the graphics API.

Compilation and Tools

The CUDA device code is programmed in *.*cu*-files. If the CUDA host code is written in C or C++ and the C/C++ API is used, those files must also have this extension. Host and device code can exist together in the same .cu-file. The *Nvidia Cuda Compiler* (nvcc) then compiles the code. The compiler first extracts and compiles the device code and then uses the native C/C++

compiler to compile the host code.

The device code can be compiled to **.cubin* binary files which can be executed immediately. A binary file however is compiled only for a specific graphics chip. So, in order to be able to run the same device code on multiple versions of graphics chips, like on a GeForce 200 and a GeForce 600, two separate binaries would have to be generated and the appropriate one has to be loaded at runtime.

The other way to compile CUDA device code is to compile to *PTX* format. PTX is an assembly-like intermediate language, used by Nvidia's graphics cards. The PTX-files can then be loaded and automatically *just-in-time* (JIT) compiled by the graphics driver for the current graphics chip on which the code needs to be executed on. Since this JIT-compilation can take some time, the JIT-compiled code is temporarily stored by the graphics driver. Only when a new version of the PTX exists, the JIT-compilation is performed again.

For debugging CUDA device code, Nvidia released a debugging tool called Nsight. Nsight is available as a plug-in for Microsoft's Visual Studio and Eclipse. With the help of the plug-in it is possible to debug CUDA device code almost like CPU code, which means setting breakpoints, stepping through code as well as variable inspection. Without Nsight, these debugging features for CUDA device code are not possible and debugging can only be done by looking at the data results calculated by a CUDA kernel. Furthermore, Nsight also provides a profiler so investigate what parts of the code consume the most time or bandwidth.

CUDA and C#

The host languages supported by Nvidia for programming CUDA are C and C++. Both APIs, the runtime and driver API, are C or C++ APIs. To use the features of CUDA in another programming language, one has to gain access to those APIs first. In case of C#, which was used as the host language in this thesis (see Chapter 5), the freely available runtime library called CUDA.NET was used to gain access to the APIs. The CUDA.NET library itself performs unsafe calls to C/C++ methods from the CUDA APIs. More details on accessing CUDA in C# are given in the section on the implementation.

3.2.3 CUDA and OpenCL

OpenCL is an open industry standard which also allows for parallel general-purpose programming on supported devices. Supported devices include diverse CPUs (Intel, AMD and Cell architectures), GPUs (Nvidia, AMD and Intel), as well as ARM-processors for cell-phones. OpenCL offers roughly the same features as CUDA, but is not limited to only Nvidia graphics cards.

However, at the time of the beginning of the implementation for this thesis, OpenCL was in an early state and some limitations existed concerning memory management and efficient sharing of graphics resources. Also, some of the needed SDKs had not been released, or were only in beta-phase. On the contrary, Nvidia provided an online platform with helpful resources for CUDA-programming and announced the debugging tool Nsight. Moreover, Nvidia's CUDA has always been ahead of the OpenCL specification, so it has been possible to use the latest features available on graphics cards. It is most likely that this will continue in the future. Based

on the support for CUDA from Nvidia in terms of online resources and tools as well as of the power and possibilities of the language, it was finally decided to use CUDA for this thesis.

CHAPTER 4

Ray Tracing on the GPU

This chapter first gives an overview of the most important steps towards real-time ray tracing. After that, as a contribution, we present a canonical iterative version of the ray tracing algorithm. It has been derived from several collected publications. Building on that algorithm, furthermore a parallel version is given. Later on, the section on "KD-Trees for GPUs" describes the main methods for implementing and traversing kD-Trees on GPUs. Finally, the last section presents our new data structure, the *Über-kD-Tree*.

4.1 Advent of Real-Time Ray Tracing

One of the very first attempts to make ray tracing work in real-time was done by Muuss [MM95] in 1995 from the U.S. Army Research Laboratory for the development of missile automatic target recognition. He used an array of 8 network computer with 12 CPUs each to render 5 NTCS-frames per second. A few years later, in 1999, Parker et al. [PMS+99] used a supercomputer with up to 64 cores to render ray-traced images with a resolution of 600x800 in real-time. In 2001, Wald et al. [WSBW01] first developed a highly optimized ray tracer for the CPU, which could render images at interactive frame rates. Later the same year, they also released a version for network distributed rendering [WSB01]. Finally, in 2002 Purcell et al. [PBMH02] mapped ray tracing to the back then newly programmable rendering pipeline on GPUs. At that time, the vertex- and the fragment-stage of the former so-called *fixed-function pipeline* became programmable. Purcell et al. implemented a ray tracer using the fragment shader.

Besides research for ray tracing in real-time on CPU and on GPU, some attempts have been made to build custom hardware for ray tracing acceleration. In 2004, Schmittler et al. [SWW+04] presented *SaarCOR*, an FPGA-chip for accelerating dynamic scenes. One year later, Woop and Schmittler [WS05] developed the *RPU*, the "Ray Processing Unit". In 2006, Woop et al. [WMS06] released the *DynRT*-architecture using *B-kD-Trees*, a hybrid data structure of BVHs and kD-Trees. Also, commercial attempts have been made for custom hardware, like the *CausticOne* by Caustic Graphics, Inc. [CG] in 2010.

During the last decade, however, graphics cards have reached a high level of computational power, and researchers have tried to utilize this power as it became available. One of the first attempts to ray tracing on the GPU using kD-Trees was made by Foley in 2005 [FS05]. They presented two new traversal methods for traversing kD-Trees on the GPU, the *kd-restart* (Section 4.4.2) and the *kd-backtrack* algorithms (Section 4.4.3). The two algorithms do not need a stack, which was back then very expensive to use on the GPU.

Acceleration data structures are crucial for fast ray tracing. Therefore, Popov et al. [PGSS06] as well as Wald and Havran [WH06] investigated methods on how to build good quality kD-Trees and how to build them fast. In the same year, Woop et al. [WMS06] presented the *B-kD-Tree* (*bounded* kD-Tree). The B-kD-Tree stores two splitting planes for each node, instead of one, like for normal kD-Trees. Wächter and Keller [WK06] developed the *Bounding Interval Hierarchy* (BIH). The BIH is basically a kD-Tree with object partitioning. For each level, it stores also two splitting planes. They furthermore use a new global heuristic for setting the locations of the splitting planes.

In 2007, Popov et al. [SPS07] released an improved version of the kD-restart algorithm which uses ropes (Section 3.1.3) and packet traversal (Section 2.3.2). At the same time, Horn et al. [HSHH07] improved the kd-restart algorithm by adding a *short stack* (Section 4.4.4). Also in 2007, Shevtsov et al. [SSK07] presented an interactive ray-tracing algorithm for the CPU. They also used kD-Trees and the algorithm scales linearly to available CPUs.

Zhou et al. [ZHWG08] presented a real-time ray tracer in 2008. It runs completely on the GPU and rebuilds the kD-Tree every frame, which allows arbitrary animations. In the same year, Bikker presented his Arauna CPU real-time ray tracer [Bik11]. It is written in highly optimized C/C++ code and uses different BVHs for static and dynamic parts of the scene.

Up until 2009, the main bottle-neck for GPU ray tracing programs where thought to be the limited memory bandwidth. However, Ailia and Laine from Nvidia showed in 2009 [AL09] that the main limiting factor, before memory bandwidth takes any effect, is the under-utilization of the GPU and the performance penalty for branching code. They released a follow-up paper in 2012 for current Nvidia graphics cards [ALK12]. In 2009, Stich et al. [SFD09] presented the *SBVH*, the spatial-split BVH. In this data structure, they allow that also spatial splits can be made when constructing the BVH in addition to the conventional object partitioning. Thus, costly overlapping of cells can be reduced. Popov et al. [PGDS09] presented a similar work, where they investigate different possibilities for spatial splits for BVHs.

In 2010, Pantaleoni and Luebke, also from Nvidia, presented their HLBVH algorithm [PL10], which allows real-time ray tracing of fully dynamical scenes by constructing the BVH from scratch every frame. The HLBVH is a BVH which uses the Z-Morton curve [Mor66] to sort and cluster the primitives in a scene, and then emits the hierarchy based on this sorted order. In the same year, Danilewski et al. [DPS10] presented their real-time ray tracer for fully dynamic scenes using kD-Trees which are rebuilt every frame. They used a binned SAH kD-Tree builder and implemented several so-called *stages* to fully utilize the computational power of the GPU for processing different tree-levels. Also in 2010, Nvidia introduced OptiX [PBD+10]. OptiX is a programmable ray-tracing system which allows developers to develop their own real-time ray tracing application. Currently OptiX uses HLBVH internally.

In 2011, Garanzha et al. [GPM11] improved the HLBVH algorithm by using work queues

instead of the *compress-sort-decompress scheme* [GL10] used in the original algorithm. Besides the dominance of kD-Trees and BVHs on current real-time ray-tracing research, Kalojanov et al. [KBS11b] showed that using a two-level uniform grid can be especially useful for dynamic scenes, where fast rebuilding of the data structure for each frame is important. Moreover, Wu et al. [WZL11] showed how to build kD-Trees using SAH entirely on the GPU.

Also in 2011, a new category of ray-tracing algorithms has been introduced, the so-called *divide-and-conquer ray tracing* (DACRT) (Section 3.1.6). DACRT does not need an explicitly stored acceleration data structure like a BVH or kD-Tree, but subdivides the scene on-the-fly when tracing rays. Mora's DACRT algorithm [Mor11b] is a CPU implementation and uses a kD-Tree-like spatial subdivision scheme which he called axis-aligned spatial subdivision (AASS). He also introduced the direct-trace library [Mor11a], which is a ray-tracing library which uses DACRT. It supports CPUs as well as GPU acceleration. Recently, Keller and Wächter [AK11] and Áfra [Áfr12] presented DACRT algorithms using a BVH-like approach instead of the AASS.

Our implementation of the traversal of the kD-Tree is similar to the method used in Zhou et al. [ZHWG08]. It is a stack-based traversal with a stack per ray. This type of traversal is described in Section 4.4.1. As far as kD-Tree construction is concerned, we use the construction algorithm on the CPU which was already implemented in Aardvark and convert the resulting kD-Trees to a format suitable for the GPU.

In the following, the adaption of the basic ray tracing algorithm, introduced in Section 2.3, for efficient implementation on the GPU will be described as well as variants of kD-Trees for GPUs.

4.2 Iterative Ray Tracing

On GPUs, recursion was not supported until recently and still, recursion is inefficient on GPUs. Therefore, we present a canonical iterative ray-tracing algorithm that we derived from various information collected from a number of publications. The iterative algorithm of the basic ray tracing algorithm (Algorithm 1) is shown in Algorithm 3. Note that only the $Trace()$-function changes, as it is now implemented iteratively. All the other functions remain the same as in Algorithm 1.

The iterative version has to make use of a stack to store the rays to be traced. With the given pseudo-code in Algorithm 3, the ray tree (c.f. Section 2.3.2) is traversed in a depth-first, left-first manner. If the tracing of reflection rays is done, the refraction rays are traced. If they again create new reflection rays, they are first traced again until the stack of rays is empty.

4.3 Parallel Ray Tracing

The parallel version of the basic ray tracing algorithm is the same as Algorithm 1, with the exception that the $for\ each$-loop in line 2 in the $DoRayTracing()$-method is executed in parallel. Since the calculations for a pixel are independent of other pixels, as many pixels as possible can be calculated in parallel. Therefore, an own thread is started for each pixel and its primary ray. The primary ray and its secondary rays are traced independently of the other pixels. When all

Algorithm 3 Iterative $Trace()$-function

```
1:  function TRACE(primRay)
2:      color ← black
3:      ray ← primRay
4:      refraction stack ← new ray stack          → stack for refraction rays
5:      depth stack ← new int stack               → stack for storing recursion level
6:      tree depth ← 0
7:      continueLoop ← true
8:
9:      while continueLoop do
10:         hit ← INTERSECT(ray, scene)
11:
12:         if hit then
13:             color += SHADE(ray, hitPoint)
14:             tree depth ← tree depth + 1
15:             if Material is reflective and tree depth <= maximum tree depth then
16:                 if Material is transparent and not total internal reflection then
17:                     refraction stack.PUSH() ← RAY(hitPoint, refracted(ray.direction))
18:                     depth stack.PUSH() ← tree depth
19:                 end if
20:                 ray ← RAY(hitPoint, reflected(ray.direction))
21:             else          → Diffuse Material
22:                 continueLoop ← false
23:             end if
24:         else          → no hit
25:             color += BackgroundColor
26:             continueLoop ← false
27:         end if
28:
29:         if not continueLoop and stacks not empty then
30:             ray ← refraction stack.POP()
31:             tree depth ← depth stack.POP()
32:             continueLoop ← true
33:         end if
34:     end while
35:     return color
36: end function
```

calculations for a pixel have been done, the calculations for the next pixel which has not yet been calculated can be started.

On CPUs, multiple threads can be used to parallelize the algorithm, and SIMD and packet traversal (Section 2.3.2) can be used as optimizations to gain performance. On GPUs, several hundreds of threads are started in parallel. The limits of parallel execution are determined by the warps and block sizes.

4.4 KD-Trees for GPUs

4.4.1 Stack-based Iterative Traversal

On GPUs, recursive traversal is nowadays possible in principle, however it is comparably slow. Therefore, an iterative traversal is favored. In this case, one way for traversing a kD-Tree is to maintain a stack.

Algorithm 4 shows the iterative version of the $IntersectNode()$ function. All other functions remain the same as in Algorithm 2. The main loop is the outer while-loop. It can only be broken when a leaf found an intersection or if the traversal did not find any intersection at all, meaning that all paths have already been traversed, i.e., that the stack is empty. This is similar to the recursive variant, when there are no more recursive calls left. The while-loop for the leaf is necessary because if a node is popped from the stack, the new node can be a leaf again. When traversing an inner node, there are still the three following cases. The ray can be on the left or right side of the splitting plane, or crossing it. In the former two cases, just the new node is set and the loop is continued. Only when the ray crosses the splitting plane, the node further away is pushed onto the stack and the traversal continues with the nearer one. Since the nodes are pushed on the stack and are later possibly retrieved again, this leads to the same traversal steps as with the recursive variant.

Maintaining a stack for each ray on the GPU was inefficient on graphics cards before the release of Nvidia's Fermi-architecture in 2010. With Fermi, a conventional cache hierarchy for memory access was introduced [Coo10]. Furthermore, there had been an overall speedup, such that the implementation of stacks became feasible. Therefore, prior to this architecture, traversal methods have been invented which did not need a stack. They will be described in the next sections.

4.4.2 KD-Restart

In 2005, Foley and Sugerman [FS05] released the first two algorithms for traversing a kD-Tree on graphics cards. Back then, recursion was not supported on graphics hardware at all, and using a stack for traversing a kD-Tree on the GPU was inefficient. Therefore, they developed two stackless traversal methods.

The first one is the *kD-Restart* algorithm. Instead of maintaining a stack for a ray, they only keep its values for t_{min} and t_{max}, the minimum and maximum t-values for the ray (see Figure 4.1 left). Then, when a leaf is tested for intersection with the ray but the ray does not hit any primitive in it, the traversal with this ray is *restarted* from the root with new values for t_{min} and t_{max}. The new t_{min} is set to the former t_{max} and the new t_{max} is set to the border of

Algorithm 4 Iterative $IntersectNode()$-function maintaining a stack

```
1:  function INTERSECTNODE(node, ray)
2:      stack ← new stack
3:      while true do
4:          while node is leaf do
5:              foundHit ← INTERSECTLEAF(node, ray)
6:              if foundHit then return foundHit
7:              else
8:                  if stack not empty then node ← stack.POP()
9:                  else return no intersection
10:                 end if
11:             end if
12:         end while
13:
14:         if ray on left of node's splitting plane then
15:             node ← node.ChildLeft
16:         end if
17:         if ray on right of node's splitting plane then
18:             node ← node.ChildRight
19:         end if
20:         if ray crosses node's splitting plane then
21:             if node.ChildLeft is nearer than node.ChildRight then
22:                 stack.PUSH() ← node.ChildRight
23:                 node ← node.ChildLeft
24:             else
25:                 stack.PUSH() ← node.ChildLeft
26:                 node ← node.ChildRight
27:             end if
28:         end if
29:     end while
30: end function
```

the scene. This way, the traversal will take its path to the nodes that would usually have to be pushed on the stack. However, due to the re-traversal of the data structure, kD-restart leads to redundant traversal steps.

Popov et al. [SPS07] presented an improved version of the kD-restart algorithm by adding *ropes* to the leafs of the kD-Tree. These ropes are links to the neighboring cells of the leaf (see Section 3.1.3). When intersecting a leaf does not result in an intersection, the rope to the neighbor cell is followed and the leaf cell or cells pointed to are tested. This way, the redundant traversals are eliminated, but at the cost of higher memory usage for the ropes. Popov et al. further used packet traversal (Section 2.3.2) to exploit ray coherence.

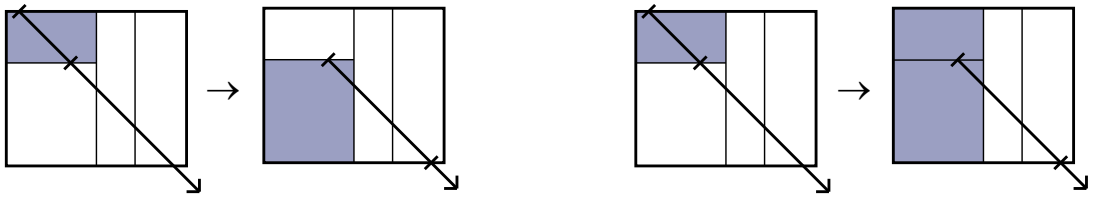

Figure 4.1: Left: KD-Restart. When the ray traversal unsuccessfully tested a leaf for intersection, the ray traversal is restarted from the root with new values for t_{min} and t_{max}. Right: KD-Backtrack. When the ray traversal unsuccessfully tested a leaf for intersection, a "backtrack" traversal is started, until the node is found which would have been pushed on a stack, and traversal continues from there. (Figures adapted from [FS05].)

4.4.3 KD-Backtrack

The second stackless kD-Tree traversal presented by Foley in 2005 [FS05] is the *kD-backtrack* algorithm. They already noticed that the kD-restart algorithm needs lots of redundant traversal steps. To remedy this, they added a parent link to each node. This way, when a leaf is tested for intersection with a ray but the ray does not hit any primitive in it, the traversal is "back tracked". This means that they look for the lowest parent node in the leaf's ancestors which intersects the appropriate t_{min} and t_{max} values (Figure 4.1, right). When this node is found, the normal "down traversal" continues from this ancestor node. As in the improved kD-restart version by Popov et al. [SPS07], the kD-backtrack needs more memory because the parent links as well as the bounding boxes for each node have to be stored.

4.4.4 Short-Stack and Push-Down

Another stackless algorithm was published by Horn et al. in 2007 [HSHH07]. They also built their algorithm on kD-restart, but added a short, fixed-sized stack where nodes can be pushed and popped as usual. Whenever a stack underflow occurs, the algorithm reverts to the standard behavior of the kD-restart algorithm. In case of an overflow, the deepest node in the stack is discarded.

They also added *push down*. In the kD-restart algorithm, the traversal of the data structure is restarted always at the root. Horn et al. observed that they could push the entry node for the restart down the tree hierarchy, as long as the ray does not cross the splitting plane. Hence, they save unnecessary traversal steps when restarting the traversal.

Horn et al. already observed in their implementation the main limiting factors for ray tracing on the GPU: the parallel workload is not distributed equally, the memory latency and last but not least, the penalty payed for divergent code.

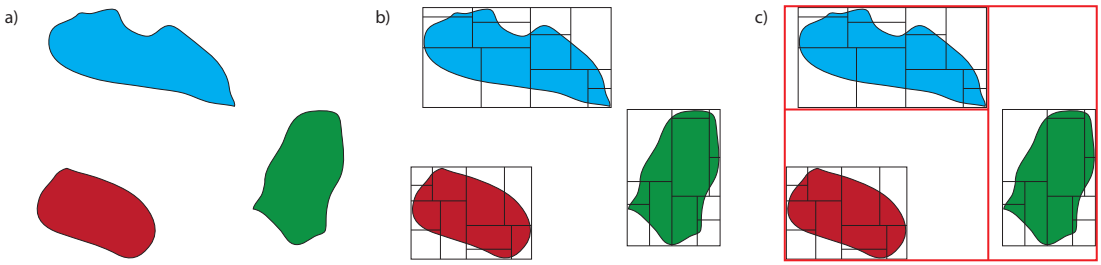

Figure 4.2: Über-kD-Tree. a) Some objects in the scene. b) Objects with their Object-kD-Trees. c) The Über-kD-Tree (red) is a kD-Tree over the Object-kD-Trees.

4.5 Über-kD-Tree

In this thesis, we developed a new data structure which we call the *Über-kD-Tree*. It is a kD-Tree which consists of kD-Trees in its leaves. The kD-Trees for the leaves are kD-Trees per geometrical object and we call them *Object-kD-Trees*. Figure 4.2 shows the idea of the Über-kD-Tree.

The main reason why we wanted to do implement such a data structure is to interactively add and delete objects to the scene without having to deal with major data structure rebuilds. This way, only the Über-kD-Tree needs to be rebuilt, which can be done quite fast. Furthermore, when there are only a few objects in a scene, a list of those Object-kD-Trees is sufficiently fast. However, for lots of objects, having a kD-Tree over the Object-kD-Trees to cull objects can be beneficial. Shevtsov et al. [SSK07] mentioned that they experimented with two-level kD-Trees and reported a speedup when using this data structure with four or more non-overlapping objects.

To traverse the Über-kD-Tree, first the Über-kD-Tree is traversed. If a ray hits a leaf which contains an Object-kD-Tree, this Object-kD-Tree is traversed to find an intersection of the ray with the geometry.

Both, the Object-kD-Tree and the Über-kD-Tree are implemented in the CUDA ray tracer for this thesis (see Chapter 6 and Section 6.4). Results using the Über-kD-Tree will be presented in Section 7.3.

CHAPTER 5

CUDA Library

This chapter takes a closer look at the CUDA library which has been developed for the VRVis-internal rendering engine Aardvark. First, the host side, including context and memory management as well as data-types, is presented. Later on, an overview of the device side of the library is given.

5.1 Overview

CUDA is by default only accessible from C or C++ (see Section 3.2.2). To access CUDA functionality from within C#, the function-calls to the CUDA-APIs have to be wrapped. Since the CUDA-API is already very large, this would be a lot of work to do manually. Fortunately, there is a library for C# called CUDA.NET [GAS] which is freely available. CUDA.NET wraps the function calls of the CUDA-API 3.0 in both versions, the runtime API and the driver API. However, the CUDA-API and hence the wrapped functions are very low-level. To make working with CUDA convenient in terms of object orientedness, it is useful to implement a higher-level library on top of the low-level API. Besides that, as mentioned above, the CUDA.NET library in its current version wraps the CUDA-API version 3.0. The CUDA-API version current during the main programming tasks for the thesis was 4.2. Since the API partially changed, some of those new API functions were wrapped manually to access new functionality.

After several iterations, the final implementation of the CUDA library *CUDALib* supports built-in data types, ready to use within Aardvark and C#, as well as semi-automatic memory-management for the GPU.

The CUDALib is separated in two parts, the host side and the device side (Figure 5.1). The host side part contains the management code for CUDA, hence, the C# code. The part of the device side contains CUDA device code which can be used from within any CUDA kernel. Also, the ray tracer described in Chapter 6 is now part of the library, such that the ray tracer can be used from within any Aardvark application.

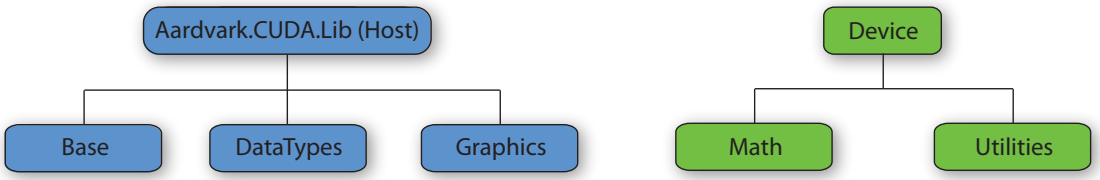

Figure 5.1: The CUDALib host and device parts. The host part has its root-namespace in *Aardvark.CUDA.Lib* with sub-namespaces: *Base*, which includes all the main-functionality like CUDA-Context, -Device, -Module and -Function management, as well as device memory management, namespace *DataTypes*, which provides read-to-use data structures for working with CUDA, and finally the namespace *Graphics*, which provides data types for graphics resource sharing. The device part has no particular namespace, but is logically subdivided into *Math*, which includes vector-, color- and matrix-classes, and some utility-functions bundled in *Utilities*.

5.2 Host Side

The host side is the main part of the CUDA library. It provides a high-level abstraction of the CUDA-API in C#. The library is integrated tightly into Aardvark and can be used from any of Aardvark's research-projects to gain access to the GPU-computing power of graphics cards.

5.2.1 Management

Context Creation

On the host side, the main object is the *CudaContext* (Figure 5.2), which encapsulates the CUDA context in a very convenient way. When a new *CudaContext* is created, it first selects the CUDA-device automatically if no preferred device is specified. Then the CUDA-context is created on this device with the given flags, like graphics resource sharing or others. Also, a new memory manager is created, which will be described below.

When context creation is done, one or more CUDA-modules, which are the PTX-files, can be loaded. Modules can also be created by run-time compiling CUDA source-code, which can be passed as a simple C#-string to the *CUDA-runtime compiler*. This CUDA-runtime compiler was developed in collaboration with Georg Haaser at the VRVis Research Center and is an encapsulation of the Nvidia CUDA-compiler *nvcc*. It translates our custom defined compiler-switches to actual ones for nvcc and then calls it with the translated commands. This way we can compile CUDA-code during the runtime of a C#-program. The advantage is that the CUDA-device code can be customized to specific needs of the currently running environment.

After the CUDA-modules are loaded, the functions, i.e. the CUDA-kernels, can be loaded from the modules. The layout of the grid, which arranges the threads into blocks, is done per function. In the current implementation, one CUDA-context per CUDA-device is supported. Since a CUDA-context can be shared among CPU-threads, more than one CUDA-context is

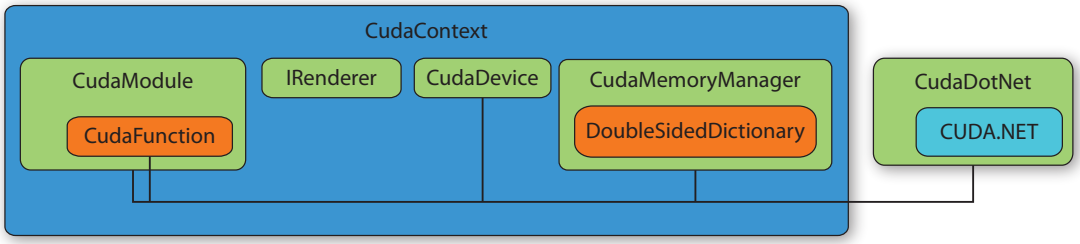

Figure 5.2: The *CudaContext* is the central part of the CUDALib. It contains and manages the *CudaDevice*, the loaded *CudaModules*, the *CudaMemoryManager* for managing device-memory and, if sharing of graphics resources is needed, also a concrete Aardvark-Renderer.

not necessary. However, if a system has more than one CUDA-capable device, the support of multiple devices is important and therefore supported by the library.

Memory Management

The CUDALib furthermore has its own GPU memory manager, the *CudaMemoryManager*. The memory manager maintains a mapping from C#-(CPU-)objects to GPU-"objects". It does this by storing the references from C#-objects to the actual memory addresses on the GPU. To maintain this mapping, a $DoubleSidedDictionary\langle S, D\rangle$ has been implemented. It is a dictionary which can look up two values $\langle S, D\rangle$ (*source* and *destination*, respectively) fast by storing them as key-value-pairs in two normal C#-dictionaries, but one time with $\langle S, D\rangle$ as key-value-pair and one time reversed as $\langle D, S\rangle$.

For the memory manager, the double-dictionary is created as $DoubleSidedDictionary\langle IntPtr, object\rangle$. The $IntPtr$ are the pointers to the GPU memory location, thus, the address of an object in GPU-memory. The $object$ is the reference to a normal C#-object.

When a new C#-object is added to the memory manager, the C#-object reference is added to the dictionary. One can register the C#-object in the memory manager first without copying it to the GPU, and copy it to the GPU later. In this case, a "virtual" pointer for the GPU-address is created, which is replaced by the actual one later. To copy a C#-object to the GPU, it is first pinned so that its address can be taken. *Pinning* in C#-terms means, that an object is fixed to its current memory location and the .NET-runtime can not move it as long as it is pinned. The object is then copied to the GPU and the returned memory address is stored as an $IntPtr$ together with the reference to the C#-object in the dictionary. Finally, the C#-object does not need to stay pinned anymore and is unpinned again. When an object is copied back from the GPU, the GPU-memory location is looked-up in the dictionary and the corresponding data is downloaded from the GPU.

When it comes to a scene hierarchy with lots of geometric objects which may share textures or material properties, the same C#-object could be registered several times. To prevent loading the same object to the GPU more than once, the memory manager implements a reference counting approach. Therefore, when an object is added to the memory manager, it first checks if the object has been registered already with this memory manager. If so, only a reference-count

to this object in the memory manager is increased and the current GPU-handle is returned. If the object is not already registered with the manager, it is added. Likewise, the reference count is decreased when a C#-object is unregistered from the manager. If the reference count becomes zero, the memory for the object on the GPU is freed. An example using the memory manager is shown in Listing 5.1.

In C#, besides arrays, structs provide the correct data-layout for working with CUDA. However, they are value types in C# and therefore no pointer to them can be maintained. After several attempts we came up with an elegant solution. To prevent writing a wrapper-class for each struct, any struct was encapsulated into an array of length 1. This way, the memory manager could also keep track of the mapping between C#-structs and their CUDA-representation. This is, however, not an integrated feature of the library itself, but rather a direction on how to use structs with the library, such that data changes in structs are visible for the memory manager. An example is shown in Listing 5.2.

The memory manager provides a convenient way to manage memory on the GPU. CPU-objects are registered first, can then be loaded to the GPU automatically or manually, updated if necessary and unregistered if not needed anymore. Currently the library supports only C#-structs and arrays of such to be managed by the memory manager due to the memory-layout of structs in C#. Support for classes could optionally be implemented.

Kernel Launch

Besides the memory management, one of the most convenient features of the library is that CUDA-kernels can be launched as easy as normal C#-functions. Kernel launches with the use of our library are simply of the form $myKernel.Call(...myParameterList...)$ (see Listing 5.1). $Call()$ is a C#-function with a variable parameter list. The passed parameters are checked by the memory manager if one of them is registered in it. If so, the stored GPU-address is passed as parameter to the kernel. Otherwise, the data is copied to the GPU. The passed parameters are furthermore automatically correctly aligned.

Without this convenient kernel-call, the parameters would have to be mapped manually, the actual program code would get much longer and therefore prone to errors.

Other Features

The library also supports other important CUDA-features. The CUDALib is implemented in such a way that it completely supports CUDA-streams. Modern CUDA-capable GPUs can run different CUDA-kernels in parallel, as well as executing CPU↔GPU memory transfer for one kernel in background when the GPU is concurrently executing another kernel. Per default, all kernels and memory transfers belong to stream 0. When using different streams for different kernels and their associated memory transfers, those kernels can be executed either interleaved or in parallel, and their memory transfers can be hidden by running in the background.

Furthermore, CUDA exposes a timer to measure the runtime of GPU operations. This timer works a little different than conventional CPU timers. The CUDA-timer works with *events*. To use the timer, a start event is created and inserted into the GPU-instructions. When then the event is passed, or "executed", the current time is recorded. Similarly, a stop event is created

```
var cudaContext = CudaContext.Create();
var cudaModule = cudaContext.LoadModule("myCUDAModule");
var cudaKernel = cudaModule.LoadFunction("myCUDAFunction");

// retrieve the memory manager
var cmm = CudaContext.CudaMemoryManager;

// create some C#-object. Let's create an array of floats:
var myObj = new float[] { 0.0f, 1.7f, 3.0f };

// register the object in the memory manager
cmm.Register(myObj);

// copy myObj-data to GPU
cmm.ToDevice(myObj);

// do something, like starting a CUDA-kernel:
// set grid-layout first
// (needs to be done only once per kernel)
cudaKernel.SetKernelLaunchLayout(myKernelLayout);

// then launch kernel
cudaKernel.Call(myObj /* ...other kernel parameters... */);

// after kernel has finished,
// copy myObj-data back from GPU
myObj = cmm.FromDevice<float[]>(myObj);

// unregister from memory manager if myObj not needed anymore
cmm.Unregister(myObj);
```

Listing 5.1: CUDALib example memory manager and kernel launch. First, a CUDA-context is created and a module including a function is loaded. After that, a reference to the *CudaMemoryManager* is retrieved. Then some C#-object is created and is registered in the memory manager. When copying the data to the GPU, the "virtual" pointer created by default in the memory manager is replaced by the actual one. Next, the kernel launch layout ist set and the CUDA-kernel is called. Finally, when the kernel has finished, the data is copied back and, if the data is not needed anymore, unregistered from the memory manager. If there are no more references to *myObj*, its data on the GPU is deleted and the corresponding memory freed.

```
// define some C#-struct for demonstration
struct MyStruct
{
    public int a;
    public int b;
}

// create a struct and fill it with data
var str = new MyStruct();
str.a = 17;
str.b = 29;

// create an array of length 1 which contains the struct
var structArray = new MyStruct[1] { str };

// create CUDA-context, load module and function
var cudaContext = CudaContext.Create();
var cudaModule = cudaContext.LoadModule("myCUDAModule");
var cudaKernel = cudaModule.LoadFunction("myCUDAFunction");

// retrieve the memory manager
var cmm = CudaContext.CudaMemoryManager;

// register the object in the memory manager
cmm.Register(structArray);

// change some data in the struct
structArray[0].a = 333;

// copy the data to GPU. The changed value for
// structArray[0].a will be visible on the GPU!
cmm.ToDevice(structArray);

// set grid-layout
cudaKernel.SetKernelLaunchLayout(myKernelLayout);

// launch kernel
cudaKernel.Call(structArray /* ...other kernel parameters... */);

// copy the data back from GPU
structArray = cmm.FromDevice<MyStruct[]>(structArray);

// unregister from memory manager if data not needed anymore
cmm.Unregister(structArray);
```

Listing 5.2: CUDALib example on how to encapsulate structs in arrays. For demonstration purpose, first, a struct needs to be defined, constructed and filled with some data. After that, the struct is encapsulated into an array of length one. This way, changes of the data of the struct are visible to the memory manager and hence later on transfered to the GPU. The remainder of this example is similar to Listing 5.1.

```
var cudaContext = CudaContext.Create();
var cudaModule = cudaContext.LoadModule("myCUDAModule");
var cudaKernel = cudaModule.LoadFunction("myCUDAFunction");

// create an C#-array of floats
var floatArray = new float[] { 0.0f, 1.7f, 3.0f };

// create a CudaArray from it
var cudaArray = new CudaArray<float>(floatArray, cudaContext);

// CudaArrays can be worked with as normal C#-arrays
cudaArray[1] = 2.0f;

// copy data to GPU
cudaArray.ToCudaDevice();

// set grid-layout
cudaKernel.SetKernelLaunchLayout(myKernelLayout);

// launch kernel
cudaKernel.Call(cudaArray /* ...other kernel parameters... */ );

// copy data back from GPU
cudaArray.FromCudaDevice();
```

Listing 5.3: CUDALib CudaArray example. This listing shows the same example as Listing 5.1, but using a *CudaArray* instead of manually registering a C#-array in the *CudaMemoryManager*. *CudaArray*s can be worked with as normal arrays in C#.

and inserted where the stop time should be recorded, for example after the memory transfers and kernel execution. CUDA can then provide the elapsed time between the start and stop events. Since memory transfers and kernel launches can run asynchronously, measuring time with CPU timers may report incorrect timings and hence CUDA-timers should be used in that case. Furthermore it should be noted that the stop event mentioned above is recorded only when it is actually executed. For this reason, before the elapsed time can be read from the CUDA-timers, one has to make sure that the events have been recorded already. This is simply done by a CUDA-synchronize instruction for the stop event. The synchronize instruction tells CUDA to execute all GPU code until the given event. After that it is guaranteed that the events have been recorded and the correct elapsed time can be read. All this synchronization is done automatically by the library, or, if required, it can be performed manually as well.

5.2.2 Built-In Data-Types

When programming with CUDA, one observes that certain CUDA-internal data types are used quite frequently, but are cumbersome to use especially from within C#. That is why four special data types have been implemented in the CUDALib. They can be seen as two groups of data types: arrays, containing homogeneous data, and a composite data structure, containing

heterogeneous data.

A conventional array on the GPU is provided by the CUDALib as the $CudaArray\langle T\rangle$, which contains elements of type T. They can be worked with as usual C#-arrays, can be used as kernel-parameters and can be conveniently loaded from and to the GPU. Listing 5.3 shows the same code-example of Listing 5.1 with the use of a $CudaArray$.

A similar purpose to the $CudaArray$ is fulfilled by the $CudaPageLockedArray\langle T\rangle$ of type T. The difference is that the data in the RAM can not be paged anymore when *page-locked*, or *pinned*. Such arrays can additionally be mapped into the GPU memory space. Page-locked arrays allow very fast updates, however, since using them reduces overall physical memory for the operating system, they should be used sparingly. The last array data structure is the $CudaTexture$. The CudaTexture is a 1D, 2D or 3D array which is internally mapped to the CUDA-internal CUDAArray. It provides all functionality expected for textures, like border wrapping or clamping, filtering, normalized coordinates and so on.

Besides the array data structures, it is often required to have objects with heterogeneous data. For this reason, the $CudaStruct\langle T\rangle$ was implemented, where T can be any C#-struct. This way, the library also permits to work with heterogeneous data with CUDA in an easy way.

5.2.3 Graphics-Resource Sharing

CUDA is often used in computer graphic programs alongside with the graphics APIs OpenGL and DirectX. In such cases, CUDA can be used to accelerate computationally intensive tasks. Those computations are often done on data which is already on the GPU in buffers or textures from one of the graphics APIs. Such data can be for example geometry data stored in buffers or image data stored in textures. When CUDA-kernels have to perform computations on this data, it would be adverse to copy the data into CUDA-arrays. Therefore, the graphics resources of graphics APIs can be shared with CUDA.

To make sharing of those resources as convenient as possible, the CUDALib provides three classes for sharing DirectX10 buffers and textures with CUDA. The $CudaSharedBuffer$ implements sharing of graphics-buffers with CUDA and $CudaSharedTexture$ shares textures. It should be noted, however, that CUDA can only *read* but not write to textures. To be able to directly write to a texture anyway, the $CudaSharedTextureBuffer$ was implemented as a workaround. It shares a DirectX linear-buffer as a CUDA-buffer, but using the DirectX shader-resource view to access the buffer in DirectX shaders as a texture. This way, direct writing from CUDA to a DirectX-texture can be obtained. The $CudaSharedTextureBuffer$, however, is a special case which is only needed because of current limitations in Aardvark's abstract renderer-implementation. The same behavior could basically also be achieved with a $CudaSharedBuffer$. Currently, a new renderer-backend for Aardvark is in development which also considers the needs for CUDA and OpenCL. When this is done, the implementation of graphics resource sharing can be simplified.

To use graphics resource sharing, a graphics resource must first be registered with CUDA. After that, before being able to actually read or write from or to the shared graphics resource from CUDA, the resource has to be *mapped* into and *unmapped* again from CUDA each time before the graphics API can access the resource again. Since there were also rules implemented for Aardvark's scene graph, this mapping can be done automatically.

To make graphics resource sharing possible inside Aardvark, several C#-extensions have been implemented for Aardvark's abstract renderer-interfaces. Also, for sharing resources from the targeted graphics API DirectX10, some extensions for concrete Aardvark-SlimDX classes have been programmed. The integration of other APIs, like any other DirectX version or OpenGL, can be done without much effort by implementing further C#-extensions, targeting the desired API.

5.3 Device Side

The counterpart of the host side of the CUDALib is the device side part. The methods and data types provided in device code can be used by any CUDA kernel which includes the header of the device side library. Most of this library was implemented concurrently with the development of the CUDA ray tracer which is described in the next section. Therefore, the device side currently contains only a math-library with vector, color and matrix support, as well as some utility-functions which are useful programming CUDA-kernels. The utility functions calculate a linear offset from the CUDA-thread- and -block-index. The offset can then be used for directly writing into a buffer.

The ray tracing specific code is not part of the core of the device side library, but the ray tracer itself is included as a part of the library so that any class, struct or method can be reused if needed. The ray tracer itself will be described in detail in the following chapter.

5.4 Examples

For demonstrating the usage of the CUDA-library, a *CUDAExample*-project has been created in Aardvark. It contains 14 examples on different topics on how to use CUDA-features in Aardvark with the help of the library. The examples are:

- *CudaArray* Example:
  Demonstrates the usage of the *CudaArray*-type of the library.
- Page-locked Memory Example:
  Demonstrates the usage of the *CudaPageLockedArray*-type of the library.
- *CudaStruct* Example:
  Demonstrates the usage of the *CudaStruct*-type of the library.
- Global Variable Example:
  Demonstrates how to set and use CUDA's global variables via *CudaModule* from the library.
- Shared Memory Example:
  Demonstrates how to set CUDA's shared memory via *CudaFunction* from the library.
- Timer Example:
  Example on how to use *CudaTimer* from the library. It measures data processing one time

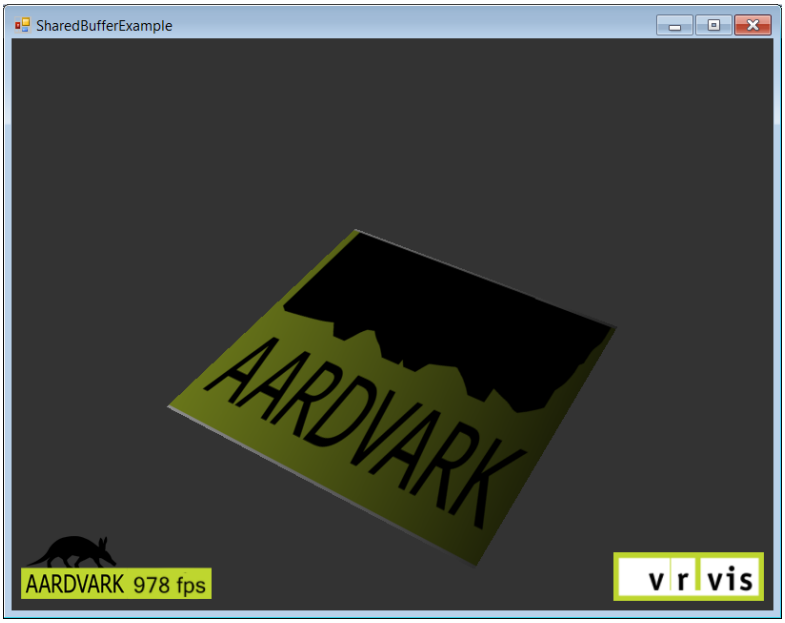

Figure 5.3: CUDALib Shared Buffer example demonstrates sharing a DirectX vertex-buffer with CUDA. Each frame, the vertices are moved by CUDA and DirectX renders the quad with the new vertices.

with a *CudaArray* and one time with a *CudaPageLockedArray*. The *CudaPageLockedArray*-variant should be faster on any CUDA-capable hardware.

- Cuda-Event Example:
  Shows the usage of *CudaEvent*.
- Stream Example:
  Shows usage of *CudaStream* by execution two kernels concurrently in different CUDA-streams.
- Texture1D, Texture2D and Texture3D Examples:
  Demonstrate the usage and capabilities of *CudaTexture*.
- Shared-Buffer, Texture and Texture-Buffer Examples:
  These examples demonstrate the usage and capabilities of sharing graphics resources with CUDA. Figure 5.3 shows a screenshot of the “Shared Buffer”-demo.

CHAPTER 6

CUDA Ray Tracer

This chapter gives detailed information on the implementation of the CUDA ray tracer which was implemented for this thesis. After a short overview, the program flow of the application is examined. After that, the implemented CUDA ray-tracing kernel is described. Close attention is further paid to the implemented acceleration data structures, including creation and conversion, data layout and traversal. Since the ray tracer is fully configurable at runtime, those parameters are presented. Finally, issues with debugging are mentioned as well as solutions to those.

6.1 Overview

The CUDA ray tracer implemented for this thesis is called *CURA*, which stands for *CU*da *RA*ytracer. It is part of the VRVis-internal rendering engine Aardvark and can be used from within any Aardvark application. The ray tracer can handle arbitrary triangle meshes and supports reflections and hard shadows. The ray-tracing code runs completely in CUDA, which means on the GPU only. Therefore the *whole* ray tracing algorithm and hence all the needed data structures, including vectors, colors, rendertargets, cameras, triangle meshes, acceleration data structures and so on, are implemented on the GPU using CUDA. The CPU is used solely for updating the current camera position and for starting the ray tracing kernel. Therefore the CPU is free to do other things while the GPU is busy calculating the ray-traced image.

Aardvark provides an abstract render-interface which is used by CURA as well as all other Aardvark applications. In case of CURA, it is a simple DirectX10 rendering application which just displays a textured full-screen quad every frame. Hence, the application has one render target which is a DirectX10 texture. It is shared between DirectX and CUDA, such that the CUDA ray-tracing kernel can render into this texture. The completely rendered texture-image is then displayed on a full screen quad by the DirectX part of the application. Since the application is interactive, the CUDA ray tracing kernel is executed every frame.

6.2 Program Flow

The program cycle is as follows (see Figure 6.1). When the program is launched, the Aardvark kernel, which is responsible for maintaining a DirectX render-loop, is started. After that, the DirectX10 renderer is initialized and the CUDA context is created. Also, the ray-tracing kernel is loaded and configured as well as the render target, which is a DirectX10 buffer used as a full screen texture. Next, the scene is loaded, but not yet onto the GPU.

Then the call to start the ray tracing kernel happens in the pre-render phase of Aardvark's rendering loop. If the scene is not ready for the GPU, the scene data gets converted and finally loaded onto the GPU. This allows updates for scene changes and animations. Finally, the ray tracing kernel is started and executed on the CUDA device. When the CUDA kernel has finished generating the image, the Aardvark render-method is called and displays the render target as a full screen quad.

The program loops over the rendering functions, thus generating a ray-traced image every frame. If the scene is not changed nor animated, only the camera is updated with the current position.

When the program is exited, all data on the GPU is cleaned up automatically by the memory manager of the CUDALib.

6.3 The CUDA Ray Tracing Kernel

For ray tracing to be efficient on GPUs, a few adaptations to the original ray-tracing algorithm have to be made. First, the $DoRayTracing()$-function from Algorithm 1 is now implemented as a CUDA kernel and therefore called $RayTracingKernel()$, as shown in Algorithm 5. CUDA kernels are executed on the CUDA device, running in many parallel threads. For the purpose of the ray-tracing kernel, there are as many threads started as the render target has pixels. Hence, the for-loop of the $DoRayTracing()$-function can be omitted.

The $Render()$-function (also in Algorithm 5) is part of the host code and is therefore implemented in C#. It starts the CUDA kernel $RayTracingKernel()$ on the device in as many threads as needed. Each thread has its own CUDA thread-index in the block it belongs to. Likewise, each block has its own CUDA block-index in the grid. From these indices, the coordinates which a thread corresponds to in the output image can be computed. Each thread calculates one pixel of the output image.

Recursive functions are still slow on GPUs. For this reason, an iterative version of the ray tracing algorithm was implemented (see Section 4.2 and Algorithm 3). Since the primary use of the ray tracer is to render curved (i.e. non-planar) reflections, the implemented version does not support refraction. Another reason for omitting refraction is that with refraction, due to the inner reflections and the resulting fan out of the ray tree, the implementation would require a stack for rays, which in turn would slow down rendering performance.

The implemented $Trace()$-function is listed in Algorithm 6. The variable ray holds the currently processed ray. Initially this is the primary ray. If there is no intersection between the primary ray and the scene, the background color is returned. Otherwise, the hitpoint is shaded. If the material at the hitpoint is reflecting, a reflection ray is created, tested for intersection with

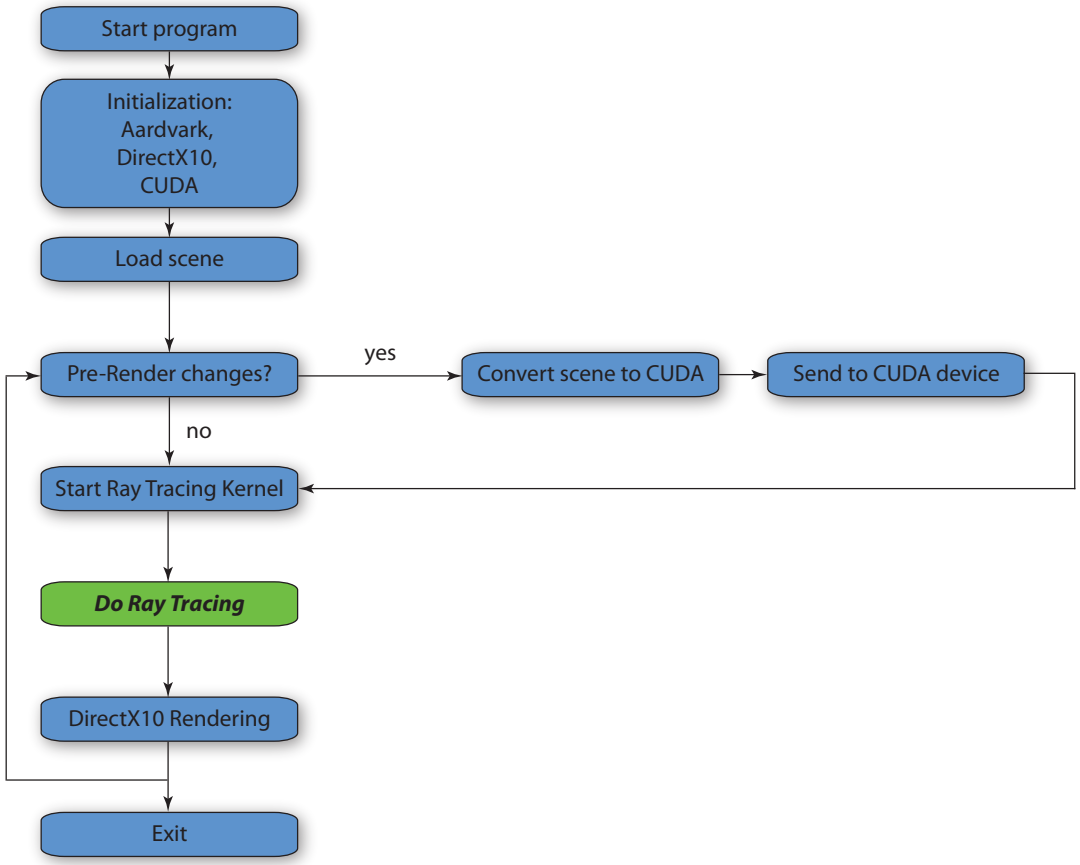

Figure 6.1: CURA program flow. The blue boxes are executed on the CPU (C#), the green one is executed on the GPU (CUDA). When the program is started, Aardvark (the rendering engine), DirectX and CUDA are initialized, and the scene is loaded. The scene gets then converted to a CUDA-capable format and is sent to the device. Each frame, the CUDA ray-tracing kernel is started, and the scene is ray traced on the GPU. Finally, DirectX displays a full-screen quad with the output buffer from the ray tracer as a texture.

the scene, shaded, and if the surface at the new hitpoint is again reflective, another reflection ray is traced. To prevent reflection rays bouncing between specular surfaces, a maximum iteration level is provided. This is the same as the maximum recursion level pointed out in the section on the ray-tracing algorithm (Section 2.3).

6.4 Acceleration Data Structures

The acceleration data structures implemented in CURA are kD-Trees. There are two variants of kD-Trees that have been implemented. The first one is a kD-Tree per geometric object. Since it is created per object, it is called *Object-kD-Tree*. The second variant is a kD-Tree per scene

Algorithm 5 CUDA-kernel

```
1: [Host]
2: procedure RENDER()
3:     numberOfThreads ← number of pixels
4:     LAUNCHCUDAKERNEL(RayTracingKernel, numberOfThreads)
5: end procedure
6:
7: [Device]
8: procedure RAYTRACINGKERNEL()
9:     (x, y) ← GETCOORDSFROMTHREADINDEX()
10:    primaryRay ← CREATEPRIMRAY(x, y)
11:    outputColor ← TRACE(primaryRay)
12:    WRITEOUTPUT(x, y, outputColor)
13: end procedure
```

and is built on top of the Object-kD-Trees, so it is a kD-Tree of kD-Trees and therefore called *Über-kD-Tree* (see Section 4.5). For performance comparison, it is also possible to render the scene *brute force*, i.e. to use no acceleration structures at all and to intersect every ray with every primitive in the scene. This is however only usable for scenes which consist of a maximum of only up to a few hundred primitives.

6.4.1 Creation and Conversion

Since Aardvark has already had built-in support for kD-Trees, these have been reused and the kD-Trees are created on the CPU using Aardvark's *KdIntersectionTree*. The *KdIntersectionTree* uses a variant of the SAH as the cost function and has support for empty-space optimization (Section 3.1.7).

After the CPU kD-Trees have been constructed, they are converted to a CUDA capable format (Listing 6.1). $CudaKdTree$ is the CUDA format of the kD-Tree and consists of the bounding box of the whole kD-Tree as well as two arrays. The first array $TreeArray$ contains the inner nodes of the kD-Tree, the other one, $LeafArray$, the indices to the primitives in the leaf nodes.

$CudaKdTreeNode$ represents an inner node of the CUDA kD-Tree. It contains the following fields. The first one is the axis along which the split for that node has been made. The second field holds the position of the splitting plane on along this axis. Next is the index of the left child node. If this index is below zero, the index indicates a leaf node. If the left child is a leaf, the $LeftCount$ gives the number of primitives in the leaf node. The last two fields contain the same information for the right child node.

Algorithm 6 Implemented $Trace()$-function

```
1:  function TRACE(primRay)
2:      color ← black
3:      ray ← primRay
4:      iteration level ← 0
5:
6:      while not reached maximum iteration level do
7:          hit ← INTERSECT(ray, scene)
8:          if hit then
9:              color += SHADE(ray, hitPoint)
10:             if Material is reflective then
11:                 reflectionRay ← RAY(hitPoint, reflected(ray.origin))
12:                 ray ← reflectionRay
13:                 iteration level ← iteration level + 1
14:             else
15:                 break loop
16:             end if
17:         else
18:             return BackgroundColor
19:         end if
20:     end while
21:
22:     return color
23: end function
```

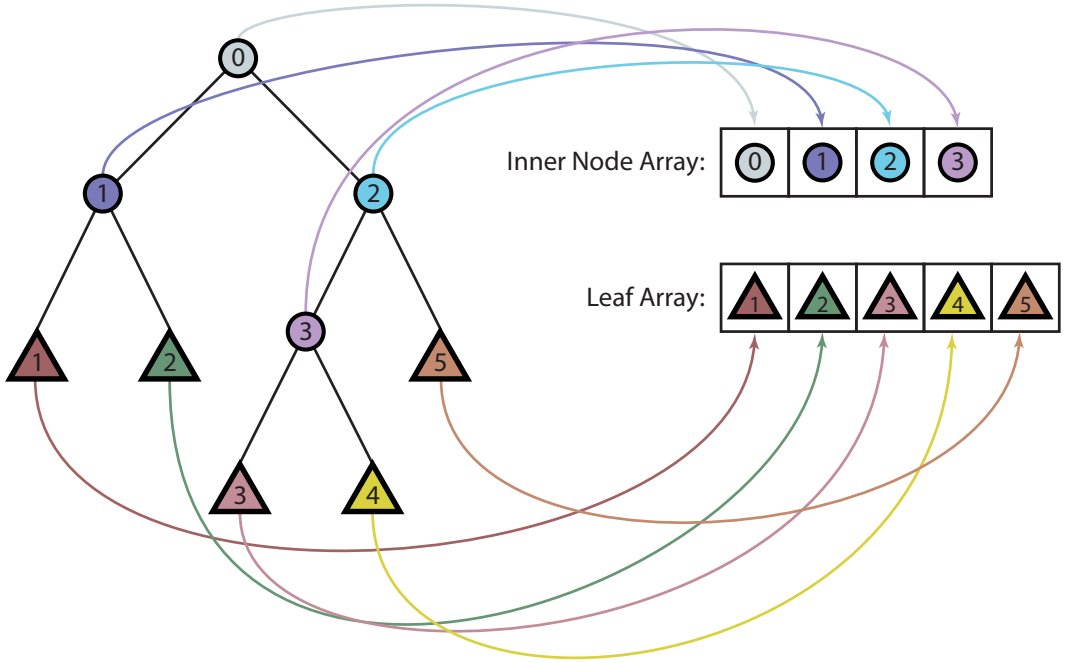

Figure 6.2: CURA kD-Tree conversion. The CPU kD-Tree is converted to two arrays, one for the inner nodes and one for the leaf nodes. The conversion processes the tree in a depth-first, left-first manner.

```
struct CudaKdTree
{
  AABB             BoundingBox   // scene's bounding box
  CudaKdTreeNode[] TreeArray     // array of inner nodes
  int[]            LeafArray     // array of leaf nodes
}

struct CudaKdTreeNode
{
  int   Axis                     // axis of subdivision
  float Position                 // position of subdivision

  int   Left                     // index of left inner or leaf node
  int   LeftCount                // number of primitives if left is a leaf

  int   Right                    // index of right inner or leaf node
  int   RightCount               // number of primitives if right is a leaf
}
```

Listing 6.1: CUDA kD-Tree Format (C#-representation)

The conversion of the tree from the CPU to the CUDA representation is then done in a depth-first order by ascending the left path first. This way, the left child of a node always is the next entry in the tree array and the leafs are stored from the lower-left leaf of the tree to the lower-right of the tree (see Figure 6.2). The converted kD-Tree arrays are then copied to the GPU together with other scene information.

6.4.2 Scene Traversal

In this section, the different scene-traversal methods will be presented. Each of the traversal methods implements its own *Intersect()*-method (c.f. Algorithm 3). In CURA, every object has its own model matrix. Therefore, for intersecting the rays with the ADS respective the objects itself, the rays are transformed into the local coordinate system of the object.

The easiest way to traverse the scene is using brute force. Hence, all rays intersect all primitives. The pseudo-code for the *Intersect()*-method is given in Algorithm 7.

The second traversal method is to traverse the scene using the Object-kD-Tree. Every object in the scene stores its own kD-Tree. Therefore, all objects need to be tested for the closest intersection. The implemented kD-Tree traversal method is similar to the traversal used in Zhou et al. [ZHWG08]. It is the stack-based iterative traversal explained in Section 4.4.1. Algorithm 8 shows the pseudo-code of the implemented version. The call to the kD-Tree *IntersectScene()*-method is similar to the one from Algorithm 2, but with the iterative version of the *IntersectNode()*-function from Algorithm 4.

Finally, the last implemented traversal method is to use the Über-kD-Tree. There is one kD-Tree for the whole scene, which in turn contains the Object-kD-Trees as its primitives. Therefore, all that has to be done to get the closest intersection is to intersect the ray with the Über-

Algorithm 7 Brute-Force Traversal

```
1:  function INTERSECT(ray, scene)
2:      bestHit ← no hit
3:
4:      for each object obj in scene
5:          transformedRay ← transform(ray, obj.Transformation)
6:          for each primitive prim in obj
7:              hit ← intersect(prim, ray)
8:              if hit nearer than bestHit then
9:                  bestHit ← hit
10:             end if
11:         end for each
12:     end for each
13:
14:     if bestHit != no hit then
15:         bestHit ← transform(bestHit, obj.BackwardTransformation)
16:     end if
17:     return bestHit
18: end function
```

Algorithm 8 Object-kD-Tree Traversal

```
1:  function INTERSECT(ray, scene)
2:      bestHit ← no hit
3:
4:      for each object obj in scene
5:          transformedRay ← transform(ray, obj.Transformation)
6:          hit ← obj.KdTree.INTERSECTSCENE(ray)
7:          if hit nearer than bestHit then
8:              bestHit ← hit
9:          end if
10:     end for each
11:
12:     if bestHit != no hit then
13:         bestHit ← transform(bestHit, obj.BackwardTransformation)
14:     end if
15:     return bestHit
16: end function
```

Algorithm 9 Über-kD-Tree Traversal

```
1:  function INTERSECT(ray, scene)
2:      hit ← scene.UeberKdTree.INTERSECTSCENE(ray)
3:      return hit
4:  end function
```

kD-Tree. When the ray hits a non-empty leaf, the Object-kD-Tree of the leaf will be traversed with the ray. The pseudo-code for the traversal is shown in Algorithm 9.

To efficiently create code paths for both types of kD-Trees, the kD-Tree is implemented as a template. The *IntersectLeaf()*-methods (Algorithm 2) are specialized variants, one for each kD-Tree type. The *IntersectLeaf()*-method for the Object-kD-Tree intersects the ray with the triangles of the leafs of the kD-Tree, whereas the counterpart of the Über-kD-Tree implementation intersects the ray with each of the Object-kD-Trees.

6.5 Runtime Parameters

The ray tracer implemented in CURA is fully configurable at runtime. A list of the parameters is given in Table 6.1. As mentioned in the previous section, the usage of the different types of ADSs can be switched. Furthermore, the maximum recursion depth can be set dynamically. In the actual implementation, the recursion depth is an iteration count for rays, but conceptually this is the same. Also, a global ambient term can be set to make the scene brighter or darker at runtime. Since CURA supports animations, those can also be triggered. The animations however are calculated on the CPU and only the changes are updated on the GPU.

Since shadow computation can take a considerable amount of time, especially when there are many light sources, shadows can be turned off. To avoid self intersections when tracing the shadow ray, the actual origin of the shadow ray is moved a small distance ϵ away from the surface of the hitpoint. This ϵ can be set dynamically too. Furthermore, it is possible to switch on and off a specific light source, or to toggle them all.

Mainly for debugging purposes, the background can be switched. The black background is the standard background used in many scenes. However, for debugging it is better to have a non-black background because a black pixel can often reveal an error in the traced ray path. This is why there is the debug background with a green color. To make a scene look good, there is also the possibility to provide a user-defined background.

Since the supported geometric primitives are triangles only, to render smooth-looking surfaces the normals have to be interpolated along the triangle surface. This behavior can also be switched on and off, as well as rendering the surface normals as surface color. Finally, the so-called debug pixel described in the next section can be overlaid to the rendered image.

The influences of some of the parameters can be seen in Chapter 7 in Figure 7.3.

6.6 Debugging

As mentioned earlier, Nvidia developed Nsight, a debugging plug-in for Microsoft's Visual Studio and Eclipse. With Nsight it is possible to debug CUDA device code the same way as CPU code, like using breakpoints, step through the code, variable inspection and so on. The first versions of Nsight were released during the development of this thesis. Unfortunately, these releases were very unstable. Nsight was primarily targeted to support CUDA developers who use C/C++ as host language. Because of that, the configuration for using Nsight with C# took a considerable amount of time. Furthermore, as newer versions of Nsight were released, the support for the CUDA APIs of versions below 4.0 was dropped. Even though a few API functions

Parameter	Possible values	Default
General		
RenderMode	Brute Force, Kd-Tree, Über-Kd-Tree	Kd-Tree
MaxRecursionDepth	0..n	2
GlobalAmbient	0..n	1.0
Animations	on, off	off
Lights and Shadows		
RenderShadows	on, off	on
Epsilon	0..n	0.25
Toggle single Lightsource	on, off	off
Toggle all Lightsources	on, off	on
Debug		
UseBackground	Black, Debug, Scene	Scene
InterpolateNormals	on, off	on
ShowNormals	on, off	off
ShowDebugPixel	on, off	off

Table 6.1: Runtime Parameters

of the CUDA API version 4.x were wrapped manually in the CUDALib, the core of the library uses CUDA.NET internally, which supports only CUDA API 3.0. That is why Nsight couldn't be used to successfully debug CUDA device code with CURA.

For these reasons, complex parts of the CUDA device code, especially the ray traversal in the kD-Trees, were debugged on the CPU. To do this, the *whole* CUDA device code had to be rewritten in C#, such that the C# version mirrored exactly the whole CUDA program. With this, single frames could also be rendered on the CPU, having full debugging support from Visual Studio.

An image of a single frame, however, has many pixels and each of them traces its own ray. During development, only some of them behave erroneously. Therefore it is advisable to only consider a specific pixel, i.e., debug only a specific ray. To do so, a *debug pixel* was used which gets a special overlay color in the render target so it is visible. Then, one could move the camera until the debug pixel was on the incorrectly rendered pixel, and then trigger rendering and debugging for this pixel only on the CPU. This was very helpful because, especially when debugging acceleration data structures, errors and faultily programmed special cases occur seldom. Hence, debugging should only be done when such a special case with wrong behavior is encountered. The precondition for this to work is that the CUDA code and the C# code stay mirrored, so that the currently rendered and displayed image from CUDA is the same as the CPU version would produce. Otherwise, debugging via the CPU would lead to misleading results because of different code versions.

With the help of these debugging "tools" it was possible but tedious to properly debug the CUDA ray tracer and its data structures.

CHAPTER 7

Results

7.1 Test Setup

All parts of this diploma thesis have been developed targeting Nvidia's Fermi architecture. In particular, an Nvidia GeForce GTX 480 graphics card with 1.5GB RAM was used for all tests. The test machine consists of an Intel Core i7 920 CPU running at 2.67GHz, 12GB RAM and Microsoft Windows 7 Professional 64-bit SP1 installed. The tested scenes are some well-known ray-tracing benchmark scenes. They can be seen in Figure 7.1, details are given in Table 7.1.

7.2 Results

For each scene, a camera position has been chosen such that the whole model is in view, except for the Sponza scene, where the camera is placed inside the building (Figure 7.1). Each scene consists of the model itself and a sky-like environment. The Bunny and the Happy Buddha scenes also have a ground plane. Furthermore, each scene has two light sources, one directional and one point light source, except the Sponza and Turbine Blade scenes which have two point

Name	Nr. Triangles	Kd-Tree Creation [sec]
Bunny (low detail)	2.9k	<1
Bunny (high detail)	69.5k	6.8
Sponza	66.5k	6.4
Buddha	293k	22
Blade	1 765k	128
Soda Hall	2 145k	216

Table 7.1: The test scenes. The kD-Trees are created on the CPU using the implementation in Aardvark.

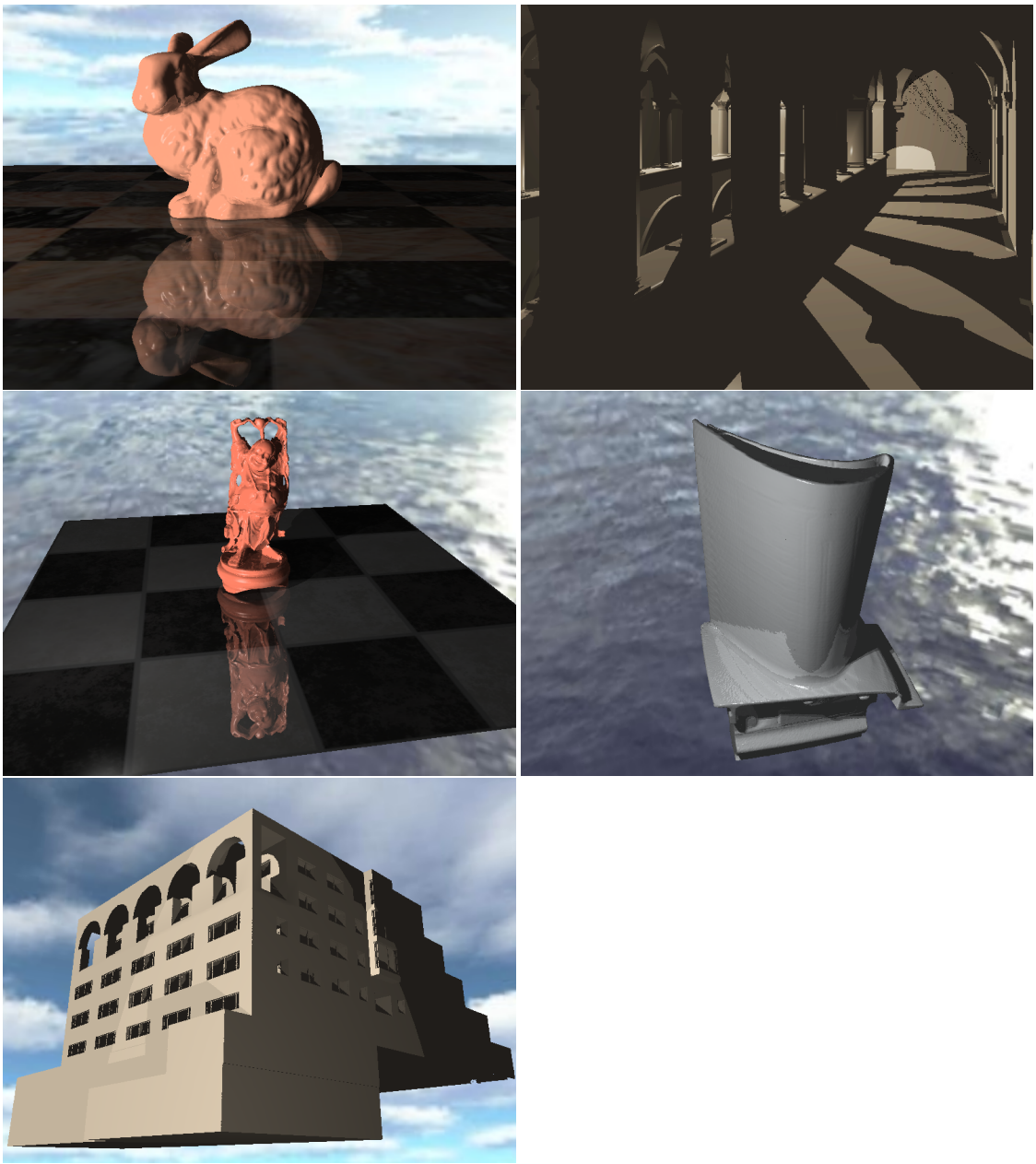

Figure 7.1: The tested scenes: Bunny (in two versions of mesh-resolutions), Sponza Atrium, Happy Buddha, Turbine Blade and Soda Hall.

light sources. Several measurements have been made related to the rendering performance of primary rays, shadows and reflections. All measurements in this section are done by using the Object-kD-Trees as acceleration data structures. The brute-force method is only feasible for scenes with a maximum of a few hundred triangles and hence too slow for the given test scenes to perform any reasonable measurements. In the chosen test scenes, the Über-kD-Tree performs just a little worse than the Object-kD-Trees. The reason is that in the given test scenes, there are only one or two Object-kD-Trees and traversing them in a sequence is faster than the overhead of traversing an Über-kD-Tree. Measurements for the Über-kD-Tree and a comparison of the Über-kD-Tree and the Object-kD-Trees with more suitable scenes are done in Section 7.3.

The behavior of primary rays with different light configurations is shown in Table 7.2. It can be seen that the directional light usually performs slightly better. This may be due to simpler calculations. Furthermore, the influence of higher screen resolutions and the subsequent impact of the higher number of rays on the rendering performance, which decreases considerably, are visible. An interesting result is the behavior of the Soda Hall scene. Its performance increases with higher screen resolutions from 640x480 to 1024x768. Furthermore, the jump of Mrays/sec from resolution 1024x760 to 1600x1200 is quite high compared to the other scenes. We have not yet found the reasons for the unusual behavior of this scene.

Table 7.3 presents the measurements for shadows. This again shows that the directional light performs better than the point light. One reason may be that the shadow rays for the point light might be more coherent as the shadow rays for directional shadow rays. Hence, those shadow rays can exploit memory and cache coherence better, which in turn results in higher rendering performance. Note that in our current implementation we do not yet support early exit for shadow rays.

The results for reflection rays can be seen in Table 7.4. It shows that with each reflection bounce there are fewer reflection rays created, which means that the other reflection rays either hit a non-reflecting material or get reflected out of the scene. Moreover, the values in the table show that the tracing of reflection rays gets more expensive with each bounce. This is the expected behavior, since reflection rays get more and more incoherent with each bounce. Thus, memory and cache coherence can not be utilized well anymore and result in a penalty on rendering time.

In Table 7.5, the results for a "full" scene setup can be seen, including shadows for two light sources and reflection with two bounces. The first interesting thing to note is that the amount of secondary rays, which are all the shadows and reflection rays together, is almost as many as the primary rays casted. However, the rendering performance for the full setup drops far lower than half of the performance for primary rays. The reason is most likely again that secondary rays exhibit less coherence and hence traversing them takes longer due to incoherent memory access. The second interesting thing is the scaling of rendering time with respect to number of pixels. If 640x480 is taken as 100%, then the given three higher resolutions have a factor of 1.56, 2.56 and 6.25 respectively more pixels. Since for every pixel one CUDA-thread is started, when rendering an image of higher resolution, the additional amount of threads is of the same ratio as the higher resolution image has more pixels. The rendering performance however scales sublinearly with the number of pixels. The main reason may be that with higher resolution, the rays of nearby pixels are more likely to hit the same objects in the scene and hence access the

Name	Resolution	Primary Rays								
		#rays	no light		directional		point		both	
			FPS	Mrays/s	FPS	Mrays/s	FPS	Mrays/s	FPS	Mrays/s
Bunny (low detail)	640 x 480	307.2k	111.1	34.1	104.2	32.0	103.1	31.7	100.0	30.7
	800 x 600	480.0k	72.5	34.8	69.9	33.6	69.0	33.1	67.1	32.2
	1024 x 768	786.4k	46.1	36.2	45.5	35.7	44.1	34.6	42.9	33.8
	1600 x 1200	1,920.0k	20.6	39.6	20.0	38.4	19.6	37.6	19.2	36.9
Bunny (high detail)	640 x 480	307.2k	81.3	24.9	80.0	24.6	78.7	24.2	76.9	23.6
	800 x 600	480.0k	55.5	26.7	54.1	26.0	53.2	25.5	52.6	25.3
	1024 x 768	786.4k	38.5	30.2	37.0	29.1	37.0	29.1	35.7	28.1
	1600 x 1200	1,920.0k	16.7	32.0	16.7	32.0	16.1	31.0	15.6	30.0
Sponza *)	640 x 480	307.2k	62.5	19.2	62.5	19.2	62.5	19.2	58.8	18.1
	800 x 600	480.0k	43.5	20.9	41.7	20.0	41.7	20.0	40.0	19.2
	1024 x 768	786.4k	27.8	21.8	27.0	21.3	27.0	21.3	26.3	20.7
	1600 x 1200	1,920.0k	13.0	25.0	12.5	24.0	12.5	24.0	12.1	23.3
Buddha	640 x 480	307.2k	52.6	16.2	52.6	16.2	52.6	16.2	50.0	15.4
	800 x 600	480.0k	40.0	19.2	40.0	19.2	38.5	18.5	38.5	18.5
	1024 x 768	786.4k	32.3	25.4	32.3	25.4	32.3	25.4	32.3	25.4
	1600 x 1200	1,920.0k	14.3	27.4	14.0	26.9	14.0	26.9	13.5	26.0
Blade *)	640 x 480	307.2k	15.4	4.7	15.2	4.7	15.2	4.7	14.9	4.6
	800 x 600	480.0k	13.3	6.4	13.2	6.3	13.2	6.3	13.0	6.2
	1024 x 768	786.4k	9.3	7.3	9.3	7.3	9.2	7.2	9.1	7.1
	1600 x 1200	1,920.0k	5.1	9.7	5.1	9.7	5.0	9.6	5.0	9.6
Soda Hall	640 x 480	307.2k	7.4	2.3	7.2	2.2	7.2	2.2	7.2	2.2
	600 x 600	480.0k	7.9	3.8	7.9	3.8	7.9	3.8	7.8	3.8
	1024 x 768	786.4k	8.2	6.4	8.1	6.4	8.1	6.4	8.0	6.3
	1600 x 1200	1,920.0k	5.5	10.5	5.5	10.5	5.5	10.5	5.4	10.4

Table 7.2: Measurements for primary rays for the test scenes at different resolutions. Frames per seconds and the corresponding Mrays/sec are given. The primary rays were measured with no lights on, with one directional light on, with one point light source on and with both lights on. None of them casts shadows in these tests. Results for shadows and reflections are given in Table 7.3 and Table 7.4 as well as a "full" setup in Table 7.5. The Sponza and Blade scenes have a second point light source instead of the directional light source.

same data, which in turn leads to higher memory coherence and less penalty for memory access.

The rendering performance of primary, shadow and reflection rays and the "full" setup for the "Bunny (high detail)" scene is depicted in Figure 7.2. The impact of rendering shadows and, even more, of reflections is clearly visible.

Finally, Figure 7.3 shows the "Blade" scene with different parameters set. The first image (upper left) corresponds to the "no light" value in table "Primary Rays" (Table 7.2). It traces primary rays only, without any light sources. The second image (upper right) includes shading for two light sources and corresponds to the "both" value of that same table. The lower left image includes shadows for the two light sources. Rendering performance is given in the "both" values in the "Shadows"-table (Table 7.3). Finally, the lower right image shows the "full" setup from Table 7.5 with two light sources including shadows and two reflection bounces.

Name	Resolution	Primary Rays			Shadows								
					directional			point			both		
		FPS	#rays	Mrays/s	FPS	Δ_{dir}	Mrays/s	FPS	Δ_{point}	Mrays/s	FPS	Δ_{both}	Mrays/s
Bunny (low detail)	640 x 480	100.0	307.2k	30.7	86.9	35.9k	23.9	72.9	199.0k	53.8	64.9	234.9k	35.2
	800 x 600	67.1	480.0k	32.2	58.8	56.1k	26.7	50.0	311.0k	61.0	45.5	367.0k	51.7
	1024 x 768	42.9	786.4k	33.8	40.8	91.9k	76.6	34.5	509.4k	89.4	31.3	601.3k	69.1
	1600 x 1200	19.2	1,920.0k	36.9	17.5	254.1k	50.8	14.3	1,281.6k	71.2	13.0	1,535.7k	61.4
Bunny (high detail)	640 x 480	76.9	307.2k	23.6	66.6	34.9k	17.4	48.1	199.3k	25.6	42.9	234.2k	22.7
	800 x 600	52.6	480.0k	25.3	45.5	54.5k	18.2	35.0	311.5k	32.4	30.0	366.0k	25.6
	1024 x 768	35.7	786.4k	28.1	32.3	89.3k	29.8	25.0	510.3k	42.5	22.0	599.6k	34.3
	1600 x 1200	15.6	1,920.0k	30.0	13.9	247.1k	30.9	10.8	1,284.2k	44.3	10.0	1,531.3k	42.5
Sponza *)	640 x 480	58.8	307.2k	18.1	34.5	159.5k	13.3	37.0	145.7k	14.6	26.3	305.2k	14.5
	800 x 600	40.0	480.0k	19.2	24.4	249.3k	15.6	26.3	227.7k	17.5	18.2	477.0k	15.9
	1024 x 768	26.3	786.4k	20.7	16.1	408.5k	17.0	16.9	372.9k	17.8	12.2	781.4k	17.8
	1600 x 1200	12.1	1,920.0k	23.3	7.6	1,026.2k	20.7	8.0	919.0k	21.6	5.6	1,945.2k	20.6
Buddha	640 x 480	50.0	307.2k	15.4	34.5	12.7k	1.4	24.4	187.2k	8.9	20.4	199.9k	6.9
	800 x 600	38.5	480.0k	18.5	27.8	19.9k	2.0	20.0	292.5k	12.2	18.9	312.4k	11.6
	1024 x 768	32.3	786.4k	25.4	24.4	32.6k	3.3	16.1	479.3k	15.5	14.3	511.9k	13.1
	1600 x 1200	13.5	1,920.0k	26.0	11.8	90.3k	8.2	8.3	1,271.5k	27.1	7.6	1,361.9k	23.9
Blade *)	640 x 480	14.9	307.2k	4.6	8.2	77.1k	1.4	8.1	76.5k	1.3	5.3	153.6k	1.3
	800 x 600	13.0	480.0k	6.2	7.4	120.5k	2.1	7.4	119.5k	2.1	4.9	240.1k	1.9
	1024 x 768	9.1	786.4k	7.1	5.8	197.5k	3.1	5.8	195.8k	3.1	4.0	393.3k	2.8
	1600 x 1200	5.0	1,920.0k	9.6	3.1	545.3k	4.5	3.7	540.9k	4.3	2.2	1,086.2k	4.3
Soda Hall	640 x 480	7.2	307.2k	2.2	6.5	91.8k	6.1	5.2	170.4k	3.1	4.7	262.2k	3.6
	800 x 600	7.8	480.0k	3.8	6.9	143.4k	9.0	5.0	266.2k	3.7	4.4	409.6k	4.1
	1024 x 768	8.0	786.4k	6.3	6.8	234.8k	10.2	4.4	436.2k	4.2	3.8	671.0k	4.9
	1600 x 1200	5.4	1,920.0k	10.4	4.2	630.3k	12.5	2.6	1,188.2k	6.0	2.4	1,818.5k	7.7

Table 7.3: Measurements for shadows for the test scenes at different resolutions. The measurements were done for a directional light source, a point light source and both light sources together. The FPS are the total measured performances. The "#rays" column gives the total number of primary rays casted. The Δ-values give only the newly created shadow rays for each light source. The "Mrays/s" give the million rays per second with respect to the value of the column before only. The Sponza and Blade scenes have a second point light source instead of the directional light source.

Name	Resolution	Primary Rays			Reflection											
					1^{st} bounce			2^{nd} bounce			3^{rd} bounce			4^{th} bounce		
		FPS	#rays	Mrays/s	FPS	$\Delta_{0,1}$	Mrays/s	FPS	$\Delta_{1,2}$	Mrays/s	FPS	$\Delta_{2,3}$	Mrays/s	FPS	$\Delta_{3,4}$	Mrays/s
Bunny (low detail)	640 x 480	100.0	307.2k	30.7	45.5	206.7k	17.2	32.3	54.1k	2.6	29.4	14.4k	0.60	28.6	1.7k	0.07
	800 x 600	67.1	480.0k	32.2	32.3	322.9k	20.1	23.0	84.4k	3.0	20.8	22.5k	0.68	20.0	2.6k	0.08
	1024 x 768	42.9	786.4k	33.8	20.8	529.0k	21.4	15.4	138.3k	3.3	14.1	36.9k	0.77	13.5	4.3k	0.09
	1600 x 1200	19.2	1,920.0k	36.9	8.7	1,335.3k	21.2	6.7	370.8k	3.8	6.3	102.2k	0.96	6.1	12.0k	0.11
Bunny (high detail)	640 x 480	76.9	307.2k	23.6	30.3	206.3k	10.3	21.3	53.4k	1.6	19.2	15.4k	0.39	18.5	2.4k	0.06
	800 x 600	52.6	480.0k	25.3	20.8	322.4k	11.1	14.9	83.6k	1.7	13.2	24.1k	0.42	13.0	3.9k	0.07
	1024 x 768	35.7	786.4k	28.1	14.1	528.1k	12.3	10.2	136.8k	2.0	9.2	39.4k	0.49	9.1	6.3k	0.08
	1600 x 1200	15.6	1,920.0k	30.0	6.3	1,332.9k	14.2	4.7	367.7k	2.5	4.2	109.2k	0.63	4.1	17.6k	0.10
Buddha	640 x 480	50.0	307.2k	15.4	22.7	188.7k	7.9	15.4	21.1k	0.47	12.3	8.5k	0.14	11.1	3.7k	0.053
	800 x 600	38.5	480.0k	18.5	17.2	294.8k	9.2	11.1	33.0k	0.52	9.2	13.2k	0.16	8.3	5.8k	0.061
	1024 x 768	32.3	786.4k	25.4	11.4	483.0k	8.5	7.6	54.1k	0.54	6.4	21.5k	0.17	5.7	9.5k	0.066
	1600 x 1200	13.5	1,920.0k	26.0	5.2	1,281.8k	10.8	3.4	149.9k	0.69	2.9	59.7k	0.27	2.6	26.5k	0.086
Blade	640 x 480	14.9	307.2k	4.6	6.9	82.4k	1.06	5.6	15.4k	0.137	4.8	4.3k	0.030	4.5	2.3k	0.015
	800 x 600	13.0	480.0k	6.2	5.8	128.8k	1.37	4.4	24.1k	0.163	3.8	6.7k	0.036	3.5	3.7k	0.017
	1024 x 768	9.1	786.4k	7.1	4.3	211.1k	1.70	3.2	39.5k	0.196	2.7	11.0k	0.042	2.4	8.9k	0.020
	1600 x 1200	5.0	1,920.0k	9.6	2.1	582.8k	2.10	1.6	109.6k	0.262	1.5	30.4k	0.063	1.4	16.6k	0.031

Table 7.4: Measurements for different reflection bounces for the test scenes at different resolutions. The FPS are the total measured performances. The "#rays" column gives the total number of primary rays casted. The Δ-values give only the newly created reflection rays for the corresponding bounce. The "Mrays/s" give the million rays per second with respect to the value of the column before only. Since Sponza and Soda Hall have no reflecting materials, they have no values and hence have been omitted in this table.

7.3 KD-Tree vs. Über-kD-Tree

As mentioned before, the chosen test scenes are not well suited for the Über-kD-Tree. To test the performance of this data structure, two additional test scenarios have been created. The Über-kD-Tree becomes advantageous when there are many objects in the scene such that the Über-kD-Tree can cull most of the objects efficiently.

Two simple test cases have been constructed to show a scenario where the Über-kD-Tree becomes faster. In both tests, the scene consists of the high detailed version of the bunny, which is instantiated many times such that a row of bunnies is created. In the first test the camera faces the first bunny from the side and in the second test from the front. Only the first bunny is visible, and all the others are either hidden behind the first one or not in the viewing region at all (see Figure 7.4).

The results of the tests are given in Table 7.6. As can be seen, the Über-kD-Tree performs almost constant in both scenes at about 5 FPS, whereas when rendering with the Object-kD-Trees, performance slowly decreases from 10-12 FPS to about 3 FPS for about 120 and more bunnies. The crossing point where rendering with the Über-kD-Tree gets faster is for both scenes at around 60 objects.

Shevtsov et al. [SSK07] also experimented with two-level kD-Trees in one scene they tested. They also created kD-Trees per object and a top-level kD-Tree on top of them. For their scene of some dancers in a theater hall, they found that their version of the Über-kD-Tree pays off already for four and more different, non-overlapping objects. However, when the lower level kD-Trees overlap, they report that their performance significantly decreases. It should be noted that their ray tracer was implemented on the CPU, which makes comparison of the results difficult.

7.4 Lessons learned

As usual with the development of complex systems, some parts are harder or take longer to implement than others. During development of the CUDA library and the CUDA ray tracer, the following tasks turned out to be the most time-consuming ones (in decreasing order of time consumed).

- *CUDA Debugging*

  The by far most time-consuming and tedious process was debugging CUDA code. Since the *whole* ray tracer runs completely on the GPU, the whole code necessary for ray tracing had to be implemented in CUDA. Hence, the CUDA kernel consists of the same amount of code as a ray tracer on the CPU would. However, debugging possibilities for CUDA are limited. To make matters worse, C# was the host language used, since Aardvark is implemented in this language.

  One way to debug was to write some special values into the frame buffer. However, this method is not feasible for complex and branching code. Approximately at the beginning of the implementation for this thesis, Nvidia released their then new debugging tool *Nsight* for debugging CUDA code. With the help of Nsight, it should have been possible to debug CUDA code almost like CPU code. However, the first releases were very buggy and hence

Name	Pixels	Primary rays					Full				
		#rays	Mrays/s	FPS	ms	x	Δrays	Mrays/s	FPS	ms	x
Bunny (low detail)	307.2k (x1.00)	307.2k	34.1	111.1	9	1.0	289.0k	20.2	22.5	45	1.0
	480.0k (x1.56)	480.0k	34.8	72.5	14	1.5	451.4k	23.2	16.5	61	1.4
	786.4k (x2.56)	786.4k	36.2	46.1	22	2.4	739.6k	25.6	11.1	90	2.0
	1,920.0k (x6.25)	1,920.0k	20.6	39.6	45	5.0	1,906.4k	29.0	5.0	201	4.5
Bunny (high detail)	307.2k (x1.00)	307.2k	25.0	81.3	12	1.0	287.7k	13.4	14.9	67	1.0
	480.0k (x1.56)	480.0k	26.7	55.5	18	1.5	449.6k	14.2	10.1	99	1.5
	786.4k (x2.56)	786.4k	30.2	38.5	26	2.2	736.4k	16.6	7.2	139	2.1
	1,920.0k (x6.25)	1,920.0k	32.0	16.7	60	5.0	1,899.0k	19.4	3.3	300	4.5
Sponza	307.2k (x1.00)	307.2k	19.2	62.5	16	1.0	305.2k	16.1	26.3	38	1.0
	480.0k (x1.56)	480.0k	20.9	43.5	23	1.4	477.0k	17.4	18.2	55	1.4
	786.4k (x2.56)	786.4k	21.8	27.8	36	2.3	781.4k	19.1	12.2	82	2.2
	1,920.0k (x6.25)	1,920.0k	24.9	13.0	77	4.8	1,945.2k	21.8	5.6	177	4.7
Buddha	307.2k (x1.00)	307.2k	16.2	52.6	19	1.0	221.0k	6.6	8.7	115	1.0
	480.0k (x1.56)	480.0k	19.2	40.0	25	1.3	345.4k	8.2	6.9	145	1.3
	786.4k (x2.56)	786.4k	25.4	32.3	31	1.6	566.0k	9.9	5.1	197	1.7
	1,920.0k (x6.25)	1,920.0k	27.4	14.3	70	3.7	1,511.7k	11.7	2.3	430	3.7
Blade	307.2k (x1.00)	307.2k	4.7	15.4	65	1.0	169.0k	2.0	3.4	295	1.0
	480.0k (x1.56)	480.0k	6.4	13.3	75	1.2	264.2k	2.5	2.7	374	1.3
	786.4k (x2.56)	786.4k	7.3	9.3	107	1.6	432.8k	2.7	1.8	551	1.9
	1,920.0k (x6.25)	1,920.0k	9.7	5.1	197	3.0	1,195.8k	3.7	0.9	1061	3.6
Soda Hall	307.2k (x1.00)	307.2k	2.3	7.4	136	1.0	262.2k	2.7	4.7	221	1.0
	480.0k (x1.56)	480.0k	3.8	7.9	126	0.9	409.6k	3.9	4.4	227	1.0
	786.4k (x2.56)	786.4k	6.4	8.2	122	0.9	671.0k	5.5	3.8	261	1.2
	1,920.0k (x6.25)	1,920.0k	10.5	5.5	182	1.3	1,818.5k	8.9	2.4	421	1.9

Table 7.5: Rendering times for one frame, for primary rays only and the "full" setup (one directional, one point light source, shadows, two reflection bounces), measured for the four screen resolutions 640x480, 800x600, 1024x768 and 1600x1200. Primary rays: The "#rays" column gives the number of primary rays casted. Furthermore, the Mrays/sec are given as well as the FPS and the corresponding rendering time in ms. Full setup: The "Δrays" column gives the number of secondary rays casted (shadow rays and reflection rays). The Mrays/sec are averaged values for the whole rendering time, including casting primary and secondary rays. Also, the FPS and corresponding rendering time in ms are given. The values in the "x" columns show the factor when comparing the ratio of rendering times of different resolutions to the ratio of the number of pixels if the screen resolution 640x480 (i.e., 307.2k pixels) is taken as 100%. It can be seen that the rendering times scale sublinearly with respect to the number of pixels.

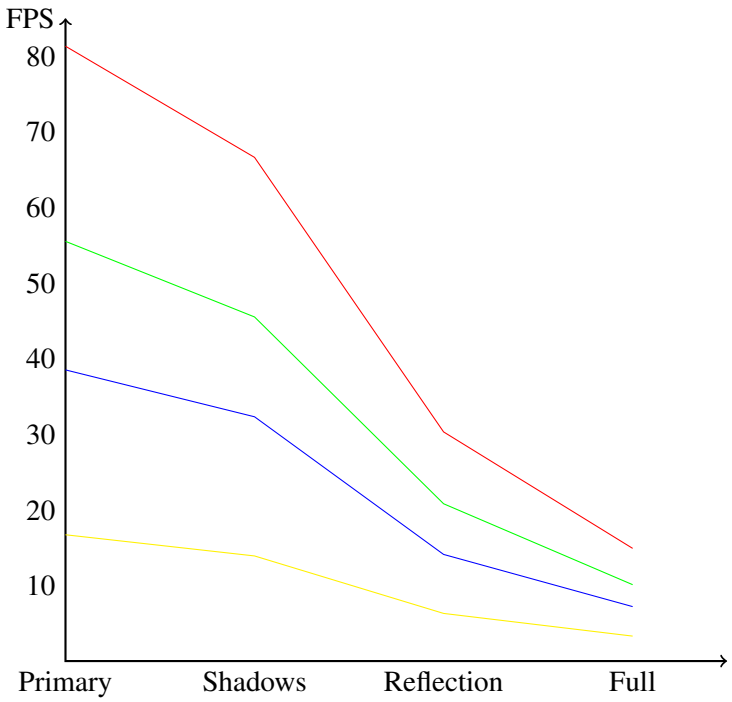

Figure 7.2: Rendering performance for the "Bunny (high detail)" scene, given for four measured screen resolutions: 640x480 shown in red, 800x600 in green, 1024x768 in blue and 1600x1200 in yellow. Values are taken from Tables 7.2, 7.3, 7.4 and 7.5. "Shadows" are the measured values for one directional light casting shadows, "Reflection" consists of one reflection bounce and no shadows. For measuring the values for "Full", one directional, one point light source, both casting shadows and two reflection bounces were used. The impact on the performance of rendering reflection-rays is clearly visible.

rendered the tool useless most of the time. Furthermore, since C# was the host language, the setup to debug CUDA code with C# as host language was indeed possible, but very tedious to accomplish. As the development of the thesis progressed, newer versions of Nsight were released. However, in the newer versions of Nsight, the support for CUDA API 3.x was dropped. This API version was the one used in the CUDA library and hence also in the CUDA ray tracer. This was the reason why Nsight could not be used for debugging anymore.

What's more is that the CUDA compilers before versions 4.x were buggy as well. Especially when compiling bigger CUDA kernels, like the ray tracing kernel, the compiler often showed unexpected behavior. In such cases, workarounds had to be found or even a reimplementation of specific parts had to be done such that the compiler could handle them.

Finally, the kD-Tree traversal needed to be debugged. The kD-Tree traversal happens in an iterative manner (see Section 4.4.1). As this traversal has several special cases and

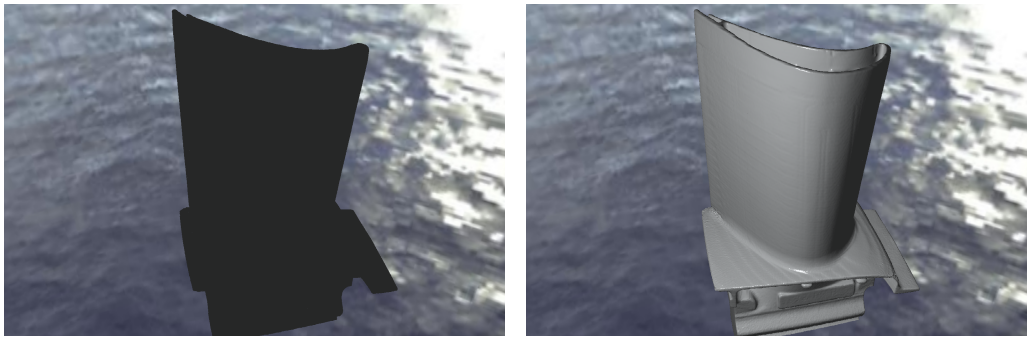

(a) Primary rays only without light sources on.

(b) Primary rays with lights on.

(c) Primary rays and shadows.

(d) Primary rays, shadows and reflections.

Figure 7.3: Turbine Blade.

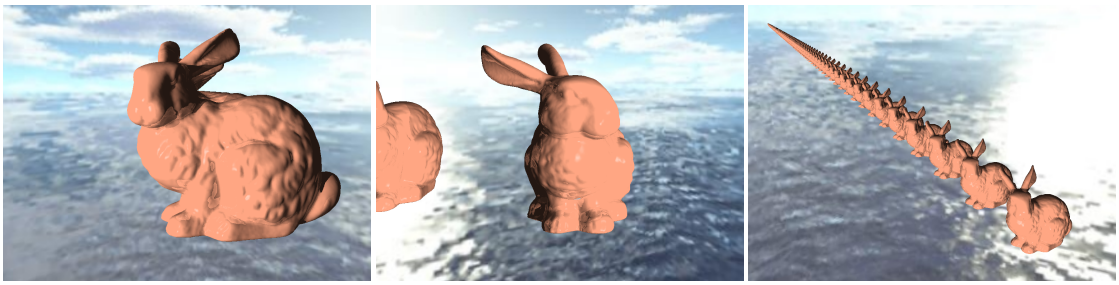

Figure 7.4: The tested scenes. Left: Test 1, facing the bunnies from the side. Middle: Test 2, facing the bunnies from the front. The picture on the right shows the array of 150 bunnies.

#Bunnies	Scene 1		Scene 2	
	Object-kD-Trees	Über-kD-Tree	Object-kD-Trees	Über-kD-Tree
1	10	7	12	9
2	8	6	7	5
3	8	6	7	5
4	7	5	7	5
5	7	5	7	5
10	6	5	6.5	5
15	6	5	6	5
20	6	5	6	5
25	5.5	5	6	5
30	5	5	6	5
35	5	5	5	5
40	5	5	5	5
50	5	5	5	5
60	4	5	5	5
70	4	5	4	5
80	4	5	4	5
90	4	5	4	5
100	4	5	4	5
110	3	5	4	5
120	3	5	3	5
130	3	5	3	5
140	3	5	3	5
150	3	5	3	5

Table 7.6: This table shows the measured performances, given in FPS, for the two test scenes (see Figure 7.4). It can be seen that the performance of the Über-kD-Tree stays almost constant, whereas the performance of the Objects-kD-Trees decreases slowly with more and more objects in the scene. The crossing point where the Über-kD-Tree has better performance for the given scenes is around 60 objects.

therefore special code paths, some of the errors appeared only seldom. Since Nsight did not work, there was no way to set breakpoints inside the CUDA code, nor was there any other way to debug like one would do on the CPU. The solution was to rewrite the *complete* CUDA code in C# and introduce a "debug-pixel". The debugging procedure with the help of the debug-pixel is described in Section 6.6.

Despite all the troubles with debugging, however, the ray tracer is well debugged and works without problems known so far.

- *Data exchange between CUDA and C# and Aardvark integration*

  The first part of the thesis was the development of the CUDA library for Aardvark. This library needed to provide a way to maintain a mapping between dynamic C#-objects and CUDA-memory locations within hierarchical data structures and to provide the possibility to update only certain parts (fields) within such data structures. Most of the data types used

in CUDA are organized in structs and arrays. In C#, structs are value types, which leads to special maintenance for the mapping and support for data updates. To successfully accomplish and maintain such a mapping, several attempts have been implemented until a clean solution has been found.

Another time-consuming task was to implement graphics resource sharing between graphics APIs, like DirectX in versions 9 and 10, and CUDA. In Aardvark, the renderer is abstracted away behind a renderer interface. The problem was, however, that in the first place this interface did not allow access to certain low-level data like the DirectX resource pointers, which are needed to implement graphics resource sharing with CUDA.

- *HILITE interface*

  Concurrently to the development of the ray tracer, the HILITE-Viewer, which is the main rendering application of the HILITE project, was developed. One of the goals of the project is a hybrid rendering algorithm, combining rasterization and ray tracing. To make the integration of the ray tracer into the HILITE-Viewer as easy as possible, an additional layer of abstraction between the CUDA-representation and the Aardvark-representation of the scene data had to be introduced. Furthermore, an interface had to be defined for the data transition from the HILITE-Viewer into the CUDA ray tracer. Due to the ongoing development of the HILITE-Viewer, however, the requirements to this interface changed over time and several refactoring processes were necessary.

CHAPTER 8

Conclusion and Future Work

8.1 Conclusion

In this thesis, I presented a CUDA ray tracer for the HILITE research-project at the VRVis research center. With the CUDA ray tracer it is possible to render correct curved reflections with interactive to real-time frame rates, depending on the scene complexity. The ray tracer runs completely on the GPU. Per pixel, one ray is traced in parallel using CUDA. The parallel ray traversal was implemented in an iterative manner. From the geometry side, the ray tracer can handle triangle meshes. Multiple reflection bounces and shadows for directional and point light sources are supported and can be fully configured interactively at runtime. The ray tracer was integrated by another student into the HILITE Viewer, the main application of the HILITE-project, during the writing of the thesis.

As far as acceleration structures are concerned, the ray tracer supports two variants of kD-Trees (Section 6.4). The first one is the Object-kD-Tree, which is a kD-Tree per geometrical object in the scene. Since each object has its own transformation matrix, rigid animations are possible with this data structure. The second variant is our newly developed Über-kD-Tree. The Über-kD-Tree is a two-level kD-Tree, having the Object-kD-Tree as leaves inside the Über-kD-Tree. Both kD-Tree variants are constructed on the CPU first, then converted to a GPU-capable format and traversed on the GPU. The traversals of the kD-Trees are implemented as stack-based iterative traversals.

During research for available literature and resources, it turned out that it is hard to find complete algorithms on how to implement an iterative, massively parallel ray tracer in CUDA. The same holds true on how to store a kD-Tree in a GPU-capable format and how to implement a stack-based iterative traversal for kD-Trees in CUDA. For these reasons, Chapter 4 summarizes the algorithms for iterative and parallel ray tracing and diverse kD-Tree traversal methods.

It turned out that developing a complete ray tracer on the GPU, consisting of a few-thousand lines of code in a big CUDA kernel, is cumbersome to develop and to debug. What's more is that, since C# was the host language, most of the few debugging possibilities available for CUDA could not be used. To remedy this, the only solution was to rewrite the CUDA code in

C# and debug the code on the CPU. After debugging the CPU mirror-code, it was necessary to translate the code back to CUDA. This slowed down development tremendously. Doing so, I came up with a new method on how to debug the kD-Trees (Section 6.6). This can be applied to all interactive CUDA rendering applications using acceleration data structures. KD-Trees are hard to debug in general, but because of the limited debugging possibilities on the GPU they are even harder to debug there. The introduced debugging method uses a "debug pixel". This is a fixed pixel on the screen for which CPU debugging can be triggered. This only works if the CPU representation of the kD-Tree code is an exact mirror of the GPU code. Otherwise, wrong code paths will be debugged.

Finally, as a prerequisite to implement the ray tracer, a CUDA library for the VRVis-internal rendering engine has been developed. This has the advantage that research projects using Aardvark can now utilize the power of GPU computing. The library has an easy-to-use interface for high-level access to CUDA functionality. CUDA resources like the CUDA-context, -device, -modules and -functions are managed by the library. It also provides memory management for GPU resources by a memory manager using a reference-counting scheme. A special challenge was that structs in C# are value types and can not be referenced by default. Hence, memory management would not be possible with this data type. However, besides arrays, they are the most important ones for GPU computing. The most satisfying solution to this was finally to encapsulate the structs into an array of length 1. When working with CUDA, the data types used most of the time are either arrays or compound types like structs. For this reason, ready-to-use data types have been created, which can be used from within C# as normal C#-objects, as well as from CUDA. Whats more is that CUDA-kernels can be called almost like any other C#-function, providing flexibility and convenience when working with CUDA. This way, one does not have to worry about parameter mappings and conversion issues. To provide efficient data sharing between CUDA and graphics APIs, graphics resource sharing has been implemented as well, even if Aardvark did not support the needed low-level access to graphics resources in the first place. Finally, the library also supports CUDA-Streams and -Events for parallel kernel execution and timing measurements.

8.2 Future Work

Even if the targeted goals of this diploma thesis have been met, there are lots of possibilities to enhance and extend the ray tracer.

The first one is the integration into the HILITE Viewer, the main application of the HILITE project. During writing of this thesis, this task has already been done by another student.

In order to achieve better photorealism, transparency should be implemented. Further, common effects like depth of field, motion blur, ambient occlusion, subsurface scattering and soft shadows are also candidates for future implementations.

Another important feature would be the implementation of multi-sampling and anti-aliasing, as well as adaptive rendering in such a way, that when the camera moves and the frame rate drops too low, only each n-th pixel is rendered. To enhance rendering time, algorithms like packet traversal (as described in Section 2.3.2) could be added as well. Additionally, hybrid rendering

could be implemented by handling the primary rays with rasterization and then starting the ray tracing task for the secondary rays only.

Furthermore, the CUDA code could be even further optimized. Especially the time for memory access can be reduced. To avoid the penalty of threads in a warp waiting for longer running threads in this warp to finish, ray pools and persistent threads as in [AL09] could be implemented as well.

Since the construction of the kD-Trees on the CPU take a considerable amount of time especially for bigger scenes, it would be nice to implement kD-Tree construction on the GPU.

An interesting research topic would be the implementation of BVHs and to compare their performance to kD-Trees in terms of rendering performance, construction time and memory footprint.

Besides that, the CUDA library currently supports the CUDA 3.x API and parts of the 4.x API, which are incompatible with the newer versions of Nvidia's debugging-tool Nsight. Hence, the API should be updated to fully support version 4.x.

Bibliography

[AK87] James Arvo and David Kirk. Fast Ray Tracing by Ray Classification. In Proceedings of the 14th annual conference on Computer graphics and interactive techniques, SIGGRAPH '87, pages 55–64, New York, NY, USA, 1987. ACM.

[AK11] C. Wächter A. Keller. Efficient Ray Tracing without Auxiliary Acceleration Data Structures, 2011. HPG 2012, Poster.

[AL09] Timo Aila and Samuli Laine. Understanding the Efficiency of Ray Traversal on GPUs. In Proceedings of the Conference on High Performance Graphics 2009, HPG '09, pages 145–149, New York, NY, USA, 2009. ACM.

[ALK12] Timo Aila, Samuli Laine, and Tero Karras. Understanding the Efficiency of Ray Traversal on GPUs - Kepler and Fermi Addendum. NVIDIA Technical Report NVR-2012-02, NVIDIA Corporation, June 2012.

[Ben75] Jon Louis Bentley. Multidimensional Binary Search Trees used for Associative Searching. Commun. ACM, 18(9):509–517, September 1975.

[Bik11] Jacco Bikker. Arauna - Real-time Ray Tracing. `http://igad.nhtv.nl/~bikker`, 2011. Last accessed: 23nd of February, 2013.

[Cab10] João Cabeleira. Combining Rasterization and Ray Tracing Techniques to Approximate Global Illumination in Real-Time. Master's thesis, Technical University of Lisbon, Instituto Superior Técnico, 2010.

[CG] Inc. Caustic Graphics. CausticOne. `https://caustic.com/caustic-rt_caustic-one.php`. Last accessed: 22nd of April, 2013.

[Cooa] Nvidia Coorp. CUDA. `http://developer.nvidia.com/category/zone/cuda-zone`. Last accessed: 23nd of February, 2013.

[Coob] Nvidia Coorp. CUDA LLVM Compiler. `https://developer.nvidia.com/cuda-llvm-compiler`. Last accessed: 16nd of April, 2013.

[Cooc] Nvidia Coorp. CUDA Programming Guide, Version 4.2. Part of the CUDA SDK. Downloadable at `http://developer.nvidia.com`. Last accessed: 23nd of February, 2013.

[Coo10] Nvidia Coorp. NVIDIA's Next Generation CUDA Compute Architecture: Fermi, 2010. Whitepaper.

[DPS10] P. Danilewski, S. Popov, and P. Slusallek. Binned SAH kD-Tree Construction on a GPU. Technical report, Saarland University, 2010.

[EMD+05] Pau Estalella, Ignacio Martin, George Drettakis, Dani Tost, Olivier Devillers, and Frederic Cazals. Accurate Interactive Specular Reflections on Curved Objects. In In Proc. of VMV 2005, 2005.

[EMDT06] Pau Estalella, Ignacio Martin, George Drettakis, and Dani Tost. A GPU-driven Algorithm for Accurate Interactive Reflections on Curved Objects. In Proceedings of the 17th Eurographics conference on Rendering Techniques, EGSR'06, pages 313–318, Aire-la-Ville, Switzerland, Switzerland, 2006. Eurographics Association.

[Áfr12] Attila T. Áfra. Incoherent Ray Tracing without Acceleration Structures. Eurographics 2012 short paper, 2012.

[FS05] Tim Foley and Jeremy Sugerman. KD-Tree Acceleration Structures for a GPU Raytracer. In Proceedings of the ACM SIGGRAPH/EUROGRAPHICS conference on Graphics hardware, HWWS '05, pages 15–22, New York, NY, USA, 2005. ACM.

[GAS] Company for Advanced Supercomputing Solutions Ltd. GASS. CUDA.NET. `http://www.cass-hpc.com/category/cudanet`. Last accessed: 23^{nd} of February, 2013.

[GL10] Kirill Garanzha and Charles T. Loop. Fast Ray Sorting and Breadth-First Packet Traversal for GPU Ray Tracing. Comput. Graph. Forum, 29(2):289–298, 2010.

[Gmb] VRVis GmbH. HILITE. `http://vrvis.at/projects/hilite`. Last accessed: 23^{nd} of February, 2013.

[GPM11] Kirill Garanzha, Jacopo Pantaleoni, and David McAllister. Simpler and faster HLBVH with Work Queues. In Proceedings of the ACM SIGGRAPH Symposium on High Performance Graphics, HPG '11, pages 59–64, New York, NY, USA, 2011. ACM.

[GPP+10] Olivier Gourmel, Anthony Pajot, Mathias Paulin, Loïc Barthe, and Pierre Poulin. Fitted BVH for Fast Ray Tracing of Metaballs. Computer Graphics Forum, 29(2), May 2010.

[GS87] Jeffrey Goldsmith and John Salmon. Automatic Creation of Object Hierarchies for Ray Tracing. IEEE Comput. Graph. Appl., 7(5):14–20, May 1987.

[Gue08] Paul Guerrero. Approximative Real-time Soft Shadows and Diffuse Reflections in Dynamic Scenes. Master's thesis, Vienna Unitersity of Technology, Institute of Computer Graphics and Algorithms, 2008.

[Hav00] Vlastimil Havran. Heuristic Ray Shooting Algorithms. PhD thesis, Faculty of Electrical Engineering, Czech Technical University, Prague, 2000.

[HBZ98] Vlastimil Havran, Jirí Bittner, and Jirí Zára. Ray Tracing with Rope Trees. In in Proceedings of 13th Spring Conference On Computer Graphics, Budmerice in Slovakia, pages 130–139, 1998.

[Hec90] Paul S. Heckbert. Adaptive Radiosity Textures for Bidirectional Ray Tracing. In Proceedings of the 17th annual conference on Computer graphics and interactive techniques, SIGGRAPH '90, pages 145–154, New York, NY, USA, 1990. ACM.

[HQL+10] Qiming Hou, Hao Qin, Wenyao Li, Baining Guo, and Kun Zhou. Micropolygon Ray Tracing with Defocus and Motion Blur. In ACM SIGGRAPH 2010 papers, SIGGRAPH '10, pages 64:1–64:10, New York, NY, USA, 2010. ACM.

[HSHH07] Daniel Reiter Horn, Jeremy Sugerman, Mike Houston, and Pat Hanrahan. Interactive kD-Tree GPU Raytracing. In Proceedings of the 2007 symposium on Interactive 3D graphics and games, I3D '07, pages 167–174, New York, NY, USA, 2007. ACM.

[ICG86] David S. Immel, Michael F. Cohen, and Donald P. Greenberg. A Radiosity Method for Non-Diffuse Environments. In Proceedings of the 13th annual conference on Computer graphics and interactive techniques, SIGGRAPH '86, pages 133–142, New York, NY, USA, 1986. ACM.

[Kaj86] James T. Kajiya. The Rendering Equation. In Proceedings of the 13th annual conference on Computer graphics and interactive techniques, SIGGRAPH '86, pages 143–150, New York, NY, USA, 1986. ACM.

[KBS11a] Javor Kalojanov, Markus Billeter, and Philipp Slusallek. Two-Level Grids for Ray Tracing on GPUs. In Oliver Deussen Min Chen, editor, EG 2011 - Full Papers, pages 307–314, Llandudno, UK, 2011. Eurographics Association.

[KBS11b] Javor Kalojanov, Markus Billeter, and Philipp Slusallek. Two-Level Grids for Ray Tracing on GPUs. Computer Graphics Forum, 30(2):307–314, 2011.

[KK86] Timothy L. Kay and James T. Kajiya. Ray Tracing Complex Scenes. In Proceedings of the 13th annual conference on Computer graphics and interactive techniques, SIGGRAPH '86, pages 269–278, New York, NY, USA, 1986. ACM.

[Lás99] Szirmay-Kalos László. Monte-Carlo Methods in Global Illumination, 1999. Scriptum.

[MB05] Marc Stamminger Marcel Beister, Manfred Ernst. A hybrid gpu-cpu renderer. Vision, Modeling, and Visualization 2005, 2005.

[MM95] Michael John Muuss and Michael John Muuss. Towards Real-Time Ray-Tracing of Combinatorial Solid Geometric Models, 1995.

[Mor66] G. M. Morton. A Computer Oriented Geodetic Data Base; and a new Technique in File Sequencing. Technical report, IBM Ltd., Ottawa, Canada, 1966.

[Mor11a] Benjamin Mora. Direct-Trace Library: Ray Tracing for the Masses. `http://www.directtrace.org`, 2011. Last accessed: 23^{nd} of February, 2013.

[Mor11b] Benjamin Mora. Naive Ray Tracing: A Divide-and-Conquer Approach. ACM Trans. Graph., 30(5):117:1–117:12, October 2011.

[M.R85] Kaplan M.R. Space Tracing: A Constant Time Ray Tracer, State of the Art in Image Synthesis. In SIGGRAPH '85 course notes, page 11f, 1985.

[PBD+10] Steven G. Parker, James Bigler, Andreas Dietrich, Heiko Friedrich, Jared Hoberock, David Luebke, David McAllister, Morgan McGuire, Keith Morley, Austin Robison, and Martin Stich. OptiX: A General Purpose Ray Tracing Engine. In ACM SIGGRAPH 2010 papers, SIGGRAPH '10, pages 66:1–66:13, New York, NY, USA, 2010. ACM.

[PBMH02] Timothy J. Purcell, Ian Buck, William R. Mark, and Pat Hanrahan. Ray Tracing on programmable Graphics Hardware. In Proceedings of the 29th annual conference on Computer graphics and interactive techniques, SIGGRAPH '02, pages 703–712, New York, NY, USA, 2002. ACM.

[PGDS09] Stefan Popov, Iliyan Georgiev, Rossen Dimov, and Philipp Slusallek. Object Partitioning considered harmful: Space Subdivision for BVHs. In Proceedings of the Conference on High Performance Graphics 2009, HPG '09, pages 15–22, New York, NY, USA, 2009. ACM.

[PGSS06] S. Popov, J. Günther, Hans-Peter Seidl, and P. Slusallek. Experiences with Streaming Construction of SAH kD-Trees. IEEE Symposium on Interactive Ray Tracing, pages 89–94, 2006.

[PL10] J. Pantaleoni and D. Luebke. HLBVH: Hierarchical LBVH Construction for Real-time Ray Tracing of Dynamic Geometry. In Proceedings of the Conference on High Performance Graphics, HPG '10, pages 87–95, Aire-la-Ville, Switzerland, Switzerland, 2010. Eurographics Association.

[PMS+99] Steven Parker, William Martin, Peter-Pike J. Sloan, Peter Shirley, Brian Smits, and Charles Hansen. Interactive Ray Tracing. In Proceedings of the 1999 symposium on Interactive 3D graphics, I3D '99, pages 119–126, New York, NY, USA, 1999. ACM.

[RH06] David Roger and Nicolas Holzschuch. Accurate Specular Reflections in Real-Time. Computer Graphics Forum (Proceedings of Eurographics 2006), 25(3), sep 2006.

[SFD09] Martin Stich, Heiko Friedrich, and Andreas Dietrich. Spatial Splits in Bounding Volume Hierarchies. In Proceedings of the Conference on High Performance Graphics 2009, HPG '09, pages 7–13, New York, NY, USA, 2009. ACM.

[SPS07] Hans-Peter Seidel Stefan Popov, Johannes Günther and Philipp Slusallek. Stackless kD-Tree Traversal for High Performance GPU Ray Tracing. Technical report, Saarland University, 2007.

[SSK07] Maxim Shevtsov, Alexei Soupikov, and Er Kapustin. Highly Parallel fast kD-Tree Construction for Interactive Ray Tracing of Dynamic Scenes. In EUROGRAPHICS 2007, volume 26, Number 3, 2007.

[Suf07] Kevin Suffern. Ray Tracing from the Ground Up. A K Peters/CRC Press, Westminster College, Salt Lake City, Utah, USA, 2007.

[SWW+04] Jörg Schmittler, Sven Woop, Daniel Wagner, Wolfgang J. Paul, and Philipp Slusallek. Realtime Ray Tracing of Dynamic Scenes on an FPGA Chip. In Proceedings of the ACM SIGGRAPH/EUROGRAPHICS conference on Graphics hardware, HWWS '04, pages 95–106, New York, NY, USA, 2004. ACM.

[Tra06] Gilles Tran. Glasses. Persistence of Vision Raytracer (POV Ray) - Hall of Fame, `http://hof.povray.org`, 2006. Last accessed: 23^{nd} of February, 2013.

[WH06] Ingo Wald and Vlastimil Havran. On building fast kD-Trees for Ray Tracing, and on doing that in O(N log N). In IN PROCEEDINGS OF THE 2006 IEEE SYMPOSIUM ON INTERACTIVE RAY TRACING, pages 61–70, 2006.

[Whi80] Turner Whitted. An improved Illumination Model for Shaded Display. Commun. ACM, 23(6):343–349, June 1980.

[WK06] Carsten Wächter and Alexander Keller. Instant Ray Tracing: The Bounding Interval Hierarchy. In IN RENDERING TECHNIQUES 2006 – PROCEEDINGS OF THE 17TH EUROGRAPHICS SYMPOSIUM ON RENDERING, pages 139–149, 2006.

[WMS06] Sven Woop, Gerd Marmitt, and Philipp Slusallek. B-KD Trees for Hardware Accelerated Ray Tracing of Dynamic Scenes. In Proceedings of the 21st ACM SIGGRAPH/EUROGRAPHICS symposium on Graphics hardware, GH '06, pages 67–77, New York, NY, USA, 2006. ACM.

[WS05] Sven Woop and Jörg Schmittler. RPU: A Programmable Ray Processing Unit for Realtime Ray Tracing. In ACM Trans. Graph, pages 434–444, 2005.

[WSB01] Ingo Wald, Philipp Slusallek, and Carsten Benthin. Interactive Distributed Ray Tracing of Highly Complex Models. In In Rendering Techniques 2001: 12th Eurographics Workshop on Rendering, pages 277–288. Springer, 2001.

[WSBW01] Ingo Wald, Philipp Slusallek, Carsten Benthin, and Markus Wagner. Interactive Rendering with Coherent Ray Tracing. In Computer Graphics Forum, pages 153–164, 2001.

[WZL11] Zhefeng Wu, Fukai Zhao, and Xinguo Liu. SAH KD-Tree Construction on GPU. In Proceedings of the ACM SIGGRAPH Symposium on High Performance Graphics, HPG '11, pages 71–78, New York, NY, USA, 2011. ACM.

[ZHWG08] Kun Zhou, Qiming Hou, Rui Wang, and Baining Guo. Real-time kD-Tree Construction on Graphics Hardware. In ACM SIGGRAPH Asia 2008 papers, SIGGRAPH Asia '08, pages 126:1–126:11, New York, NY, USA, 2008. ACM.